Assessment of Control Loop Performance for Nonlinear Process

By

Nelendran Pillay

(Student Number: 19752683)

A thesis submitted in fulfilment for the requirements for the Doctors Degree in Engineering (Electrical Engineering: Light Current)

Department of Electronic Engineering

Faculty of Engineering, Science and the Built Environment

Durban University of Technology

The work presented in this thesis represents my own work

_____

Nelendran Pillay

APPROVED FOR FINAL SUBMISSION

_____ _____

Supervisor: Dr Poobalan Govender Date

Department of Electronic Engineering

Durban University of Technology

Durban University of Technology

Faculty of Engineering, Science and the Built Environment

Department of Electronic Engineering

The undersigned certify that they have read and recommend to the Faculty of Engineering, Science and the Built Environment for acceptance, a thesis entitled **Assessment of Control Loop Performance for Nonlinear Process** submitted by **Nelendran Pillay** in fulfilment of the requirements for the degree of **Doctor of Engineering.**

_____

Dr. Poobalan Govender (Supervisor)

Durban University of Technology

_____

Prof. Walter Commerell (External Examiner)

University of Applied Sciences ULM

_____

Prof. Md. Ali Ahammad Shoukat Choudury (External Examiner)

Bangladesh University of Engineering and Technology (BUET)

_____

Date

To my family:

Theresa & Cameron

Acknowledgements

During the study period I am grateful to my promoter Dr. Poobalan Govender. His constructive criticism of my research work has impacted positively on the results presented in this thesis. May his soul rest in peace. Gratitude must be conveyed to the Head of Department of Electronic Engineering, Mr Kevin Moorgas for his constant support throughout the research period.

Great appreciation must be given to colleagues at ABB® South Africa, who shared their invaluable expertise and knowledge with us.

This research work was financially supported by the National Research Foundation (NRF) of South Africa. Thuthuka Grant Reference Number: TTK1206121201.

Finally I must acknowledge the support of my family, during which you endured many hours of me being absent on account of this work. Without your support and understanding this research thesis would not have materialised.

Abstract

Controller performance assessment (CPA) is concerned with the design of analytical tools that are utilized to evaluate the performance of process control loops. The objective of the CPA is to ensure that control systems operate at their full potential, and also to indicate when a controller design is performing unsatisfactorily under current closed loop conditions.

Such monitoring efforts are imperative to minimize product variability, improve production rates and reduce wastage. Various studies conducted on process control loop performance indicate that as many as 60% of control loops often suffer from some kind of performance problem. It is therefore an important task to detect unsatisfactory control loop behavior and suggest remedial action. Such a monitoring system must be integrated into the control system life span as plant changes and hardware issues become apparent.

CPA is well established for linear systems. However, not much research has been conducted on CPA for nonlinear systems. Traditional CPA analytical tools depend on the theoretical minimum variance control law that is derived from models of linear systems. In systems exhibiting dominant nonlinear behavior, the accuracy of linear based CPA is compromised.

In light of this, there is a need to broaden existing CPA knowledge base with comprehensive benchmarking indices for the performance analysis of nonlinear process control systems.

The research efforts presented in this thesis focuses on the development and analysis of such CPA tools for univariate nonlinear process control loops experiencing the negative effects of dominant nonlinearities emanating from the process.

Two novel CPA frameworks are proposed; first a model based nonlinear assessment index is developed using an open loop model of the plant in an artificial neural network NARMAX (NNARMAX) representation. The nonlinear control loop is optimized offline using a proposed Nelder Mead-Particle Swarm Optimization (NM-PSO) hybrid search to determine global optimal control parameters for a gain scheduled PID controller. Application of the benchmark in real-time utilizes a synthetic process output derived from the NNARMAX system which is compared to the actual closed loop performance.

In the case where no process model is available, a second method is presented. An autonomous data driven approach based on Multi-Class Support Vector Machines (MC-SVMs) is developed and analyzed. Unlike the model based method, the closed loop performance is classified according to five distinct class groups. MC-SVM classifier requires minimal process loop information other than routine operating closed loop data.

Several simulation case studies conducted using MATLAB™ software package demonstrate the effectiveness of the proposed performance indices. Furthermore, the methodologies presented in this work were tested on real world systems using control loop data sets from a computer interfaced full scale pilot pH neutralization plant and pulp and paper industry.

List of Tables

List of Figures

List of Abbreviations

ACF	Autocorrelation function
ANOVA	Analysis of variance
ANN	Artificial neural network
ANNs	Artificial neural networks
AR	AutoRegressive
ARMA	AR Moving Average
ARMAX	AutoRegressive Moving Average with eXogenous inputs
CPA	Controller performance assessment
CSTR	Continuous stirred tank reactor
CV	Controlled variable
DCS	Distributed control system
DFA	Detrended fluctuation analysis
FCE	Final control element
FCOR	Filtering and correlation
FOPDT	First order plus dead time
GUI	Graphical user interface
HOS	Higher order statistics
HMI	Human machine interface
IAE	Integral absolute of the error
I/O	Input output
IMC	Internal model control
LTI	Linear time invariant
LTV	Linear time variant
MC-SVMs	Multi-class SVMs
MPC	Model predictive control
MSE	Mean square of the error

MV	Minimum variance
MVC	MV control
MVPLB	MV performance lower bound
NARMAX	Nonlinear ARMAX
NGMV	Nonlinear generalized minimum variance
NLCPA	Nonlinear CPA
NM-PSO	Nelder Mead- Particle swarm optimization
NMVLB	Nonlinear minimum variance lower bound
NNARMAX	Neural NARMAX
OAA	One-against-all
OAO	One-against-one
OPC	Open process control
PI	Proportional-integral
PID	Proportional-integral-derivative
PSO	Particle swarm optimization
PV	Process variable
SISO	Single input single output
SP	Setpoint
SVMs	Support vector machines
NaOH	Sodium hydroxide
H_2SO_4	Sulphuric acid

List of Symbols

a, A	white noise sequence
A_m	gain margin
b	integer value of the process dead time
c	regularization constant
C_a	concentration of the acid entering the tank
C_b	concentration of the base entering the tank
d, D	disturbance signal
deg	degree of differencing
d_{poly}	degree of the polynomial Kernel
e	control error
E	expectation operator
e^m	controller error of the model
e^p	controller error of the plant
F	regression vector matrix
F_a	acid flow rate (titrating stream)
F_b	base flow rate (process stream)
$f(.)$	nonlinear mapping function
G_c	controller transfer function
G_d	disturbance transfer function
G_p	process transfer function
g_{RBF}	width of the RBF kernel
h	Volterra model coefficients
i	NARMAX input term
I_o	initial conditions

IAE_{dim}	dimensionless integral absolute of the error
IAE_{LIM}	limit on IAE
$iqr(\rho)$	interquartile range of ACF coefficients
J	cost function
J_v	valve jump band
k	number of SVM classes
K	number of parameters
$K(.)$	nonlinear kernel function
k_c	proportional gain
K_w	ionic product of water
K_p	process gain
$K_{1,2}$	dissociation constants
l	number of lags
L	Lagrangian multiplier function
m	number of regression variables
n	number of data samples
N	number of SVM training samples
n_b	past delay term
n_e	neuron
n_u	past input term
n_y	past output term
o	NARMAX output term
r	setpoint
S_v	valve stick band
t	instantaneous time
t_s	settling time

T_p	process time constant
T_s	sampling time
t_{OP}	operating point
T_{dim}	dimensionless settling time
$tune_c$	tuneable constant
u,U	controller output
V	variance operator
var(ρ)	variance of ACF coefficients
V_{CSTR}	volume of the CTSR tank
w	N dimensional vector
w_e	weight
w_l	window length
x	sample input vector
x_a	concentration of the acid solution in the CSTR
x_b	concentration of the base solution in the CSTR
y,Y	process output
y^p	plant output
y^m	model output
z	auxiliary variables
z^{-1}	backshift operator

Greek symbols

ϑ	impulse coefficients
Θ	parameter vector matrix
Ξ	*b-step* ahead prediction error vector matrix
Ψ	regression vector
ξ	Gaussian noise
β	distance between boundary margin and samples
θ_p	process dead time
α_e	activation function
ϕ_m	phase margin
ρ	ACF coefficient
$\bar{\rho}$	mean value of the ACF coefficients
$\rho(l)$	ACF at lag *l*
$\gamma(\rho)$	mean of ACF coefficients
$\Phi(.)$	nonlinear mapping function
σ_A^2	variance of the white noise
σ_Y^2	variance of the actual process output
σ_{MV}^2	variance of the system under MV control
σ_{PID}^2	variance of system under PID control
$\hat{\sigma}_{NGMV}^2$	variance of system under nonlinear generalized minimum variance control
σ_ϕ^2	variance of system under linear generalised minimum variance control
$\eta_{MV}(b)$	minimum variance index
η_{PID}	PID controller performance index
η_{ANOVA}	ANOVA performance index
$\eta_{NL_{PID}}$	nonlinear PID controller performance index

μ_b	neural network bias term
θ_e	summation of products
τ_i	integral time constant
$\tau_{i_{optimal}}$	optimal integral time constant
τ_d	derivative time constant

Contents

Chapter 1

Introduction

1.1 AN OVERVIEW OF CONTROLLER PERFORMANCE ASSESSMENT WITH OBJECTIVES TO THIS THESIS

Controller performance assessment (CPA) is concerned with health of the automatic control system (Joe Qin, 1998; Harris *et al.*, 1999; Hugo, 2006) and aims to diagnose the state of operational efficiency of the controller. As stated by Jelali (2006);

"The main objective of CPA is to provide online automated procedures that evaluate the performance of the control system and deliver information to plant personal for determining whether specific performance targets and responses characteristics are being met by the controller process variables."

Automatic process control monitoring constitutes an integral part of performance improvement in modern industry. With the sheer number of process control loops functioning in a typical industrial facility, operators and maintenance personnel are usually inundated to manually detect and diagnose poorly performing control loops individually. Furthermore, many problematic control loops may not be easily detected from simple cursory inspection of recorded historian trends of plant data (Rengaswamy *et al.*, 2001) and therefore require continuous automatic evaluation.

Although there have been considerable technological advancements made in the area of CPA (cf. Tyler and Morari, 1996; Kendra and Çinar, 1997; Horch and Isaksson, 1999; Harris and Seppala, 2002; Huang and Jeng, 2002; Kadali and Huang, 2002; Jain and Lakshminarayanan, 2004; Julien *et al.*, 2004; Majecki and Grimble, 2004b; Ingimundarson and Hägglund, 2005; Thornhill and Horch, 2006; Ordys *et al.*, 2007; Hanna *et al.*, 2008; Howard and Cooper, 2010; Sun *et al.*, 2013), the literature has been relatively sparse on CPA studies concerning nonlinear processes. Many of the methods devised for CPA are primarily restricted to linear systems (Harris and Yu, 2007; Yu, 2007; Yu *et al.*, 2011a). In practice however, industrial control loops can include nonlinearities from the control valve, the feedback measurement, or the process itself (Yu *et al.*, 2011a). Conventional CPA techniques will yield imprecise results since they have been devised using linear models (Harris and Yu, 2007; Yu, 2007). These methods were designed without any consideration for nonlinear stochastic and/or deterministic behavior acting within a control loop.

Improved performance is the prime objective in today's industrial processes (Harris *et al.*, 1999; Desborough and Miller, 2002; Jelali, 2006). Throughputs have increased drastically, decreasing the time available to detect and control upsets (Jelali, 2013). Inadequately designed control systems, malfunctioning control equipment, poorly tuned and oscillating loops require automatic detection and diagnosis (Hägglund, 1995; Ordys *et al.*, 2007). Methods used to detect poor performing loops can be categorized under the CPA framework (Jelali, 2006).

Commercial software packages such as ABB™ Optimize^{IT} Loop Performance Manager, HONEYWELL™ Loop Scout and METSO Automation™ Loop Browser (Jelali, 2013) usually contain several different metrics to indicate the quality of the controller performance and to aid in diagnosis of controller problem. Most commercial packages employ the Harris index (Harris, 1989) in which CPA is achieved by utilizing linear time series modeling and

minimum variance control (MVC). The method is influential in that CPA is realized by merely fitting the closed-loop process variable data to a linear time series model (Joe Qin, 1998). Only the process loop dead time must be known in order to perform the Harris performance index (Harris, 1989; Harris *et al.*, 1999). The achievable theoretical minimum variance which is derived from the time series model is compared to the actual closed-loop output variance. The method is practical and easy to implement but is only applicable for the linear case (Harris and Yu, 2007; Yu *et al.*, 2011a).

Thus far the majority of research conducted in the field of CPA utilizes linear time models in determining suitable indices for CPA (Kozub, 2002; Jelali, 2006; Harris and Yu, 2007). In practice however, industrial control loops invariably include mild to severe nonlinearities in the control channel which must be considered. Within this context, these nonlinearities must be taken into account at the design stage in order to improve controller ruggedness and also to ensure accurate performance benchmarking measures.

It is well known that process loops that are mildly nonlinear can be modeled sufficiently well using linear time series models such as the parametric Auto-Regressive-Moving-Average with Exogenous input (ARMAX) structure (Astrom, 1970; Harris, 1989). However, some systems exhibiting higher degrees of nonlinearity may be more difficult to model, due to the existence of inherent complexities and a non-Gaussian output (Zhou and Wan, 2008; Zhang *et al.*, 2011). In such cases, the closed-loop process dynamics and disturbance models cannot be well characterized by either its impulse response or its equivalent linear time series model. Yu *et al.* (2010a) showed that traditional linear performance indices incorrectly yield biased performance benchmark measures in the presence of valve nonlinearity.

A survey of literature reveals that researchers investigating nonlinear systems fall into three groups. The first group focused on the diagnosis of valve stiction nonlinearity (Yu *et al.*,

2010b; Yu *et al.*, 2011a) while the second group tried to establish the minimum variance performance lower bound (MVPLB) (Harris and Yu, 2007; Maboodi *et al.*, 2015). Finally, Yu (2007) suggested using analysis of variance (ANOVA) to decompose the disturbances acting on the process in order to determine its effect on control loop performance. However, many outstanding issues still remain open for further research on CPA for nonlinear systems and will be discussed in the thesis.

1.2 RESEARCH PROBLEMS

Some of the outstanding issues concerning nonlinear CPA (NLCPA) that form the basis of the research work are given as follows:

(i) *Extension of NLCPA to systems experiencing variable setpoint changes.*

This research will have practical significance since many process loops employ cascade control, whereby the secondary control loop is constantly tracking a variable setpoint from the primary control loop.

(ii) *Performance assessment of a gain scheduled PID control algorithm.*

Although MVPLB gives a performance metric based on the MV of the closed loop process output, it does not take the controller structure into consideration (Jelali, 2013). Therefore if the controller was determined to be under-performing according to the MVPLB, the performance measure would not give any indication on how to improve the controller performance. Since most industrial controllers are of the PID type, it would be beneficial to provide a suitable performance index based on its algorithmic structure in the presence of different types of nonlinearities.

(iii) *Nonlinear process modeling for CPA.*

Process modeling using suitable techniques for systems exhibiting severe nonlinear plant dynamics need to be exploited. When the process is described by a nonlinear difference equation, development of the nonlinear MVC may be very challenging (Harris and Seppala, 2002, Yu *et al.*, 2010). Therefore an alternative performance metric is required for these dynamical systems.

(iv) *Data driven NLCPA methodology.*

In some industrial plants, nonlinear process modeling cannot be achieved due to time and/or human resource constraints. Therefore it will be highly beneficial to have a suitable non-intrusive data driven performance metric that uses routine plant data.

1.3 AIMS OF THE RESEARCH

Based on the CPA problems listed in the previous section, this research will focus on the following aspects:

(i) Development of suitable performance benchmarking methodologies for systems exhibiting behavioral characteristics attributed to nonlinear effects originating from the process.

(ii) Design of a restricted structure CPA methodology where the gain scheduled PID controller is used in the nonlinear process control loop. Consideration has been given to systems where setpoint tracking is of primary concern. This type of

control objective is chosen since it has not been considered in the literature for nonlinear CPA study.

(iii) Utilization of suitable nonlinear modeling techniques to quantify loop nonlinearities for the purpose of real time closed loop control monitoring.

(iv) Development of a model free approach to NLCPA.

1.4 SCOPE OF THE RESEARCH

The scope and delimitations of the research work include the following:

(i) Synthesis of suitable autonomous benchmarks for the purpose of evaluating controller performance operating in the presence of control channel nonlinearities.

(ii) Dynamic nonlinear models of the process control loops has been developed using well established methodologies. Emphasis has been on process and pneumatic control valve nonlinear characteristics. The effects of long term sensor degradation are not considered.

(iii) The study is limited to the PID control structure operating within a closed loop negative feedback single input-single output (SISO) scheme. SISO loops are selected for this study because it is the fundamental building block of a control loop.

(iv) In general, the study is limited to setpoint tracking capabilities of the controller, although the data driven methodology presented in the latter part of this work can be applied to systems where regulatory control of the process variable is important.

(v) NLCPA tools will be software based using MATLAB™ programming language and graphical user interface (GUI) toolboxes. Suitable interfaces that convey relevant control performance benchmarks to the control practitioner has been developed.

(vi) Data derived from simulated closed loop experiments and real world industrial process loops has been analysed using a NLCPA computer interface system.

(vii) The novel loop assessment indices developed from this work can be directly applied on a plant distributed control system (DCS) or auxiliary monitoring computer with third party software.

1.5 RESEARCH METHODS

The study design includes both descriptive and analytical elements. First, the descriptive stage of the study will involve the construction of a laboratory based continuously stirred tank reactor (CSTR) system. The main motivation for using this process system in the research stems from the effects of severe intrinsic nonlinearities present in the chosen chemical process. These nonlinearities may take the form of exothermic reaction rates, control valve nonlinearities and irregular product flow rates. From this, real world plant data will be used to develop models that describe the nonlinear process behaviour. Simulation models will be developed for

reproducing closed loop behaviour within a controlled laboratory environment. The performance of the nonlinear controller will then be compared to the actual CSTR control loop. Based on this, an index will be developed to evaluate the performance of pilot plant process loop.

Second, the analytical aspect will involve studies of typical process loop performances of specific control loop data from a pulp and paper mill, and the experimental pilot study plant. These studies will entail visual inspection of production trends retrieved from the DCS with the intention of isolating problematic control loops. Selected loops in process plants are chosen for this study because of the destabilizing control issues experienced which can include variable process gain, control valve nonlinearities, constant loop oscillations, overshoot and sluggish behaviour.

1.6 CONTRIBUTIONS OF THE STUDY

The main contributions of the research study presented in the thesis include:

(i) Classification of existing NLCPA methods according to model and system excitation requirements.

(ii) A new model based NLCPA framework for assessing setpoint tracking capabilities of a gain scheduled PID controller in real time has been proposed.

(iii) Constrained optimization of a gain scheduled PID controller for nonlinear systems using Nelder Mead-Particle Swarm Optimization hybrid algorithm.

(iv) Development of a novel control loop classification utility that uses multi-class support vector machines to classify different closed loop behaviours following setpoint changes.

(v) Proposal of a unifying approach using several statistical algorithms for the sole purpose of feature extraction.

(vi) Development of a suitable human machine interface for indicating NLCPA assessment results in real time.

(vii) The methodologies presented in this thesis were evaluated using real world data extracted from a pilot scale plant and an industrial facility.

(viii) Scientific publications originating from this study have been published or are to appear in conference proceedings and archival journals.

1.7 STRUCTURE OF THE THESIS

The thesis is organised as follows:

In Chapter 2, an overview of existing linear and nonlinear CPA benchmarking tools is provided to review current terminology and methods. Chapter 3 provides insight into the taxonomy of existing NLCPA schemes.

In Chapter 4, a new model based NLCPA benchmarking methodology is proposed. The method is discussed in detail using three stages to explain the development of the novel real

time NLCPA index. A simulation case study is provided to demonstrate its effectiveness on a nonlinear process model.

Chapter 5 provides details of the full scale pilot study plant that was designed to test the new benchmarking indices developed in this work. Nonlinear pH equations for strong acid/strong base reactions are discussed. Two case studies emanating from the CSTR pilot plant is used to demonstrate the effectiveness of the model based approach.

Chapter 6 introduces a new data driven NLCPA technique using MC-SVMs to classify closed loop performance. A brief review of MC-SVMs is given and introduces its use for NLCPA. Fifteen key ACF statistical attributes that distinguish different controller performance are presented. Feature extraction algorithms used in the development of the MC-SVM tool are introduced and simulation experiments emphasize the feasibility of the proposed classification monitoring tool.

Chapter 7 highlights practical application of the data driven NLCPA methodology on real world data sets. Several case studies are provided in order to validate and demonstrate the efficacy of the proposed framework. Chapter 8 concludes the study with a summary of the work presented in this thesis and recommendations for extending the work.

An outline of the research study presented in this thesis is illustrated in Fig.1.1.

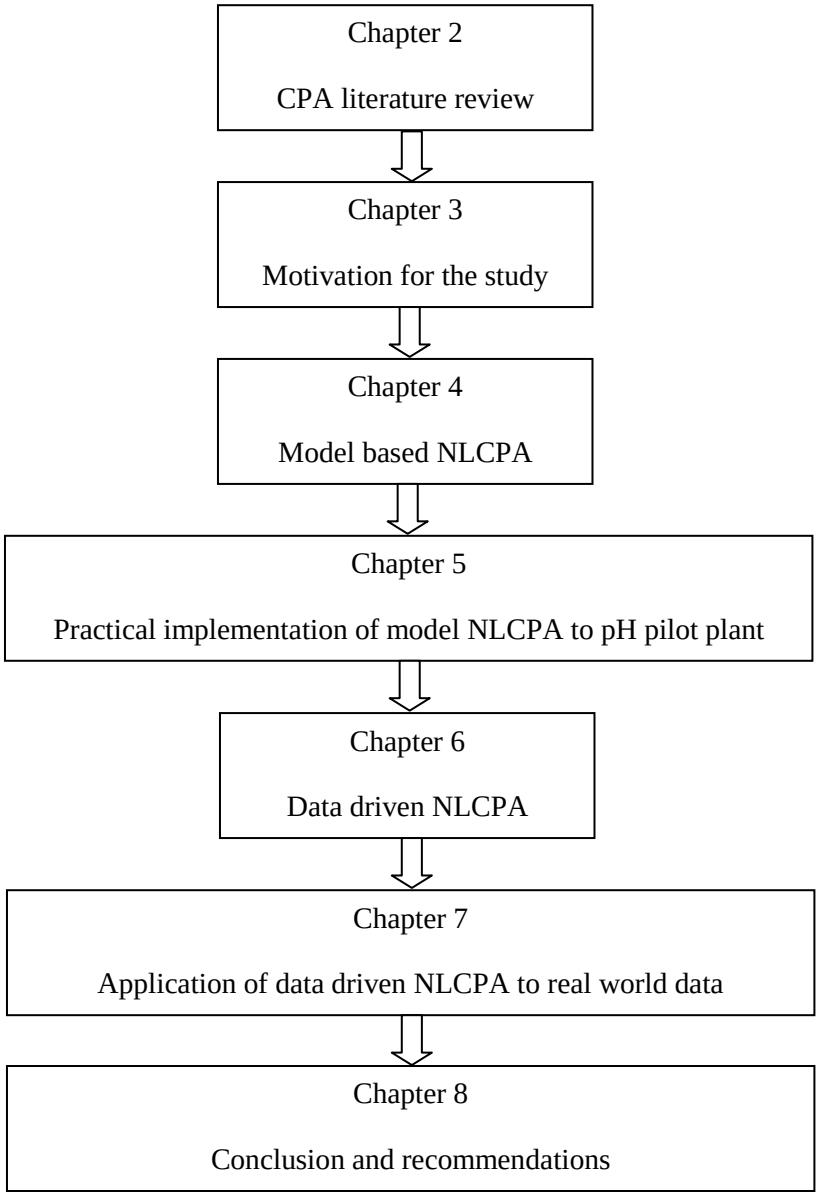

Figure 1.1: Outline of the material contained in the thesis

Chapter 2

Background Information and Literature Review

2.1 INTRODUCTION

The objective of this chapter is to provide an overview on the state of art concerning CPA for nonlinear processes. The emphasis of this work is to develop tools for the assessment of controller performance operating in nonlinear dynamic systems. Therefore in this chapter, important background information regarding existing CPA tools is provided. Relevant terminology and concepts of control performance monitoring and assessment are also reviewed.

For the sake of completeness a review of controller performance benchmarking algorithms based on linear processes is also discussed. Subsequently, the majority of the nonlinear CPA benchmarking tools proposed in the literature have their methodologies rooted in linear systems theory for which there is a rich information base.

2.2 CONTROLLER PERFORMANCE ASSESSMENT FOR LINEAR SYSTEMS

2.2.1 *Assessment based on minimum variance principles*

Originating from the underlying principles of the framework for minimum variance control (MVC) and linear time series analysis (cf. Astrom (1970) and Box *et al.* (1970)), Harris (1989) derived a well-known minimum variance based performance measure popularly referred to as the "Harris index". Harris (1989) showed mathematically that any linear time-invariant feedback control strategy can be compared to that of MVC using a linear time series model and knowledge of the process dead time (Harris *et al.*, 1999).

Consider the schematic of a typical discrete time negative feedback control system shown in Fig. 2.1. The single loop system is represented by a linear time-invariant transfer function process model and additive disturbance driven by white noise. Since the aim is for regulatory control, the setpoint signal is constant.

The linear time invariant process transfer function is given by G_p. G_c and G_d denotes the controller and disturbance transfer functions respectively; $Y(z)$ is the process output represented as:

$$Y(z) = G_p(z^{-1})z^{-b}U(z) + D(z)$$

$$= \frac{\omega(z^{-1})}{\delta(z^{-1})} z^{-b}U(z) + D(z) \qquad (2.1)$$

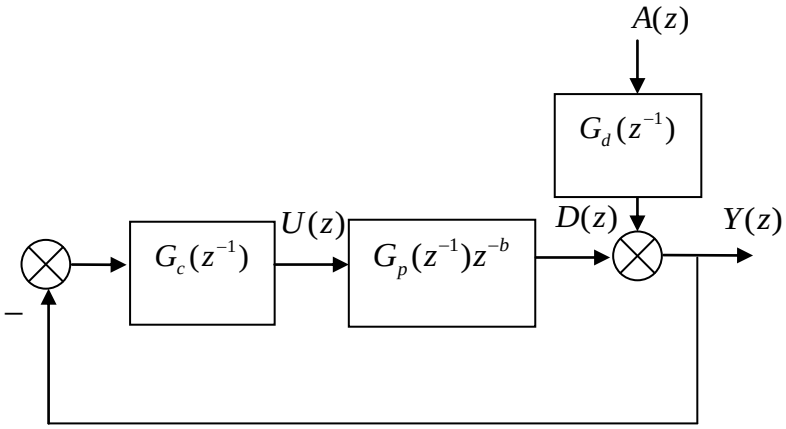

Figure 2.1: Discrete time representation of SISO negative feedback control system

The controller output is given by $U(z)$ and the process delay is represented by integer value of b where $b \geq 1$. $\omega(z^{-1})$ and $\delta(z^{-1})$ are polynomials in the backshift operator z^{-1}. The process disturbance signal is denoted by $D(z)$ and represented by an Autoregressive-Integrated-Moving-Average time series model in the form (Harris and Seppala, 2002):

$$D(z) = \left(\frac{\theta(z^{-1})}{\phi(z^{-1})\Delta^{\deg}} \right) A(z) \tag{2.2}$$

It is assumed that the disturbance signal represents all unmeasured disturbances acting on $Y(z)$ which may be deterministic or stochastic. $\theta(z^{-1})$ and $\emptyset(z^{-1})$ are stable polynomials in the backshift operator, i.e., all poles and zeroes are inside the unit circle. The operator Δ is defined as $\Delta = (1 - z^{-1})$ such that it allows the mean of the disturbance output to vary over time such that it can exhibit non stationary behaviour. The integer deg denotes the degree of differencing (typically $0 \leq deg \leq 2$ for most applications (Harris and Seppala, 2002). $A(z)$ denotes a sequence of independently and identically distributed random variables with zero mean and variance σ_A^2.

The closed loop transfer function for the system in Fig. 2.1 is given by:

$$\frac{Y(z)}{D(z)} = \frac{1}{1+\left(\frac{\omega(z^{-1})z^{-b}}{\delta(z^{-1})}\right)G_c(z^{-1})} \tag{2.3}$$

By substituting Eq.(2.2) into Eq.(2.3) and simplifying, the output can be expressed as:

$$Y(z) = \left[\frac{\alpha(z^{-1})}{\beta(z^{-1})}\right]A(z) = \vartheta(z^{-1})A(z) \tag{2.4}$$

The closed loop impulse response coefficients are given by:

$$\vartheta(z^{-1}) = 1 + \vartheta_1 z^{-1} + \vartheta_1 z^{-2} + \cdots \tag{2.5}$$

Convergence of Eq. (2.5) is only guaranteed if the closed loop system is stable (Joe Qin, 1998; Jelali, 2013). The fundamental characteristic of MVC is that the impulse response coefficients of the closed loop system beyond the process dead time would equal zero, i.e., $\vartheta_j = 0$ for $j = b, b+1, \ldots$,(Astrom, 1970; Harris, 1989; Harris *et al.*, 1999). Therefore the output variance from a closed loop system under MVC would therefore be (Harris *et al.*, 1999):

$$\sigma_Y^2 = \sigma_{MV}^2 = (1 + \vartheta_1^2 + \cdots + \vartheta_{b-1}^2)\sigma_A^2 \tag{2.6}$$

From Eq.(2.6) a simple but effective lower bound comparison can be made by utilizing just routine closed loop process operating data and *a priori* knowledge of the process time delay (Harris, 1989). The Harris index (1989) is used to provide an indication of departure from MVC and is defined as (Harris, 1989):

$$\eta_{MV}(b) = 1 - \left(\frac{1 + \vartheta_1^2 + \cdots + \vartheta_{b-1}^2}{1 + \vartheta_1^2 + \cdots + \vartheta_{b-1}^2 + \vartheta_b^2 + \cdots}\right) = 1 - \left(\frac{\sigma_{MV}^2}{\sigma_Y^2}\right) \tag{2.7}$$

The number of impulse response lags in the denominator ϑ_b^2 is user defined such that it captures the essence of the system dynamic. The controller performance index given in Eq. (2.7) represents the increase in the variance of the closed loop output that arises from not implementing a MVC and is bounded such that $0 \le \eta_{MV}(b) \le 1$.When $\eta_{MV}(b) = 0$, the controller is operating as a MVC; conversely when $\eta_{MV}(b) \to 0$, the greater the variance of the closed loop process output is relative to the best possible performance given by σ_{MV}^2 . For this, the control loop is therefore deemed to be performing poorly.

Typically well-tuned loops operate within the limits $0.3 \le \eta_{MV}(b) \le 0.5$ (Yu *et al.*, 2010b). The primary reasoning for this range is that a Harris index resulting in very low values for $0 \le \eta_{MV}(b) < 0.3$ would indicate the final control element (FCE) is operating excessively and therefore may lead to a reduction in lifespan of the FCE (Eriksson and Isaksson, 1994; Agrawal and Lakshminarayanan, 2003; Jelali, 2013). Furthermore, the index is not suitable for control loops that are oscillatory (Joe Qin, 1998; Harris *et al.*, 1999; Jelali, 2013) and is often viewed as an overly optimistic benchmark (Joe Qin, 1998; Harris and Seppala, 2002; Shahni and Malwatkar, 2011) since a comparison is drawn to the MVC. Furthermore the methodology may not be applicable to processes with short or no-dead time (Horch and Isaksson, 1999).

Moreover, the MVC benchmark may not be achievable in practice depending on the type of control algorithm implemented, process invertibility and other physical constraints of the processes (Huang, 1998). Nevertheless, it does present valuable information about how "*good"* the current controller is compared to that of MVC (Harris, 1989; Jelali, 2006) and its potential for further improvement.

If the Harris benchmark indicates "*good"* controller performance relative to MVC, further redesign and tuning of the control algorithm may neither be necessary or helpful. In this case, if further process variation reduction is sought, implementation of feed forward control or complete re-engineering of the process itself may be necessary (Huang, 1998; Harris *et al.*, 1999). This point is further supported by Ziegler and Nichols (1942):

"*In the application of automatic controllers, it is important to realize that controller and process form a unit; credit or discredit for results obtained are attributed to one as much as the other. A poor controller is often able to perform acceptably on a process, which is easily controlled. The finest controller made, when applied to a miserably designed process, may not deliver the desired performance."*

However, postponing for the moment the deficiencies associated with the benchmark, the Harris Index (1989) has several traits which makes it appealing to CPA:

(i) It is a non-invasive technique as no perturbation or external signal injection is required.

(ii) An Auto Regressive (AR) or Autoregressive Moving Average (ARMA) time series model is fitted to routine closed-loop operating data using model orders of (15 to 25) and (8 to 12) respectively, (Horch, 2000).

(iii) Only the knowledge of process dead time is required (Harris, 1989).

(iv) Currently, it is an efficient computational algorithm and used in many proprietary software CPA packages (Jelali, 2013).

Due to the success of the Harris performance index (1989), several other CPA methodologies have emerged. Whereas Harris (1989) used linear parametric models and knowledge of the process dead time to calculate the performance bound, Lynch and Dumont (1996) proposed the use of Laguerre series model and a time delay estimation techniques.

Horch and Isaksson (1999) suggested modifying Harris's index in which the closed loop poles are placed based on control design guides rather than placing all at the origin (which corresponds to MVC).

Huang (1998) used a pre-whitening filter and subsequent correlation (FCOR –filtering and correlation) analysis between the process output and the estimated stochastic disturbances obtained by the filter. The methodology eliminates the need for determining the impulse response coefficients from its estimated linear closed-loop transfer function (Jelali, 2013). Srinivasan *et al.* (2012) suggested the use of detrended fluctuation analysis (DFA) to extract information relating the autocorrelation properties of the process output. The methodology has the main advantage that no knowledge of the process dead time is required, unlike the Harris Index.

Conventional CPA algorithms are categorized according to *stochastic performance monitoring* (Joe Qin, 1998). This category is based on the assessment of the output variance due to dynamic stochastic disturbances driven by white noise. These methods provide a lower bound performance measure (Desborough and Harris, 1992; Horch and Isaksson, 1999) and do not indicate traditional benchmarks such as rise time, settling time, decay ratio and integral absolute error (IAE) of the closed loop system. These indices fall into the *deterministic performance monitoring* classification (Swanda and Seborg, 1999; Huang and Jeng, 2002). Other important CPA tools include loop oscillation detection tools (Hägglund, 1995) and assessment of controller performance designed for setpoint tracking (Yu *et al.*, 2011b). A brief overview of these methods will be discussed.

2.2.2 *Performance benchmark tools for controllers designed for setpoint tracking*

Currently there has been limited research (Swanda and Seborg, 1999; Thornhill *et al.*, 2003; Yu *et al.*, 2011b) conducted on setpoint tracking CPA for linear processes and to this author's knowledge no research has been presented for nonlinear dynamic and stochastic processes. Earliest work conducted in this area for linear processes is given in Swanda and Seborg (1999) and more recently (Yu *et al.*, 2011b). Both of these methods are based on the internal model control (IMC) principles, where the process models are assumed to be linear time invariant. In their approach, a linear time invariant (LTI) first-order plus dead time (FOPDT) model was used to develop performance benchmarks for proportional-integral (PI) and proportional-integral-derivative (PID) controllers. Swanda and Seborg (1999) proposed the use of dimensionless performance indices derived from a dimensionless settling time given by (Swanda and Seborg, 1999):

$$T_{\dim} = \frac{t_s}{\theta_p} \tag{2.8}$$

where, t_s is the settling time and θ_p is the process dead time. Systems with $T_{\dim} \leq 1$ are considered to exhibit good closed loop behaviour, whilst $T_{\dim} > 1$ indicates an increasingly poor control.

An additional closed loop performance characteristic, namely the integral absolute of the error signal (IAE) is also incorporated into the CPA design methodology given by:

$$IAE_{\dim} = \frac{IAE}{|r(t)|\theta_p} \tag{2.9}$$

where, $r(t)$ is the absolute size of a setpoint step change made by the control practitioner. With regards to Eq.(2.9), $IAE_{\text{dim}} \leq 1$ implies that the system is well controlled. In contrast, $IAE_{\text{dim}} > 1$ suggests that the control loop can be improved. Using equations (2.8 and 2.9), optimal dimensionless settling time (T_{dim}) and IAE (IAE_{dim}) for a FOPDT processes can be represented by (Swanda and Seborg, 1999):

$$T_{\text{dim}} = 2.3\frac{tune_c}{\theta_p} + 1 \tag{2.10}$$

$$IAE_{\text{dim}} = \frac{T_{\text{dim}}}{2.30} + 0.566 \tag{2.11}$$

The selection of a controller tuning parameter ($tune_c$) is dependant on the desired control objective. For FOPDT processes, the minimum recommendation given by $tune_c = \theta_p$, results in a PI controller with optimal IAE value with small or no overshoot for the closed loop control system (Swanda and Seborg, 1999). In addition to the performance benchmarks given by Swanda and Seborg (1999), they also proposed using a corresponding gain margin (A_m) and phase margin ($\emptyset_m$) as functions of the normalized settling time T_{dim}. These relationships are useful since they reveal useful performance robustness characteristics of the control loop under investigation and are described by the following (Swanda and Seborg, 1999):

$$A_m = \frac{\pi}{2}\left(\frac{T_{dim}}{2.30} + 0.565\right) \tag{2.12}$$

$$\emptyset_m = \frac{\pi}{2} - \left(\frac{1}{\frac{T_{dim}}{2.3} + 0.565}\right) \tag{2.13}$$

Using equations (2.10 – 2.13), it is possible to determine whether a control loop is performing under categories of "*high performance*", "*excessively sluggish*" or "*poorly tuned*"

(Swanda and Seborg, 1999). Table 2.1a shows useful performance classes as proposed by Swanda and Seborg (1999) for FOPDT processes. Table 2.1b gives a gain and phase margin limits for systems that are giving high performance. The methodology described above is essentially lower bounds (in terms of closed loop transient specifications) for controller performance based on the principles of IMC. Since the method is based on a linear time invariant (LTI) FOPDT model it may not be applicable to dynamic nonlinear stochastic processes which are often encountered in most industrial plants. In such cases, an alternative methodology is proposed in this research which will be discussed in the subsequent chapters.

Class	T_{dim}	IAE_{dim}	Overshoot
High performance	≤ 4.6	≤ 2.8	Not specified
Excessively sluggish	> 13.3	> 6.3	$\leq 10\%$
Poorly tuned	> 13.3	> 6.3	$> 10\%$

Table 2.1a: Proposed performance classes for PI control on FOPDT processes. (Swanda and Seborg ,1999)

A_m		$\emptyset_m$	
min	max	min	max
2.0	4.4	44	74

Table 2.1b: Proposed range for gain and phase margin for PI controllers performing under high class on FOPDT processes. (Swanda and Seborg ,1999)

2.2.3 *Restricted structure performance assessment*

Eriksson and Isaksson (1994) introduced a performance assessment framework that makes a comparison to the well-known PID controller. This prevents misinterpretation of controller

performance since the lower bound benchmark is based on achievable control actions of a typical PID controller, and not to the erratic control actions of a higher order minimum variance controller. If the primary goal of a controller is for disturbance rejection, then the variance of the process output must be considered (Desborough and Harris, 1992; Harris *et al.*, 1999). Large excursion and drift of the process variable from setpoint would obviously negatively affect product quality. Therefore, emphasis on the type of controller algorithm used on the process must be taken into account when attempting to evaluate its performance. For example, it is reasonable to compare the current performance of a PID control algorithm to its theoretical best. Furthermore, the CPA framework (Eriksson and Isaksson, 1994) can be extended to other types of controller, for example model predictive controller (MPC). Other works relating to achievable performance assessment by researchers who have subscribed to this view can be found in (Jain and Lakshminarayanan (2004); Ko and Edgar (2004); Sendjaja and Kariwala (2009)). An obvious drawback to this approach is the requirement of a process model of the process and determining the solution to the constrained optimization problem for solving optimal controller parameters. However, it does provide more realistic benchmark for which a common controller such as the PID controller can be compared against. Fig. 2.2 illustrates expected degrees of process output variance in accordance to the type of controller used. *Perfect* control will yield little or no loop output variance while a controller in open loop would give large output variance since no corrective action is taken when the loop is subjected to load changes, measurement noise and/or process nonlinearities.

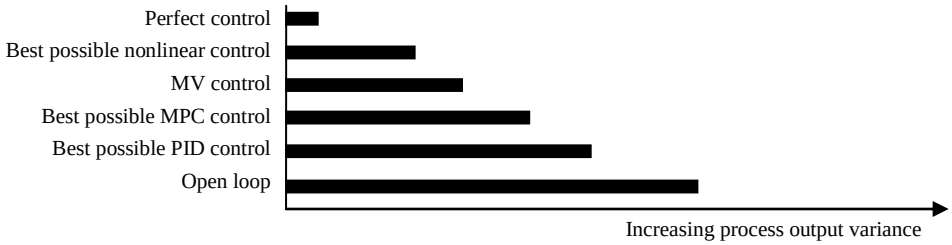

Figure 2.2: Ranking of control performance standards in terms of achievable loop output variance

A convenient feature of PID achievable performance assessment is that the optimal tuning (based on user requirements such as no overshoot or minimal absolute of the error) parameters are by-products of an assessment algorithm and may be applied to the actual controller operating in the loop. This approach requires the open loop process transfer function (G_p) and the disturbance model (G_d) in order to compute the optimal controller parameters. With reference to Fig. 2.1 under closed loop conditions, the relationship between the controlled variable and the external signals (setpoint and disturbance) is expressed as:

$$y(t) = \frac{G_c(t)G_p(t)}{1+G_c(t)G_p(t)} r(t) + \frac{G_d(t)}{1+G_c(t)G_p(t)} a(t) \tag{2.14}$$

Achievable PID performance can now be obtained by solving the following optimisation problem:

$$K_{PID} = \min_{K_{PID}} \sigma_Y^2(G_p, G_d) \tag{2.15}$$

In order to obtain optimal PID settings (K_{PID}) that give achievable minimum output variance (σ_Y^2), Ko and Edgar (2004) suggested Newton's iterative method to solve Eq. (2.15). Since the Newton iterative search method is gradient based, it is vulnerable to local minima (Veronesi and Visioli, 2010b; Pillay and Govender, 2013). Hence, other researchers have proposed alternative methods that guarantee a global optimal solution to the problem (Veronesi and Visioli, 2010a; Shahni and Malwatkar, 2011; Pillay and Govender, 2013) without dependence on gradient information of the objective function. Performance evaluation of the PID controller can now be assessed as (Ko and Edgar, 2004):

$$\eta_{PID} = \frac{\sigma_{PID}^2}{\sigma_Y^2} \tag{2.16}$$

With regards to Eq. (2.16) the performance index (η_{PID}) is defined by the ratio of output variance of the optimally tuned system (σ_{PID}^2) and the output variance of the actual system (σ_Y^2). The performance benchmark lies within the range [0, 1], where zero corresponds to very poor control and one to achievable optimal PID control. If $\eta_{PID} = 1$ is achieved then no further improvements on the controller tuning can be made. In the subsequent chapters an efficient hybrid optimisation routine is proposed by combining Nelder-Mead (NM) simplex with the Particle Swarm Optimization (PSO) algorithm and will be used to determine optimal controller parameters for nonlinear process control loops. In the following section, a brief overview of important oscillation detection methods will be discussed.

2.2.4 *Control loop oscillation detection tools*

A control loop may show signs of oscillatory behaviour for various reasons which are obviously undesirable from a control performance, profitability and/or safety point of view. Thus it is reasonable to detect an oscillatory control loop and identify its root cause. This is not a trivial task due to the sheer number of control loops and sources of the oscillation (Thornhill and Horch, 2006). The most important sources of oscillations on control loops are from aggressive controller tuning, nonlinear phenomenon emanating from the control valve stiction (Choudhury *et al.*, 2004) or the process, defective sensors and loop interactions (Jelali, 2013). The task of oscillation detection is therefore primarily focused on detection methods which can be easily automated for either on-line or stored data. As mentioned earlier, the Harris index yields misleading results when applied to oscillatory data and is therefore not recommended for use on such time series data (Harris *et al.*, 1999). This is mainly due to the underlying linear concepts of minimum variance upon which the Harris index is premised. Thus it is advantageous to automatically detect oscillatory control loops before applying the Harris index (Desborough and Miller, 2002).

There is a number of oscillation detection methods published in the literature which forms the basis for many industrial control performance assessment applications and comprises of:

(i) Time domain criteria such as the integral absolute of the error (IAE) (Hägglund, 1995; Thornhill and Horch, 2006).

(ii) Methodologies based on auto covariance function. (Miao and Seborg, 1999; He *et al.*, 2007).

(iii) Classical approach of detecting spectral peaks of the data's power spectrum. (Thornhill *et al.*, 2003; Thornhill and Horch, 2006).

A brief overview of some of the methods mentioned above will now be discussed. Hägglund's (2002b) control performance monitor is based on the simple idea that a *well-functioning* control loop should fluctuate around the setpoint and that if a large duration is detected on one side of the setpoint it is an indication of a poor performing control loop. The IAE between each period that the control signal crosses zero is given as:

$$IAE = \int_{t_{i-1}}^{t_i} |e(t)| dt \tag{2.17}$$

Where, $\left(|e(t)| = |r(t) - y(t)|\right)$ and the times of the two consecutive zero crossings are denoted by t_i and t_{i-1}. A threshold value (IAE_{lim}) is selected by the control practitioner such that when Eq.2.17 exceeds the threshold an alarm is activated. The method is simple and suitable for online implemented on a DCS. However, oscillations with relatively small amplitude and period may go undetected. Alternatively, an approach using autocorrelation function (ACF) of a stationary signal can be used in this case. For stable systems the ACF is bound within -1 and +1, and generally decays with increasing lags. For oscillating systems however, the autocorrelation will also be oscillatory (Karra and Karim, 2009; Sivalingam and Hovd, 2011). Theoretically the autocorrelation function can be used to detect oscillations in

the data set. This scheme will be exploited and incorporated into a new automatic controller performance evaluation tool for systems operating under nonlinear plant dynamics.

Finally, power spectral analysis of the data set will also give information about whether the system has periodic oscillation. The principle idea is that if the signal exhibits a purely sinusoidal oscillation at a particular frequency, the power spectrum will have a peak at that frequency. The ratio between the position of the peak and its bandwidth gives a measure of the regularity of the oscillation, but the presence of noise in the same frequency band may cause difficulties with the frequency bandwidth determination (Thornhill and Horch, 2006).

A power spectral density plot of the data may yield several peaks; where a peak is defined as a point that is more than three times greater than the average of its surrounding samples (Jelali, 2013). Fig.2.3 illustrates the response following a step change of a simulated pH control loop and its corresponding power spectral density. The data was sampled at one second. The largest peak occurs at a frequency of 10.95 Hz indicating that the system is oscillating at very low frequency. This oscillation is mainly due to the nonlinear characteristic of the pH reaction at the steep point of its titration curve which has very large gain and consequently the linear controller is ineffective. The main drawback of this approach is that the power spectrum may be corrupted by noise and nonlinear effects which cause the power spectrum to be contaminated with several spikes which is then unsuitable for frequency bandwidth determination.

The detection of process loop oscillation is simple when the signal is purely sinusoidal with a single dominant frequency. In a practical process control loops however, the signal may be contaminated by sensor noise, valve nonlinearities and/or multiple oscillations from interacting control loops (Hägglund, 2002b). In such cases, it becomes difficult to automatically detect control loop oscillation, hence the detection tool must be robust enough

to counter these effects and correctly interpret an oscillatory signal. Therefore it becomes important to consider loop nonlinearities and oscillations within the context of control loop monitoring as these destabilizing effects will inherently lead to a biased or incorrect performance assessment.

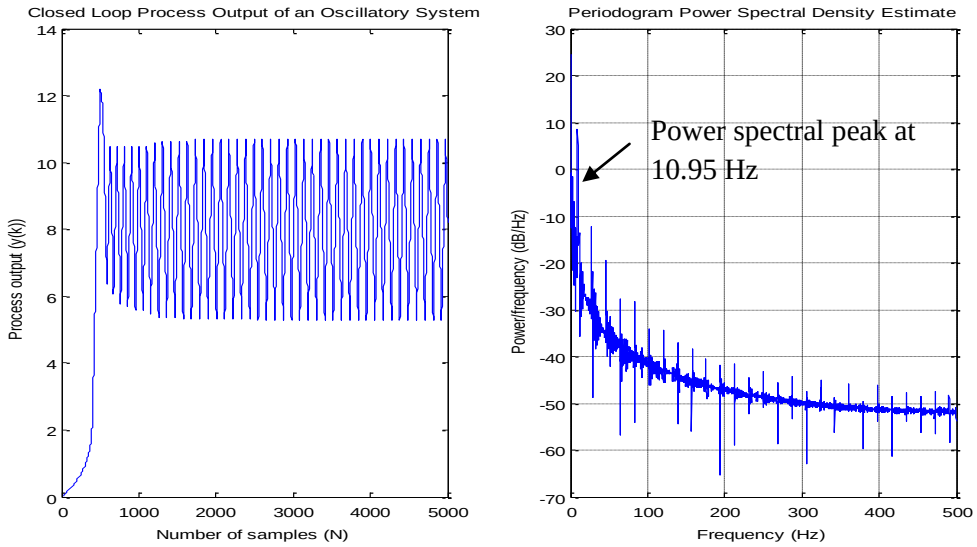

Figure 2.3: Spectral analysis of process output *y(t)* from a simulated pH control loop

2.3 FEEDBACK CONTROLLER PERFORMANCE ASSESSMENT FOR NONLINEAR SYSTEMS

2.3.1 *Detection of control loop nonlinearities*

Most of the control performance indices discussed thus far presumes that the process control loop is linear. However all processes are nonlinear to *some degree* and the presence of certain types of nonlinearities (for instance, control valve stiction, hysteresis or dead band) may cause severe performance degradation and even variability in product quality. The importance of this statement in this thesis would be to account for these nonlinearities in the design of a suitable CPA tool. Therefore, an important step in the assessment procedure should be to evaluate the degree of nonlinearities present in the control loop. Some of the earliest works in this field can be traced back to Rao and Gabr (1980) and Hinich (1982). These methods can be used to detect the presence of certain types of nonlinearities present in a time series. Such tests determines whether a time series could plausibly be the output of a linear system driven by Gaussian white noise disturbance, or whether its properties can only be explained as the output of a nonlinearity (Jelali, 2006).

A methodology for detecting valve stiction using higher order statistics (HOS) was proposed by (Shoukat Choudhury *et al.*, 2004). Whilst low order statistics (for example, mean, standard deviation and variance) are popular signal processing tools and have been extensively used in the analysis of process data, they are only sufficient when used in describing linear processes. In practice however, there are many processes that deviate from linearity and exhibit nonlinear behaviour. In such cases HOS are useful in that they can be used to extract information due to deviations from Gaussianity, to recover true phase

character of the signal and for the detection and quantification of inherent nonlinearity (Nikias and Mendel, 1993).

More recently, Liu *et al.* (2012) presented a nonlinearity measure based on the minimum variance lower bound to quantify the degree of nonlinearity. The measure which is data driven belongs to a class of Hammerstein-Wiener modelling structure. However, the algorithms mentioned above are designed to detect the presence of nonlinearity in a time series and do not provide an indicative measure of controller performance. For this case, Harris and Yu (2007) proposed the use of a minimum variance benchmark for certain classes of nonlinear systems which is discussed in the next section. In addition, several other important CPA methodologies which account for loop nonlinearities are reviewed.

2.3.2 *Extension of minimum variance benchmark to nonlinear systems*

In section 2.2.1, a theoretical discussion of minimum variance control performance benchmark was given. A critical assumption is that the process under closed loop control is linear and driven by stochastic and deterministic disturbances. This description is suitable only if the process is adequately described by the superposition of a linearized transfer function model plus additive stochastic or deterministic disturbances (cf. Fig.2.1). Unfortunately this assumption does not carry through for nonlinear systems due to the following challenges (Harris and Yu, 2007):

(i) Nonlinear processes can exhibit complex behaviours which include chaotic responses to simple inputs of asymmetric responses to symmetric inputs with its stability being input dependant.

(ii) A linear time invariant system can be completely characterised by its impulse response. This is not the case for all nonlinear systems.

(iii) For systems which admit a linear representation there are well established methods for obtaining models. For nonlinear systems there are challenges in model determination and many parameters to estimate.

Despite the difficulties mentioned above, the development of nonlinear minimum variance control laws has been proposed by a several authors (cf. Anbumani *et al.* ,1981; Grimble, 1988; Bittanti and Piroddi ,1997; Zhu *et al.* ,1999; Grimble ,2005). Early work conducted by Anbumani *et al.* (1981) showed that self-tuning MVC of nonlinear systems is possible. In their work, it was presented that nonlinear MVC gave superior performance when compared to its linear counterpart for systems adequately described by the Hammerstein model (Anbumani *et al.* ,1981).

Further research was conducted by Grimble (1988) whereby an optimal weighted minimum variance controller was designed for nonlinear systems also in the form of the Hammerstein model representation. This was later followed up by Bittanti and Piroddi (1997) who made use of Artificial Neural Networks (ANNs) as the basis of their design approach towards a generalized minimum variance neural control algorithm. The challenges experienced with using prior knowledge of the nonlinear structures were highlighted and used as motivating factors for the application of ANNs in black box system identification. ANNs offer the advantage of contributing an explicit control law based on inversion of the black box model with suitable training data set. This view of enhancing the nonlinear minimum variance control with ANNs was further supported by Zhu *et al.* (1999). They proposed using a linear model combined with ANNs to design a generalised minimum variance self-tuning controller for nonlinear discrete time systems.

Finally, a relatively recent approach given by Grimble (2005) was the use of feedback or feedforward tracking control based on internal model of the nonlinear process. The solution

of the nonlinear feedback/feedforward tracking control law is derived from nonlinear operator representation of the nonlinear function of the plant.

The major challenge associated with determining a suitable controller performance estimate for the above nonlinear control designs lies in the existence of the feedback invariance. This is the dynamic part of the closed loop system and is not affected by the feedback control law (Harris and Yu, 2007). For the general linear process, the feedback invariance can be obtained from standard time series estimation. Subsequently, this is used in the determination of controller performance index based on minimum variance principles (Harris, 1989). Underlying theoretical aspects of this approach as shown by Harris (1989) is exclusively reliant on the use of the feedback invariance of the process variable under closed loop conditions. This assumption can be used to compare the current controller to a minimum variance controller. However for the nonlinear process described by Harris and Yu (2007), it was shown that the feedback invariance does not exist and therefore the minimum variance assessment procedure is not applicable. The model considered in their work was of the form (Harris and Yu, 2007):

$$y(t) = f\left[\mathrm{u(y-b)}, \mathrm{z(t)}\right] + d(t) \tag{2.18}$$

where, f represents a nonlinear mapping function represented by nonlinear polynomial approximators. $z(t)$ denotes the auxiliary variables that are known and accounts for nonlinear dynamic terms that are functions of the previous values of the process output. All other terms have the same meanings as given in Eq. (2.1). The minimum variance control for the above process model can be derived from:

$$y(t+b) = f\left[\mathrm{u(t)}, z(\mathrm{t+b})\right] + d(t+b) + e(t+b) \tag{2.19}$$

The term $e(t+b)$ is the feedback invariance quantity which is not influenced by the feedback controller. It is important to note that the above approach is only applicable when the feedback invariance *does* exist, in which case the same methodology given in section 2.2.1 will apply. Direct estimation of the controller performance benchmark can also be calculated using the lagged regression approach (Harris and Yu, 2007):

$$\tilde{Y} = F\Theta + \Xi \tag{2.20}$$

with,

$$\tilde{Y} = \begin{bmatrix} \tilde{y}_1 \\ \vdots \\ \tilde{y}_n \end{bmatrix}$$

$$\Xi = \begin{bmatrix} e_1 \\ \vdots \\ e_n \end{bmatrix} \qquad F = \begin{bmatrix} 1 & \tilde{y}_1 & \cdots & \tilde{y}_{1-m} & \cdots & \tilde{y}_{1-M} \\ \vdots & \vdots & \ddots & & \vdots & \\ 1 & \tilde{y}_{n-1} & \cdots & \tilde{y}_{n-m} & \cdots & \tilde{y}_{n-M} \end{bmatrix}$$

$$\Theta = \begin{bmatrix} h_0' & h_1' & \cdots & h_{m\ldots M}' \end{bmatrix}$$

F is the regression variables, Θ is the parameter vector and Ξ is the vector of the *b-step* ahead prediction errors. The number of regression variables is given by m with n number of samples. Harris and Yu (2007) demonstrated their methodology using finite discrete time Volterra series approximation, for which h represents the model coefficients of the series. A parameter vector that minimizes $\left\|\tilde{Y} - F\Theta\right\|^2$ is given by (Harris and Yu, 2007):

$$\hat{\Theta} = (F^T F)^{-1} F^T \tilde{Y} \tag{2.21}$$

in which case $\|.\|$ is the Euclidean norm. It should be noted that the number of possible terms in Eq.(2.20) can be extremely large due to larger model orders and higher polynomial degrees, therefore efficient optimisation algorithms must be used to determine the parameters for the corresponding model. Harris and Yu (2007) prescribe the use of Fast Orthogonal Search or Genetic Programming techniques. Once suitable parameters have been determined, the residual error of the model can be determined (Harris and Yu, 2007):

$$\hat{\Xi} = \tilde{Y} - F\hat{\Theta} \tag{2.22}$$

Minimum variance lower bound can be found using Eq.(2.22) in conjunction with process dead time knowledge. A critical assumption is that the disturbance is represented by a linear time invariant model of specific structure that is summed at the process output. Furthermore, the method is only applicable to processes that can be suitably modelled using Volterra series models. A major drawback of the approach is the nonlinear Volterra modelling structure used in the CPA algorithm requires a large number of parameters to be estimated which may be computationally demanding (Yu *et al.*, 2012).

2.3.3 *Generalised minimum variance index for nonlinear processes.*

Maboodi *et al.* (2015) developed an extension to the nonlinear minimum variance lower bound (NMVLB) discussed in the previous section within the context of generalised minimum variance by taking the control effort into consideration (cf. Fig. 2.4). It well known that the linear MV controller is limited to practical applications due to excessive movement required by the final control element. To counter this effect, generalised minimum variance control (GMV) has been developed and is an active area of research (Zhu *et al.*, 1999;

Majecki and Grimble, 2004a; Grimble, 2005). This framework is carried over to nonlinear systems by Maboodi *et al.* (2015) and is used in the evaluation of controller performance. In their work, a generalised nonlinear generalized minimum variance controller (NGMV) is introduced based on a second order Volterra series model in the polynomial form and is shown to be more effective than the NMVLB presented by Harris and Yu (2007). Furthermore, the disturbance acting on the system is assumed to be linear with a specific form. The central design is to obtain a NGMV control algorithm that minimizes the following cost function (Maboodi *et al.*, 2015):

$$J = E\left\{\phi(t+b)^2\right\} \tag{2.23}$$

where $\phi(t+b)$ (cf. Fig. 2.4) is the generalised output signal and,

$$\phi(t+b) = Py(t+b) + Qu(t) - Wr(t) \tag{2.24}$$

With regards to Eq. (2.24), P, Q and W are appropriate weighting transfer functions and act as the NGMV design parameters. The generalised output can now be expressed in Volterra series polynomial form (Maboodi *et al.*, 2015):

$$\begin{aligned}\phi(t) = h_0 + \sum_{i=1}^{n_y} h_i^y y(t-b-i+1) + \sum_{i=1}^{n_u} h_i^u u(t-b-i+1) + \sum_{i=1}^{n_{yy}} h_i^{yy} y^2(t-b-i+1) + \\ \sum_{i=1}^{n_{uu}} h_i^{uu} u^2(t-b-i+1) + \sum_{i=1}^{n_{yu}} h_i^{yu} y(t-b-i+1)u(t-b-i+1) + \xi(t)\end{aligned} \tag{2.25}$$

where h is the corresponding Volterra model coefficients and $\xi(t)$ represents Gaussian noise disturbance.

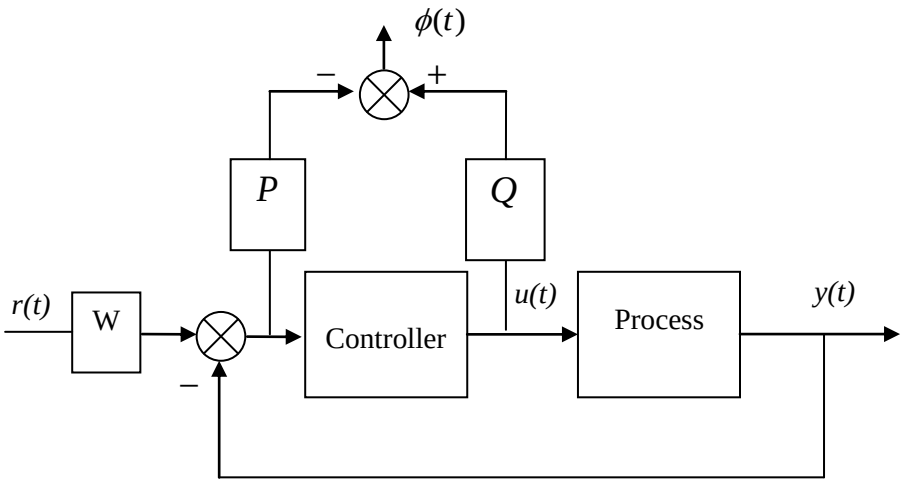

Figure 2.4: NGMV scheme for a negative feedback control system.

A vector form of Eq.(2.25) can be conveniently written as:

$$\Phi = X\Theta + \Xi \tag{2.26}$$

with

$$\Phi = \left[\phi(n) \quad \phi(n-1) \quad \ldots \quad \phi(\mathrm{K}+b)\right]^T$$

where *n* is the number of data samples and *K* is the number of parameters.

$$K = n_y + n_u + n_{yy} + n_{uu} + n_{yu} \tag{2.27}$$

With regards to Eq. (2.26), X , Θ and Ξ represents the regression variables, parameter vector and prediction error vector matrices respectively. Now the parameter matrix vector $\left(\Theta\right)$ can be estimated as (Maboodi *et al.*, 2015):

$$\hat{\Theta} = (X^T X)^{-1} X^T \Phi \tag{2.28}$$

The minimum variance of the generalised output is given in terms of the residual error variance:

$$\hat{\sigma}^2_{NGMV} = mse(\Phi - X\hat{\Theta}) \tag{2.29}$$

The nonlinear controller performance index can now be defined as (Maboodi *et al.*, 2015):

$$\eta_{NGMV} = \frac{\hat{\sigma}^2_{NGMV}}{\sigma^2_{\phi}} \tag{2.30}$$

where σ^2_{ϕ} is the actual generalised output variance and $\hat{\sigma}^2_{NGMV}$ is the minimum generalised output variance that can be theoretically obtained using a NGMV controller. The index is bounded within the interval [0,1], where values close to zero indicate poor control performance. Conversely a value of one indicates good control in relation to the theoretically achievable generalized output variance control.

2.3.4 *Analysis of variance based controller performance assessment of nonlinear processes*

The MV based performance benchmarks described in sections 2.3.2 and 2.3.3 exhibit significant theoretical difficulties when applied to general nonlinearities as described by Nonlinear Auto-Regressive-Moving-Average with Exogenous input (NARMAX) models (Yu *et al.*, 2012). Furthermore, the methodology relies heavily on the existence of the feedback invariance term which may be very difficult to estimate from nonlinear process data. Yu *et al.* (2009) proposed a more fundamental statistical approach using analysis of variance

(ANOVA) to decompose the disturbances acting on the nonlinear process. The main idea is to separate the disturbances entering the system at current time t into past group of terms and

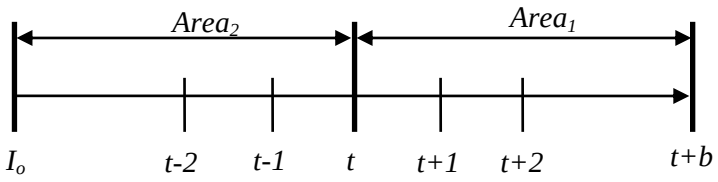

Figure 2.5: Division of disturbance sequence into groups A_1 and A_2.

a second group into future set of terms as shown in Fig. 2.5. The sensitivity of the process output after the dead time $y(t+b)$ relies on variations of the disturbance vectors from series *Area*$_1$ and *Area*$_2$ (refer to Fig.2.5). Therefore the variance of $y(t+b)$ can be decomposed into two terms (Yu *et al.*, 2009):

$$V[y(t+b)] = E_{I_0}[V_A[y(t+b)\,|\,I_o]] + V_{I_0}[E_A[y(t+b)\,|\,I_o]] \tag{2.31}$$

where A=[Area$_1$,Area$_2$] represents all the disturbances entering the system from time 0 to time *t*. $E_{Io}[.]$ denotes the expectation of [.] with respect to initial condition I_o. $V_{Io}[.]$ denotes the variance of [.] with respect to initial condition. The first term on the right hand side of Eq. (2.31) is the fractional contribution to the variance of *y* from the disturbance signal and the interaction between the disturbance and the initial condition. The second term is the fractional contribution to the output solely due to the uncertainties in the initial condition (Yu *et al.*, 2009). Using the ANOVA approach, it is possible to determine the conditional variance given the initial conditions as (Yu, 2007):

$$\begin{aligned} V_A\,|\,I_o &= V_A[y(t+b)\,|\,I_o] \\ &= V_1\,|\,I_o + V_2\,|\,I_0 + V_{12}\,|\,I_o \end{aligned} \tag{2.32}$$

where V_1, V_2 and V_{12} are represented by:

$$\begin{aligned} V_1 \mid I_o &= V_{A_1}\left[E_{A_2}[y_{k+b} \mid (A_1, I_o)]\right] \\ V_2 \mid I_o &= V_{A_2}\left[E_{A_1}[y_{k+b} \mid (A_2, I_o)]\right] \\ V_{12} \mid I_o &= V_A\left[E_A[y_{k+b} \mid (A, I_o)]\right] - V_1 \mid I_o - V_2 \mid I_o \\ &= V_A \mid I_o - V_1 \mid I_o - V_2 \mid I_o \end{aligned} \tag{2.33}$$

Given the relationship of process variance to past and future disturbance terms, a suitable performance index can be established (Yu, 2007):

$$\eta_{ANOVA} = \frac{E_{I_o}[V_1 \mid I_o]}{\sigma^2(t+b)} \tag{2.34}$$

The performance index given in Eq. (2.34) shares some properties with the Harris index in that it is strictly bound between [0,1]. If η_{ANOVA} approaches one, then this indicates the variance of the output is contributed mainly by A_1, which suffice to say that the controller is behaving as a MV controller. It is interesting to note that the methodology is not applicable to *non-ergodic* systems where the second term in Eq.(2.31) dominates and is highly dependent on user selected initial conditions. For a practical computation of the performance index given by Eq. (2.34), a closed loop NARMAX model and Monte-Carlo optimization strategy is required and can be computationally demanding.

2.3.5 *Minimum variance lower bound estimation in the presence of valve stiction*

It is well known that valve stiction is a common occurrence that results in poor control loop performance (Choudhury *et al.*, 2005). In such cases, if severe valve stiction is confirmed from limit cycle oscillation then the palpable approach would be to remove the control valve from operation and replaced. Following the removal of the undesired FCE nonlinearity from

the control loop, one can then perform suitable CPA tests for the sake of determining how well the controller is functioning under *improved* operating conditions. However if a control valve is showing moderate signs of stiction then the nonlinearity present in the control loop would be more difficult to identify. In such cases, the accuracy of the CPA tool would be compromised as shown by Yu *et al.* (2010b). Since stiction is non-differentiable, strategies involving linear polynomial ARX models are not suitable. A bias in the performance evaluation is usually incurred (Yu *et al.*, 2010b) which may lead to false information regarding control loop performance for which a judicious approach is sought. For the sake of controller performance analysis, Yu *et al.* (2010b) proposed spline smoothing to lessen the effects of the valve nonlinearity. Alternatively, one can also bypass the effects of valve stiction nonlinearity by estimating the lower performance bound at steady state conditions when the control valve is presumably stuck (Yu *et al.*, 2010b). The key problem associated with this scheme is determining when the steady state periods exactly occur from the closed loop operating trends. Thus the approach may only be applicable for circumstances whereby the control valve is stuck for relatively long periods of time.

2.4 SUMMARY AND CONCLUSIONS

This chapter provided an overview of established CPA techniques aimed at linear and nonlinear processes. While a great deal of attention has been given to systems where the process is assumed to have linear dynamics, it has been discussed that traditional linear CPA methodologies provide biased results when nonlinearities are prevalent. Generally, the Harris index (1989) will present an over estimation (Yu *et al.*, 2009; Yu *et al.*, 2012) when applied to most nonlinear systems. However it is simple to implement by control personnel without any high computational demand on hardware resources. It is recommended that before

application of the index on recorded plant data, a thorough investigation should be done to check the extent of the nonlinearity using appropriate algorithms (cf. (Hinich (1982); Choudhury *et al.* (2004)). If the nonlinearity is significant, then this would compromise the accuracy of the index.

An extension to the Harris index (1989) for certain nonlinear systems depends strictly on the existence of the feedback invariant term. The feedback invariant term may not exist for general dynamic systems represented by NARMAX models. Therefore the methodology is restricted to nonlinear systems represented by Volterra series models.

A natural extension to the nonlinear CPA (NLCPA) index to account for the large variations in the control signal was described by the NGMV approach. However the technique is also reliant on feedback invariance which is difficult to obtain on general nonlinear processes. ANOVA of process data to decompose variance of disturbances that contribute primarily to the process variance is an alternate strategy, but the technique is severely hampered by large computational demands.

Other NLCPA strategies have been proposed to account for mild valve stiction which are also based on MV principles. Thus far no research has been conducted on restricted structure CPA for general nonlinear systems which exhibit the NARMAX structure. In the subsequent chapter, a new NLCPA methodology is proposed to indicate excursion from good control where the performance bound of a gain scheduled PID structure is concerned.

Chapter 3

Motivation for the Study of Nonlinear Controller Performance Assessment

3.1 INTRODUCTION

In this chapter, a novel classification of NLCPA methods is proposed and used to support the study. Furthermore, since PID controllers are the central theme of this work, a brief overview of the algorithm is given. Practical issues surrounding its implementation and general terminologies are also discussed. We limit our attention to negative feedback control which is a powerful and flexible control design strategy often found operating in the majority of industrial process control loops. Further study of NLCPA on other control schemes is an interesting topic and may be considered as an extension to this work.

3.2 TAXONOMY OF NLCPA METHODS

3.2.1 Framework for classification of nonlinear controller performance assessment tools

In the previous chapter (Section 2.3), a review of NLCPA techniques was discussed. Based on these existing methodologies a new categorization of NLCPA is proposed. Consider the classification of existing CPA methodologies (linear and nonlinear) shown in Fig. 3.1.

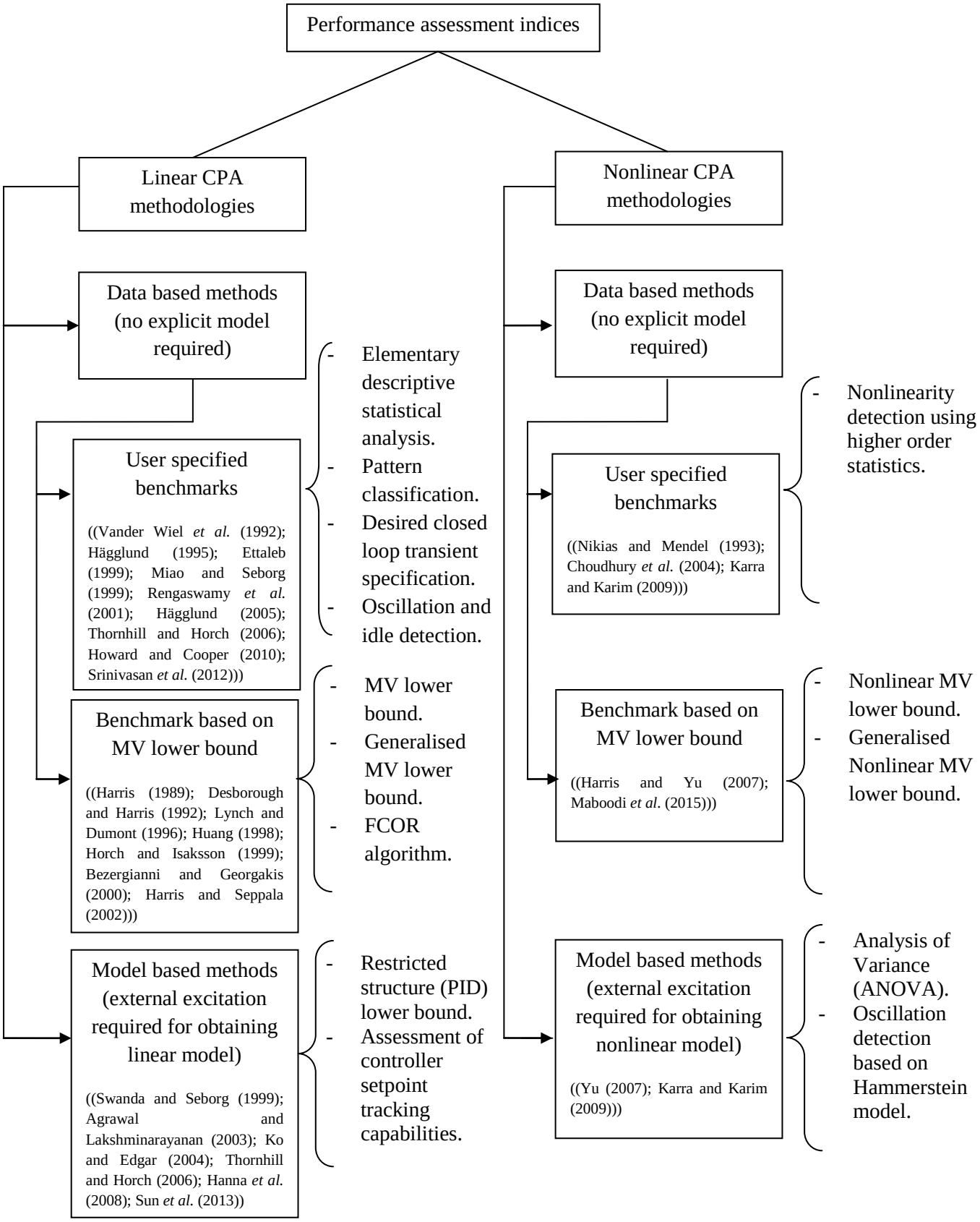

Figure 3.1: Classification of NLCPA methodologies in comparison to linear CPA methods

It is worth mentioning that the proposed classification shown in Fig. 3.1 relates to univariate CPA with the controller operating under negative feedback strategy. Other CPA techniques that deal with different control schemes, namely multivariate, feedforward and ratio control are not considered in this study. Further studies are required to extend CPA for the alternative control strategies mentioned when operating in the context of a nonlinear process control loop. These alternate control schemes have been studied by Huang (1998), Grimble (2005), and Ko and Edgar (2001) in the framework of CPA for linear systems. Such systems are important as they are frequently encountered in industry to offer tighter and improved control when negative feedback does not suffice. When control systems fail to meet their design objectives then the underlying cause for poor closed loop performance must be ascertained. These causes may include the following effects (Harris *et al.*, 1999; Choudhury *et al.*, 2004):

(i) Presence of external/internal disturbance, interaction between other loops, limits imposed on the process variable, large dead time and/or intrinsic dynamic behaviour of the process such as non-invertible zeros.

(ii) Wear or failure of control loop hardware such as final control element hysteresis, stiction and excessive sensor degradation.

(iii) Inappropriate controller tuning settings due to changes in the process dynamics or the nature of disturbances.

Many industrial PID controller loops are commissioned with default settings and not optimised due to time and human resource constraints (Desborough and Miller, 2002; Jelali, 2006). These loops are often left unattended with suboptimal controller settings. For nonlinear systems, the controller gains are frequently detuned to obtain a stable system at the expense of a sluggish closed loop response (Grimble, 2005). Moreover, when system dynamics vary then current controller settings are inappropriate and may cause the loop performance to deteriorate even to the point of instability (Leith and Leithead, 2000). In such

cases, the symptoms of poor loop performance must first be detected and the cause/s for the poor performance can then be effectively diagnosed. Therefore it is important to have a CPA tool that accounts for nonlinearities present in the control loop rather than avoiding its destabilising effects altogether.

3.2.2 Description of the novel NLCPA classification framework

The body of CPA tools is ever increasing with new indices being developed to ensure accurate and reasonable lower performance bounds for different classes of control schemes. Research of linear CPA methodologies by far outweighs the efforts made in establishing newer NLCPA techniques. The main reason for this may be attributed to theoretical difficulties encountered when analysing dynamic nonlinear systems, especially for the MV lower bound which may not even exist for the general nonlinear system (Yu *et al.*, 2012).

However, tools such as Higher Order Statistics (HOS), Artificial Neural Networks (ANNs) and data mining methods can be utilized to aid in the performance evaluation of nonlinear systems. This view is supported by Jelali (2013) and Harris *et al.* (1999). In this work, we use ANNs to model nonlinear plant behaviour for the purpose of establishing a suitable NLCPA. In addition, Support Vector Machines (SVMs) are an invaluable classification and pattern recognition tool when model based methods are not suitable. The study of utilizing these algorithms is further supported by the lack of well-established CPA procedures when dealing with general nonlinear dynamical systems.

With regards to Fig.3.1, a comparison between linear and nonlinear CPA methodologies can be drawn. We primarily focus on two distinct CPA classes; the first class given as *data based methods* and the second class as *model based methods*. For data based methods, the

process model is not a requirement and only data that has captured essential process dynamics is used in the assessment procedure. Only routine operating data records of the process variable (PV) or controlled variable (CV) is required to compute the performance measure. Simple statistical analysis of process data (for example; mean; variance and power spectrum) fall into this category (Vander Wiel *et al.*, 1992). It is worth noting that these first-order and second-order statistical tools are sufficient at only describing linear systems and alternate approaches must be sought to quantify system nonlinear characteristics (Jelali, 2006). Other user defined transient performance specifications, namely settling time, percentage overshoot and time to peak will also be included in this class. To the author's knowledge, there is currently no established procedure/s that detects oscillatory or even sluggish closed loop responses in the presence of process nonlinearity without the requirement of a nonlinear process model. Hence, the study of developing a methodology for such cases is beneficial and has practical significance in industry. The use of HOS has proved an invaluable tool in the detection of loop nonlinearity such as control valve stiction (Choudhury *et al.*, 2004; Jelali, 2006; Ordys *et al.*, 2007). Distinctive characteristics of a nonlinear time series includes the presence of self-sustained limits cycles with harmonic content and the presence of phase coupling which creates coherence between the frequency bands occupied by the harmonics such that the phases are non-random and form a pattern (Thornhill and Horch, 2006). While HOS is a useful tool when analysing nonlinear time series data, it does not provide information about closed loop performance.

When deriving a MV controller for the linear CPA methodology, the critical assumption is made that the process admits the description given by Eq. (2.1). When the process is described by a nonlinear difference equation for the purpose of capturing the process dynamic or disturbance behaviour, it may be very difficult to estimate the MV lower bound if not impossible due to the structural form of the nonlinearity (Harris and Seppala, 2002).

Therefore the MV lower performance bound for the general nonlinear dynamic system cannot be determined from routine operating data. If the linear model is used in the assessment procedure, then the assumption must be made that the process admits a local linear representation. Therefore the CPA results are locally valid and if changes to the operating point are made then the data must be properly segmented prior to the analysis. A suitable methodology for data segmentation is thus required and can be combined with existing linear CPA tools to handle nonlinear process data.

For the class of model based CPA methodologies, an explicit model of process and/or the disturbance model are a requirement. Usually a step input is used to excite the process under open loop conditions in order to capture the systems dynamic behaviour. The methods used for linear based CPA indices assume the process to be represented by a LTI FOPDT model. However, for nonlinear systems a LTI FOPDT model is inadequate for the reasons mentioned previously in Section 3.2.1.

A survey of CPA literature reveals that restricted structure performance bounds for the general nonlinear dynamic model have not been developed. Restricted controller structure refers to the PID algorithm in this study. More than 90% of control loops operating within industry use the PID type with only a small percentage functioning to their full potential as indicated by a survey conducted by Ender (1993). In light of this, it is apparent that PID controllers are widely used but poorly tuned for linear and nonlinear process control loops. To compound the effects of poor controller tuning, other loop problems such as sensor degradation and final control element wear also hinders acceptable closed loop performance. Nonlinear control valve problems such as stiction and hysteresis add to the complex dynamic behaviour of the process and play a significant role in poor performing loops which may directly affect controller tuning. Therefore, it is important to isolate hardware problems

before attempting to find appropriate PID tuning parameters in order to achieve desired performance objectives.

Despite the fact that most industrial processes are controlled using the *linear* PID controller, most chemical processes show a certain degree of nonlinear behaviour (Bhat *et al.*, 1990; Chen *et al.*, 1990; Henson and Seborg, 1994; McMillan, 1994; Bittanti and Piroddi, 1997). Therefore it is important to provide some kind of nonlinear compensation when necessary to counter the effects of the nonlinearity and ensure satisfactory control for the entire operating region of the controlled variable. Gain scheduling is probably the most widely used scheme in process industry (Leith and Leithead, 2000; Rugh and Shamma, 2000; Åström and Hägglund, 2006). One main reason is that it provides the standard *linear* PID controller to operate satisfactorily for nonlinear systems using just lookup tables or simple if/then rules. In this work, we focus on developing novel NLCPA indices based on the structure of the PID controller. The main objective is to analyse current PID controller performance applied to a nonlinear process using the gain scheduling approach. In the following section, a brief discussion of the PID controller is given.

3.3 THE PID CONTROL ALGORITHM

The PID controller is considered the *bread and butter* of process control engineering in many industrial control loops (Åström and Hägglund, 2006) and provides satisfactory closed loop performance for many practical applications due to its simple and transparent controller architecture. Despite advances made in more complex controller design algorithms, the PID controller remains the first choice of SISO controller designs operating in a feedback control loop. It is flexible to allow for combination with additional logic and may be implemented in cascade control and/or ratio control for more elaborate control schemes.

Many sophisticated control strategies, such as model predictive control (MPC) are organised hierarchically based on the common PID controller (Tan *et al.*, 2002). The PID controller has been implemented in many forms including pneumatic, analogue/discrete electronics and now primarily software based with structural modifications to suite an application. The fairly simple controller structure allows for the use of additional features to counter the negative effects of integral windup, derivative kick and high frequency noise filtering to achieve robust and satisfactory control for a variety of process control loops. Furthermore, gain scheduling allows for application of the simple linear controller in more complex dynamical nonlinear systems.

The dynamical nature of nonlinear process control loops leads to changes of operating conditions within the loop, and hence loop performance. Changes in system performance may be attributed to the presence of process nonlinearities within the control channel, process equipment aging, production strategy changes, modification to properties of raw materials and changes over equipment cycles (Poulin and Pomerleau, 1996). Often the quickest and most cost effective way to achieve continued satisfactory performance is by controller tuning. The main objective of PID controller tuning is to determine parameters that satisfy closed loop system performance specifications, and the robust performance of the control loop over a wide range of operating conditions should also be ensured. Practically, it is often difficult to simultaneously achieve all of these desirable qualities. For example if the PID controller is designed to provide good setpoint tracking capabilities, it usually results in poor response when under external disturbance load conditions and vice-versa. Therefore prior to the design stage, the desired controller objective (either setpoint tracking or disturbance rejection) should be selected. This work focuses on controllers designed for setpoint tracking, since this is commonly encountered in many industrial process control loops.

3.4 SUMMARY AND CONCLUSIONS

CPA is important to ensure the success of process control throughout the entire life cycle of a typical control loop. While significant advancements have been made with regards to univariate and multivariate CPA technologies for linear systems, far more research opportunities remain to address the challenging problems imposed by process loop nonlinearities. Factors such as imperfect control valves, noisy sensors and load disturbances add to the dynamic behaviour of the process and should be accounted for. Another important consideration is the selection of PID controller settings for which there exists a plethora of tuning methods (Aström and Hägglund, 1995; Wang *et al.*, 2000; Åström and Hägglund, 2006; O'Dwyer, 2009).

Satisfactorily accounting for most loop nonlinearities in the computation of NLCPA index reduces the possibility of obtaining misleading performance assessment results. In summary, the novel NLCPA classification framework presented in this chapter reveals that further studies in the area of nonlinear based benchmarking tools are required and necessary for accurate automated performance assessment of dynamic nonlinear systems especially where PID controllers are predominately used.

Chapter 4

A New Model based Controller Performance Index for Nonlinear Systems

4.1 INTRODUCTION

The aim of this chapter[1] is to present a novel performance benchmark based on the system's nonlinear model representation. Setpoint tracking performance of SISO nonlinear systems is of interest in this work. Given a suitable system representation, it is possible to devise a measure that describes current controller behaviour relative to an optimal nonlinear performance benchmark. This approach serves as a basis for the development of NLCPA presented in this chapter. A model based CPA strategy that can be practically implemented on a typical plant DCS is described.

First, insights into the subject of mathematical nonlinear modelling techniques used to describe real world process control loops are discussed. Since the focus of the work is based on capturing complex dynamic nonlinear behaviour for the purpose of NLCPA, it is important that the nonlinear model captures *essential qualitative behaviour* of the process such that an accurate assessment of the control loop is obtained. NARMAX models have shown to be useful in their ability to represent a broad class of nonlinear systems at a

[1] A version of this chapter is accepted for publication in December 2016 in the Journal of New Generation Sciences. Certain sections of this chapter are published in the Proceedings of the World Congress on Engineering and Computer Science (2014).

reasonable computational cost (Chen *et al.*, 1990; Sales and Billings, 1990). A general representation of nonlinear systems by NARMAX models are used in this study for system identification. NARMAX model structure is briefly reviewed and ANN based NARMAX models are motivated for the study of model based NLCPA.

Second, the acquired model is utilized for performance evaluation of the control loop. Using a constrained optimisation approach, an optimal closed loop system is derived *offline* and subsequently utilised in the NLCPA framework in *real time*. A simulation case study is used to demonstrate the efficacy of the proposed methodology in MATLAB ™ SIMULINK™. Further application of the methodology is validated on real world experiments, the results of which are presented in the subsequent chapter.

4.2 APPLICATION OF NONLINEAR MODELLING TO CONTROLLER PERFORMANCE ASSESSMENT

It is commonly known that linear models have been widely used in system identification for two main reasons (Box, 1970). First, the system dynamics from input to output (I/O) follow simple linear relationships and are relatively easily determined. Even if the system is mildly nonlinear, simple linear models are adequate for capturing system dynamics in place of more complex nonlinear models. The second reason relies on the fact that linear systems are *homogenous* (Box, 1970). However, if this assumption was extended to all process control loops that do not demonstrate this property, then the systems actual dynamics cannot been represented accurately by a simple linear model and linear methods would not be applicable. In many cases encountered within the process industry, linear models are not suitable to represent these complex systems satisfactorily and nonlinear models have to be considered (Harris and Yu, 2007; Yu *et al.*, 2009; Yu *et al.*, 2011a; Zhang *et al.*, 2011).

Due to nonlinear effects commonly encountered in practical process control loop, (such as valve hysteresis, harmonic generation, variations in process gain and the effects of imposed limits) neither of the principles of linear CPA described in Chapter 2 are valid for nonlinear systems (Harris and Yu, 2007). Any attempt to restrict attention to strictly linear methods for CPA can only lead to a compromised benchmarking index, especially for process control loops dominated by severely nonlinear dynamic behaviour. Furthermore, restricting the CPA tools to purely linear describing models severely limits the systems characteristics that can be possibly captured, and therefore compromises the integrity of the CPA index.

For linear stochastic systems, Box *et al.* (1970) proposed a systematic approach to linear time series modelling which consisted of the following four primary steps in the identification procedure:

(i) Selection of a general class of empirical models for consideration.

(ii) Identification of specific subclass of models to be fitted to time series data.

(iii) Estimation of model parameters using suitable algorithms.

(iv) Validation of model accuracy.

As shown in Chapter 2, linear *parametric* models can be used to find the MV lower bound as demonstrated by Harris (1989). Model order and its structure determination remains a secondary problem for which there are suitable tools such as the Akaike Information Criterion to aid in the guidance of appropriate model order selection (Bozdogan, 1987).

For the purpose of extending CPA to a wider class of nonlinear process control loops, an I/O model structure in the form of a NARMAX model is proposed. In the next section, representations of nonlinear systems using the NARMAX models are discussed within the context of its intrinsic properties.

4.3 NARMAX MODEL REPRESENTATION

System representation, modelling and identification are fundamental to process engineering where it is often required to approximate a real world system with an appropriate model from a set of representative I/O data vectors. The model structure needs to have sufficient representation ability to enable the underlying system dynamics to be approximated within satisfactory limits. In many real world cases, the additional requirement is often to retain model simplicity (Chen and Billings, 1989). In practice, most systems encountered in industry are nonlinear to some degree and nonlinear models are required to provide acceptable representations.

NARMAX model structures have been shown to provide useful unified representations for a wide class of nonlinear systems (Chen and Billings, 1989; Chen *et al.*, 1990; Sales and Billings, 1990). An adequately trained neural network performs nonlinear transformation of input data in order to approximate output data that is comparable to the real world system of interest. A NARMAX model provides a means of describing the I/O relationships of a system which relate the systems output to its input signals in a straight forward manner. Attractive features of the NARMAX which lends itself to a wide class of nonlinear system identification are:

(i) In some cases, the nonlinear relationship $f(.)$ is known and the task of specifying the I/O relationship of the system is reduced to determining a few of the unknown parameters (Chen and Billings, 1989).

(ii) Since the derivation of the NARMAX model is independent from the form of a nonlinear function $f(.)$, the choice of nonlinear function approximation is not

restrictive and may be expanded to include polynomials and ANNs amongst others (Chen *et al.*, 1990).

(iii) When compared to a Volterra series representation, the NARMAX model provides an efficient and convenient framework. It does not require expensive computational effort for a large number of kernel estimation as encountered with Volterra models (Yu, 2007).

(iv) NARMAX models have relatively few parameters and are numerically easy to handle. Furthermore, the model coefficients can be estimated using established estimation algorithms (Sales and Billings, 1990).

(v) Due to the discrete structure of the NARMAX representation it may be readily implemented on a digital computer, which is especially relevant for industrial control purposes.

For pragmatic reasons, the model provides adequate approximation to as large a class of systems as is possible at a reasonable computational cost. In light of these desirable features, NARMAX model representation described by Chen and Billings (1989) is an important nonlinear modelling approach that provides a unified representation for a broad class of nonlinear systems. A brief description of this significant class of nonlinear modelling framework is provided in the following subsection.

4.3.1 Description of the general nonlinear NARMAX representation

NARMAX models fall into the class of I/O descriptions that expand the current output in terms of past inputs and past outputs. The model representation has the capability of describing a broad class of nonlinear systems and may avoid the difficulty of excessive parameter usage as in the case with Volterra series (Chen and Billings, 1989). A discrete time nonlinear stochastic control system with *'O'* outputs and *'I'* inputs can be represented by the NARMAX model (Leontaritis and Billings, 1985):

$$y(t) = f(.) = f(y(t-1),...,y(t-n_y),u(t-1),...,u(t-n_u),\xi(t-1),...,\xi(t-n_\xi)) + \xi(t) \tag{4.1}$$

where

$$y(t) = \begin{bmatrix} y_1(t) \\ . \\ . \\ . \\ y_o(t) \end{bmatrix}, \qquad u(t) = \begin{bmatrix} u_1(t) \\ . \\ . \\ . \\ u_I(t) \end{bmatrix}, \qquad \xi(t) = \begin{bmatrix} \xi_1(t) \\ . \\ . \\ . \\ \xi_I(t) \end{bmatrix};$$

$f(.)$ is some nonlinear function with n_y ,n_u and n_ξ representing the number of maximum past output, input and noise lag terms for a nonlinear system respectively. $\xi(t)$ is a zero mean Gaussian noise sequence. Eq. (4.1) can be simplified by considering only additive uncorrelated noise and therefore represented by (Chen and Billings, 1989):

$$y(t) = f(y(t-1),...,y(t-n_y),u(t-1),...,u(t-n_u)) + \xi(t) \tag{4.2}$$

The I/O relationship given by Eq.(4.2) is dependent upon the nonlinear function $f(.)$ which in reality is generally very complex (Chen *et al.*, 1990). Knowledge of the structure of the

nonlinearity is generally not readily available and the solution is to approximate $f(.)$ using some known simpler function. $f(.)$ may be constructed by using suitable techniques such as lookup tables and polynomial equations.

In this work, we consider using ANNs to approximate the nonlinear relationship. It has been recognised that the field of ANNs offer a number of potential benefits for application in the field of control engineering (cf. Narendra and Parthasarathy (1990), Hunt *et al.* (1992), Bittanti and Piroddi (1997), Lightbody and Irwin (1997)) and therefore provides a tractable basis for its application in CPA. Furthermore, ANNs have gained maturity (c.f. Narendra and Parthasarathy (1990), Billings *et al.* (1992), Hunt *et al.* (1992), Bhat *et al.* (1990)) in terms of algorithmic advances and estimation theory and therefore provides a rich background and sound framework for the development of a model based NLCPA.

4.3.2 Artificial neural network based NARMAX model

As discussed previously, it is important that essential nonlinear system behaviour is captured by the model. ANNs have become an attractive tool that can be used to construct a model of a complex nonlinear process (Narendra and Parthasarathy, 1990; Haykin, 2004). This is mainly due to the fact that the ANN has the inherent natural ability to learn approximate generalised nonlinear functions arbitrarily well (Cybenko, 1989). The modelling approach therefore lends itself to possibly modelling complex dynamic behaviour effectively (such as $f(.)$) for a wide range of nonlinear system dynamics when NLCPA is of primary concern. The main motivating factors which contribute to its use in this work are:

(i) A nonlinear relationship $f(.)$, is generally unknown in most process control loops (Narendra and Parthasarathy, 1990). ANNs offer the ability to learn complex nonlinear relationships from using captured records of I/O data without prior

knowledge of the structure of the nonlinearity or process dynamics (Antsaklis, 1990).

(ii) Based on the theoretical results of Cybenko (1989) and Funahashi (1989), it has been shown that an ANN comprising of two hidden layers and a fixed nonlinearity can be trained to form any realisable vector function $f(.)$ and hence represent any nonlinear continuous model sufficiently well.

(iii) Hardware and software advances in digital technology have enabled computer simulations of ANNs to be inexpensive, with relative speed and efficiency.

(iv) In some cases it may not be appropriate to develop models from first principles due to the difficulties and *a-priori* knowledge of the process involved, especially those with severe nonlinearities. ANNs offer a simpler and proficient "black-box" alternative to the modelling of nonlinear processes (Hussain *et al.*, 2001).

(v) The output from a well-trained ANN produces a signal that is bounded to the selected threshold value when driven by new or large input signals. This is not the case when polynomial NARMAX models are used which may result in an unbounded output signal (Lightbody and Irwin, 1997).

(vi) Finally, the versatility in structure, size and application of ANNs allow them to be customized to suit many nonlinear relationships, for modelling a broad class of nonlinear systems.

Based on the attractive features of ANNs for modelling nonlinear dynamics, there is strong impetus for its usage in the development of a CPA methodology for typical nonlinear dynamical systems encountered in the process industry (Zhou, 2008).

4.3.3 Linearization of the NARMAX model

According to Leontaritis and Billings (1985), the model given by Eq.(4.1) may also be characterised by a linear ARMAX model at a specific operating point. A description of the discrete time ARMAX model is given by (Leontaritis and Billings, 1985):

$$A(z^{-1})y(t) = B(z^{-1})u(t-b) + C(z^{-1})\xi(t) \tag{4.3}$$

where, $y(t)$ is the system output, $u(t)$ is a controllable input signal, $A(z^{-1})$, $B(z^{-1})$ and $C(z^{-1})$ are the polynomials in the backward shift operator z^{-1}, and b is the system delay. Leontaritis and Billings (1985) rigorously proved that a nonlinear time variant system can always be represented by the model Eq. (4.3) in a region around an equilibrium point subject to the following two necessary and sufficient conditions (Chen and Billings, 1989):

(i) The nonlinear function $f(.)$ is of the system is finitely realizable.

(ii) A linearized model exists if the system is operated close to the chosen equilibrium point.

These conditions are important for the analysis of nonlinear control system design since it allows for the application of well-established linear design methods. In a similar context, this approach is used in the development of the NLCPA tool presented in Section 4.4 and takes advantage of piecewise linear approximation.

4.4 DEVELOPMENT OF THE NONLINEAR CONTROLLER PERFORMANCE BENCHMARK

Consider the negative feedback closed loop control system under performance inspection as is illustrated in Fig.4.1. The principal idea is to compare the closed loop performance of the actual controller to that of an optimal controller designed offline for a generalized nonlinear process (Pillay *et al.*, 2014). For the purpose of comparison, an open loop model of the nonlinear process is required.

The procedures followed to estimate the nonlinear restricted structure performance bound $\eta_{NL_{PID}}(t)$ is presented in *three stages*:

(i) Stage 1: Nonlinear plant identification,

(ii) Stage 2: Optimal PID controller design,

(iii) Stage 3: Nonlinear controller performance index.

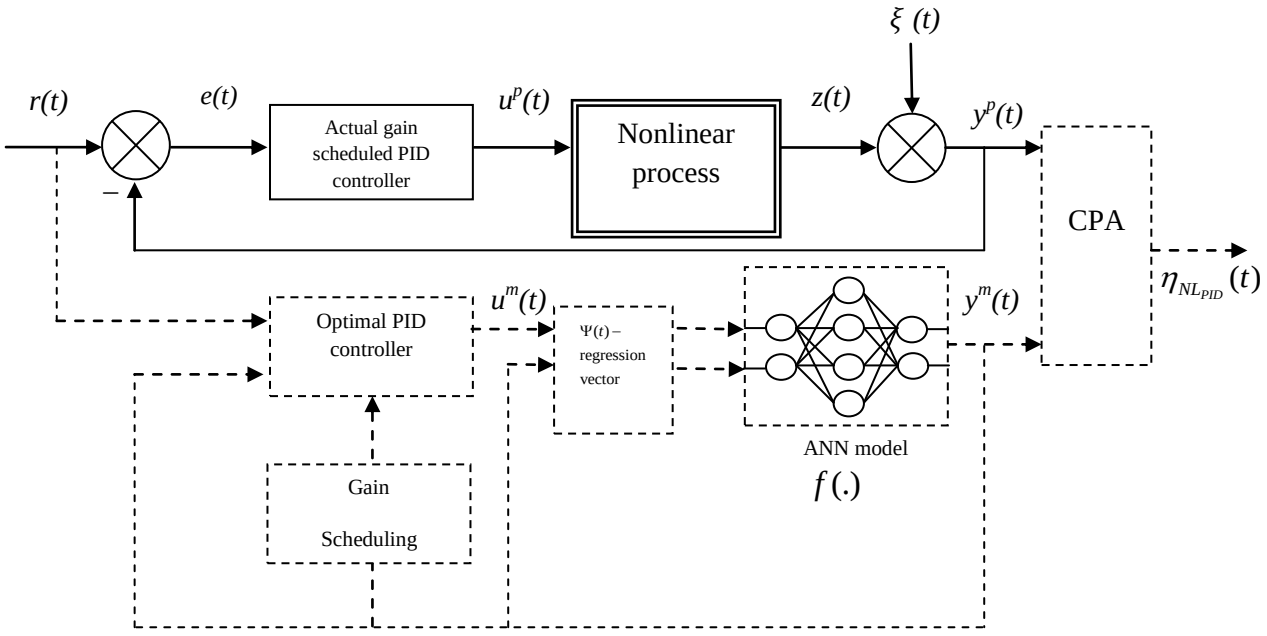

Figure 4.1: Proposed controller performance assessment scheme for single-input single-output nonlinear process.

A brief description of the purpose of each element shown in the dotted section of Fig. 4.1 is given:

(i) Optimal PID controller: Simulated PID gain scheduled controller for the nonlinear process.

(ii) Gain scheduling: Enables gain scheduled parameters for the simulated PID controller. Optimal controller parameters are preselected prior to the NLCPA.

(iii) Regression vector: Matrix containing past input and past output simulated data.

(iv) ANN model: Nonlinear representation of the process under performance inspection.

(v) CPA: Computation of proposed performance index.

4.4.1 Stage 1: Nonlinear plant identification

In this section, ANN modeling of a dynamic nonlinear system is presented. In order to establish a performance benchmark we first train a neural network to capture relationships between the real plant input $u^p(t)$ and its corresponding output $y^p(t)$. In the following stages we will use the trained neural network to design optimal controllers for real time estimation of an artificial process output $y^m(t)$ under closed loop conditions for the NLCPA procedure. A nonlinear discrete time process admitting the generalized form of a Neural NARMAX (NNARMAX) model is considered (Chen *et al*., 1990):

$$y^m(t) = f[y\ (t-1),...,y\ (t-n_y),u(t-1),...,u\ (t-n_u)] + \xi(t) \tag{4.4}$$

The process output $y^m(t)$ can be evaluated in terms of a nonlinear function $f(.)$ of the past output and input values denoted by *y(t-1)* and *u(t-1)* respectively, in which n_y and n_u are the corresponding lag terms. Here an appropriate excitation signal can be used to drive the system in order to capture its nonlinear behavior in open loop. It is important that the input signal is *rich* for adequate capturing of the system's dynamics over its entire operating range of interest. This stage of the procedure is *once-off* and only repeated if process changes occur. A neural network can be trained to map the nonlinear relationship $f(.)$ which on completion will be able to replicate the actual process output dynamic for a given input signal. If identification is satisfactory, the Gaussian noise $\xi(t)$ will be unpredictable and uncorrelated with all past inputs and outputs, which in principle can be used for model validation (Chen *et al.*, 1990).

Rewriting Eq.(4.4) in terms of a deterministic model yields:

$$y^m(t) = NNARMAX(\Psi(t)) \tag{4.5}$$

where the regression vector is defined as:

$$\Psi(t) = [y(t-1),...,y(t-n_y),u(t-1),...,u(t-n_u)] \tag{4.6}$$

Nonlinear system behavior $f(.)$ is embedded in the following parametric neural network structure with hidden layers:

$$\Theta(t) = \lambda^1\left(W^1\Psi(t)^T + \mu_b{}^1\right)$$

$$y^m(t) = \lambda^2\left(W^2\Theta(t) + \mu_b{}^2\right) \tag{4.7}$$

where λ is the activation function matrix, W represents the weight matrix and μ_b is the bias. The identification of the nonlinearity $f(.)$ is based on the *supervised learning* scheme

with suitable input and output process data. ANN training methods are well documented and the interested reader is directed to (Haykin, 2004) for a thorough treatment on the subject. Fig. 4.2 illustrates the NNARMAX architecture used in this work. The training is performed offline and implemented in the NLCPA scheme as shown in Fig. 4.1. Model based controller design methods usually employ a model for derivation of a control law; hence the effort of system identification may be disregarded in this case. Once a suitably trained ANN model has been established, it can be used to obtain linearized models for given input and output data sets at each operating point. Linearized models at any operating region may be represented as:

$$Y(z) = \left[\frac{B(z)}{A(z)}\right] U(z^{-n_b}) \tag{4.8}$$

where,

$$A(z) = 1 + a_1 z^{-1} + ... + a_{n_y} z^{-n_y}$$

$$B(z) = b_1 z^{-1} + b_2 z^{-2} + ... + b_{n_u} z^{-n_u+1}$$

z^{-1} represents the back shift operator. The system sample delay in which the input signal affects the output is denoted by n_b in Eq. (4.8). For desired operating region t_{OP} , the first partial derivative term can be used (Chen and Huang, 2004):

$$a_i = -\frac{\partial NNARMAX}{\partial y(t-i)} \mid \Psi(t) = \Psi(t_{OP}) \quad i = 1, 2, ..., n_y \tag{4.9}$$

$$b_i = \frac{\partial NNARMAX}{\partial u(t-i)} \mid \Psi(t) = \Psi(t_{OP}) \quad i = 1, 2, ..., n_u$$

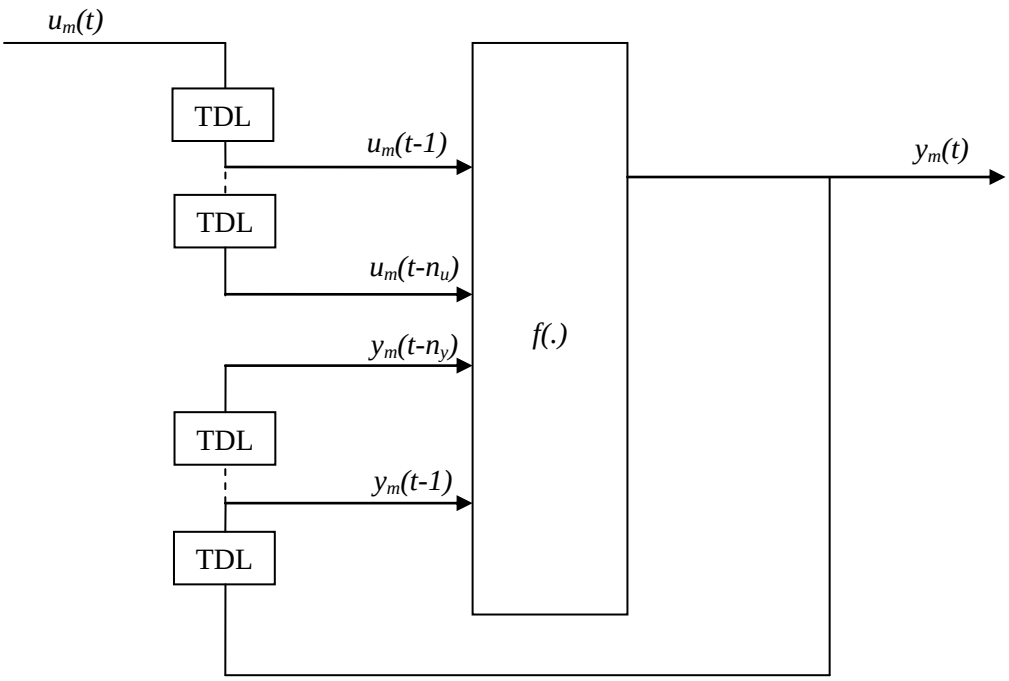

Figure 4.2: NNARMAX architecture used in modeling nonlinear process dynamics

Once a linearized model is obtained for the respective operating region, it can be applied to well established linear design techniques for control tuning. The theoretical difficulties of determining optimal PID controller settings for the nonlinear process are thus avoided since an appropriate linearized approximation for the local point can be computed. In the subsequent section, the local linearized model is used to obtain optimal controller settings under operating constraints.

4.4.2 Stage 2: Optimal PID controller design

One structure of a continuous PID controller is a parallel form realization without a derivative filter:

$$u(t) = k_c \left[e(t) + \frac{1}{\tau_i} \int_0^t e(t)dt + \tau_d \frac{de(t)}{dt} \right] \tag{4.10}$$

where the instantaneous control loop error, *e(t) = r(t) - y(t)* is deviation of the process output from the setpoint. k_c,τ_i and τ_d represent the proportional gain, integral time constant and the derivative time constant respectively. Adopting a discrete time PID version of Eq. (4.10) gives the velocity form at each sample time T_s:

$$u(t) = u(t-1) + k_c \left[\left[(e(t) - \mathrm{e(t-1)} \right] + \frac{T_s}{\tau_i} \mathrm{e(t)} + T_s \tau_d \left[e(\mathrm{t}) - 2(e(\mathrm{t-1})) + e(t-2) \right] \right] \tag{4.11}$$

For a particular preselected sampling time, the objective is to determine the best values of k_c, τ_i and τ_d that will result in optimal control in terms of the integrated absolute error (IAE) under negative feedback closed loop control. Several variations of the PID architecture are found on industrial controllers from different manufacturers. Information about the controller structure is essential and must be known prior to implementation of the NLCPA index. The benchmark is thus based on identical control structures, which will allow for a reasonable and fair comparison. Tuning of the controller for nonlinear systems is accomplished through numerical optimization.

MATLAB™ is a popular software environment used by many researchers for offline controller design. Researchers have reported good results using the *fminsearch* function available in the MATLAB™ OPTIMIZATION TOOLBOX™ version 5.0 (Agrawal and Lakshminarayanan, 2003; Sendjaja and Kariwala, 2009), for controller design. In this work, a hybrid Nelder Mead-Particle Swarm Optimization (NM-PSO) function is utilized in the determination of the optimal controller parameters (Pillay and Govender, 2013)[2].

[2] The hybrid Nelder-Mead Particle Swarm Optimization (NM-PSO) algorithm was presented at the 5th International Conference on Agents and Artificial Intelligence (2013).

The NM simplex algorithm (Nelder and Mead, 1965) is a widely used numerical method for solving nonlinear unconstrained optimization problems. The objective of the algorithm is to minimize a cost function without any gradient information thereby reducing the possibility of getting trapped in a local minimum.

In contrast, the PSO method (Eberhart and Kennedy, 1995) is based on the concept of social interaction that exists in nature such as the swarming of bees. The technique is highly stochastic in nature and is population based and can search a large feature space without succumbing to the effects of local minima for which the NM is prone. By combining the stocasticity of the PSO and the local search capabilities of the NM optimization, the hybrid algorithm (NM-PSO) is proficient in determining global optimal controller parameters. Further details of the hybrid optimization algorithm can be found in Pillay and Govender (2013) and the MATLAB™ code is listed in APPENDIX A.

During the controller design, step responses of the closed loop system for different operating conditions are simulated and the optimal controller parameters are determined using the NM-PSO algorithm to solve the following objective function:

$$J_{k_c,\tau_i,\tau_d} = \min \int \left| e(t) \right| dt = \min \sum \left| r(t) - y^m(t) \right| \tag{4.11}$$

with the following inequalities imposed:

$$y^m{}_{\min} < y^m < y^m{}_{\max} \tag{4.12}$$

$$k_{c_{\min}} < k_c < k_{c_{\max}} \tag{4.13}$$

$$\tau_{i_{\min}} < \tau_i < \tau_{i_{\max}} \tag{4.14}$$

$$\tau_{d_{\min}} < \tau_d < \tau_{d_{\max}} \tag{4.15}$$

These constraints ensure that the simulated process output does not exceed the prescribed operating regions. In addition, the controller parameters will not lead to excessive values which if applied on a real PID controller may lead to excessive final control element wear. A scheduling variable is chosen and adjusted accordingly for each operating region. The operating region is defined by the desired setpoints at which the process variable is required to be maintained. Once the optimal values are determined for each operating region, it can be used on the simulated PID algorithm to obtain $u^m(t)$ in a generalized gain scheduling scheme.

4.4.2.1 Gain scheduling

Since performance evaluation of a PID controller is the central theme of this work, the gain scheduling approach represents a convenient approach for PID implementation in nonlinear control problems. Furthermore, using the gain scheduling approach preserves well understood linear intuition for which there exists powerful linear design tools on difficult nonlinear problems (Rugh and Shamma, 2000). Computational burden of the scheduling methodology is much less demanding than for other nonlinear controller design approaches. Finally, PID gain scheduling enables a controller to respond rapidly to changing operating conditions, and is an effective and convenient method for nonlinear PID control design.

4.4.3 Stage 3: Nonlinear controller performance index

In the final stage of the methodology we use the NNARMAX model obtained from open loop system identification experimentation, and the optimal PID controller parameters computed for each operating point in the real time estimation of the NLCPA. By computing the closed

loop response of the gain scheduled optimal PID controller in series with the NNARMAX model we can obtain an artificial process output $y^m(t)$.

To establish the real time performance index, we use the synthetic signal of the simulated process output $y^m(t)$ and compare it to the actual plant process variable $y^p(t)$. The desired reference trajectory $r(t)$ is mutual to the simulated PID control and the real PID process controller. The methodology is described in Fig.4.3 and the derivation of the NLCPA index follows.

With regards to Fig. 4.3, the present time instant is represented by t and n denotes the number of past samples. Therefore a moving window of sampled data is used by the NLCPA index in a first-in first-out basis to give current controller performance during setpoint changes.

A novel dynamic performance assessment benchmark that relates current controller performance to an optimal gain scheduled nonlinear PID controlled system is derived from the simulated process IAE:

$$IAE^m = \sum_{t}^{t+n}\left[\left|e^m(t)\right| + \left|e^m(t-1)\right| + \cdots + \left|e^m(t-n)\right|\right] \tag{4.16}$$

where the simulated process error matrix is:

$$e^m = \begin{bmatrix} r^p(t) \\ r^p(t-1) \\ \vdots \\ r^p(t-n) \end{bmatrix} - \begin{bmatrix} y^m(t) \\ y^m(t-1) \\ \vdots \\ y^m(t-n) \end{bmatrix}$$

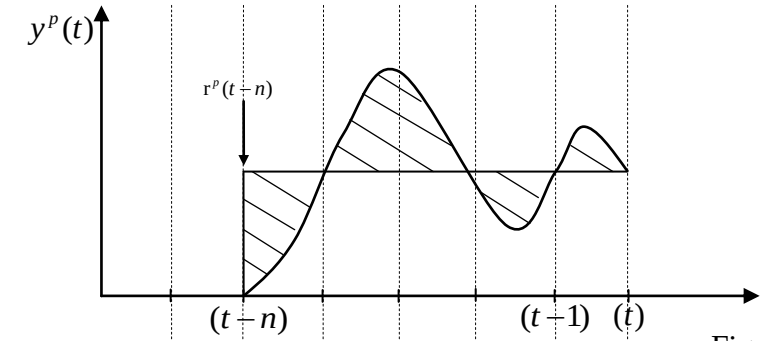

Fig 4.3a: Actual process output

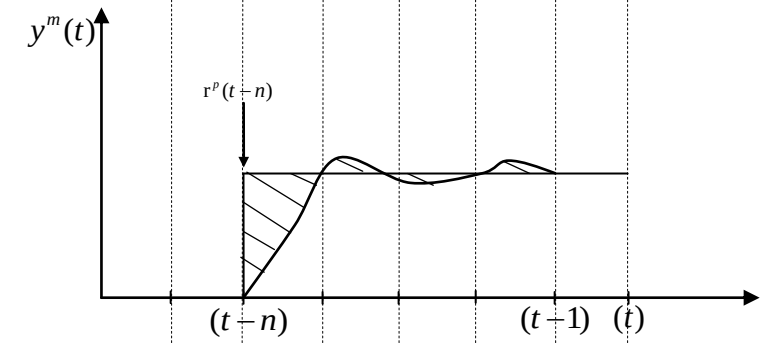

Fig 4.3b: Simulated process output

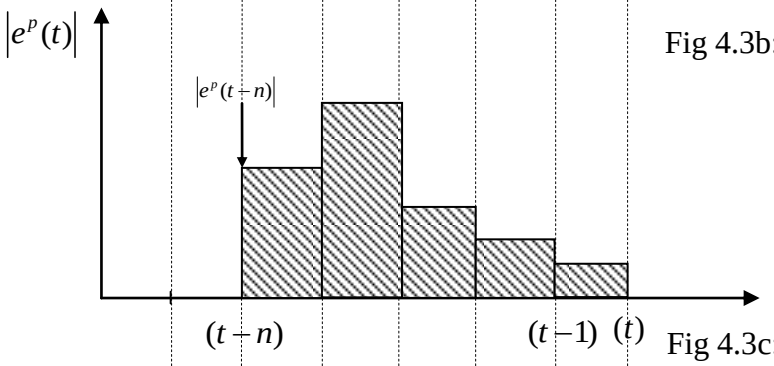

Fig 4.3c: IAE of the actual process

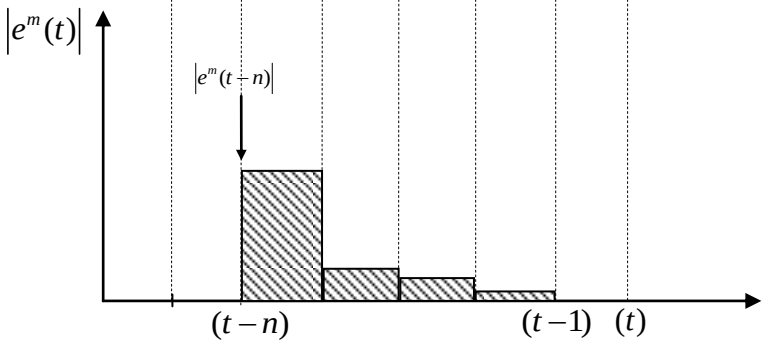

Fig 4.3d: IAE of the simulated process

Figure 4.3: Real time performance assessment based on running window IAE

Similarly the actual process IAE is given by:

$$IAE^{p} = \sum_{t}^{t+n}\left[\left|e^{p}(t)\right| + \left|e^{p}(t-1)\right| + \cdots + \left|e^{p}(t-n)\right|\right] \tag{4.17}$$

where the actual process error matrix is:

$$e^{p} = \begin{bmatrix} r^{p}(t) \\ r^{p}(t-1) \\ \vdots \\ r^{p}(t-n) \end{bmatrix} - \begin{bmatrix} y^{p}(t) \\ y^{p}(t-1) \\ \vdots \\ y^{p}(t-n) \end{bmatrix}$$

From Eq.(4.16) and Eq.(4.17) the NLCPA can be written as:

$$\eta_{NL_{PID}} = \frac{IAE^{m}}{IAE^{p}} \tag{4.18a}$$

The ratio given by Eq.(4.18a) is bounded to the 0 to 1 range as follows:

$$\eta_{NL_{PID}} = 1 - \left(\frac{IAE^{m}}{IAE^{p}}\right) \tag{4.18b}$$

$$= 1 - \left\{\frac{\sum_{t}^{t+n}\left[\left|e^{m}(t)\right| + \left|e^{m}(t-1)\right| + \cdots + \left|e^{m}(t-n)\right|\right]}{\sum_{t}^{t+n}\left[\left|e^{p}(t)\right| + \left|e^{p}(t-1)\right| + \cdots + \left|e^{p}(t-n)\right|\right]}\right\}$$

With regards to Eq. (4.18), the subscript "NL_{PID}" refers to the minimum achievable bound using an optimal nonlinear gain scheduled PID control algorithm as the benchmark. The NLCPA index is bounded in the range $0 \le \eta_{NL_{PID}} \le 1$, where $\eta_{NL_{PID}} \to 0$ would indicate good control. Conversely for $\eta_{NL_{PID}} \to 1$, the actual closed loop performance is regarded as poor relative to the artificial closed loop process output.

4.5 SIMULATION STUDY OF THE PROPOSED NLCPA TOOL

4.5.1 Preliminaries to simulation experiments

To demonstrate the efficacy of the novel NLCPA index developed in the previous section, a simulation case study is presented. All simulations were conducted in MATLAB™ SIMULINK™ with system identification and optimal PID controller settings determined prior to the performance assessment of the controller.

MATLAB™ System Identification Toolbox™ was used in the determination of open loop nonlinear discrete models for all the examples presented. A unit step up and unit step down input signal with equal magnitude was injected into the processes for the purpose of capturing nonlinear system dynamic behaviors for the examples. A NNARMAX model structure with a hidden layer of [10 20 15] neurons and corresponding activation functions of "log-sigmoid", "log-sigmoid" and "linear" was constructed for each layer respectively.

The process output variable $y(t)$ was used as the single scheduled variable for the gain scheduled nonlinear PID controller (NLPID). Two operating regions were chosen for obtaining linearized models at the prescribed operating points to demonstrate the methodology. Corresponding linearized transfer functions (Eq.4.9) were used in the computation of the optimal PID controller settings using NM-PSO optimization described by (Eq.4.11).

4.5.2 Simulation case study

Consider the following nonlinear dynamical system represented by a second order Volterra series (Harris and Yu, 2007) given by:

$$\begin{aligned} y^p(t) &= 0.2u(t-3) + 0.3u(t-4) + u(t-5) + 0.8u^2(t-3)u(t-4) \\ &-0.7u^2(t-4) - 0.5u^2(t-5) - 0.5u(t-3)u(t-5) + d(t) \end{aligned} \tag{4.19}$$

With regards to Eq. (4.17), the disturbance $d(t)$ is defined as:

$$d(t) = \frac{a(t)}{1 - 1.6(t-1) + 0.8(t-2)} \tag{4.20}$$

where $a(t)$ is a zero mean white noise sequence having a variance of 0.1.

Constraints (4.12) to (4.15) imposed on the NM-PSO search for optimal controller settings are listed in Table 4.1. These limits were arbitrarily chosen to speed up the search. The sample time was selected to provide an adequate number of I/O data points for the purpose of nonlinear plant identification. Orders of the regression variables yielding the best performing NNARMAX model are given in Table 4.1. The model orders were chosen by trial and error to best fit the actual process data. Since the intention is to assess the efficacy of the proposed NLCPA index, a suboptimal gain scheduled PI controller was used to control the process and its closed loop control performance is shown in Fig.4.4(a). Fig. 4.4(b) illustrates the corresponding dynamic NLCPA for the simulation. Similarly, the optimal gain scheduled PI controller with parameters derived from the NM-PSO search was simulated to show disparity between a well-tuned and a poorly-tuned control system. The respective controller settings are given in Table 4.2.

Constraints													
Sample time	Regression variables			Limits on PID settings						Limits on process output			
										Operating region 1		Operating region 2	
T_s (sec)	n_y	n_u	n_k	$k_{c_{\min}}$	$k_{c_{\max}}$	$\tau_{i_{\min}}$ (sec)	$\tau_{i_{\max}}$ (sec)	$\tau_{d_{\min}}$ (sec)	$\tau_{d_{\max}}$ (sec)	$y^m(t)_{\min}$ (%)	$y^m(t)_{\max}$ (%)	$y^m(t)_{\min}$ (%)	$y^m(t)_{\max}$ (%)
1	2	2	1	0.01	1	0.1	10	0	0	0	25	25	50

Table 4.1: Constraints used in the determination of the optimal PID controller settings for respective operating regions.

	PID gain scheduling settings					
	Operating region 1			Operating region 2		
	k_c	τ_i (sec)	τ_d (sec)	k_c	τ_i (sec)	τ_d (sec)
Suboptimal gain scheduled PID controller settings	0.20	0.65	0	0.25	0.55	0
Optimal gain scheduled PID controller settings	0.354	4.023	0	0.439	3.429	0

Table 4.2: Gain scheduled controller parameters at respective operating regions.

It is observed from Fig. 4.4(a) that the suboptimal gain scheduler yields excessive oscillations at setpoint r(t)=0%, whilst acceptable control performance occurs at r(t)=25% and r(t)=50%. This is because of the changes to process gain for transitions of $y^p(t)$. From Fig. 4.4(b), the poor closed loop performance is clearly indicated by the proposed NLCPA performance index, where at time t = 200 seconds, $\eta_{NL_{PID}} = 0.96$ and at time t=900 seconds the $\eta_{NL_{PID}} = 0.91$ with suboptimal gain scheduled control; the corresponding indices for the optimally tuned controller are $\eta_{NL_{PID}} = 0.13$ and $\eta_{NL_{PID}} = 0.12$, respectively.

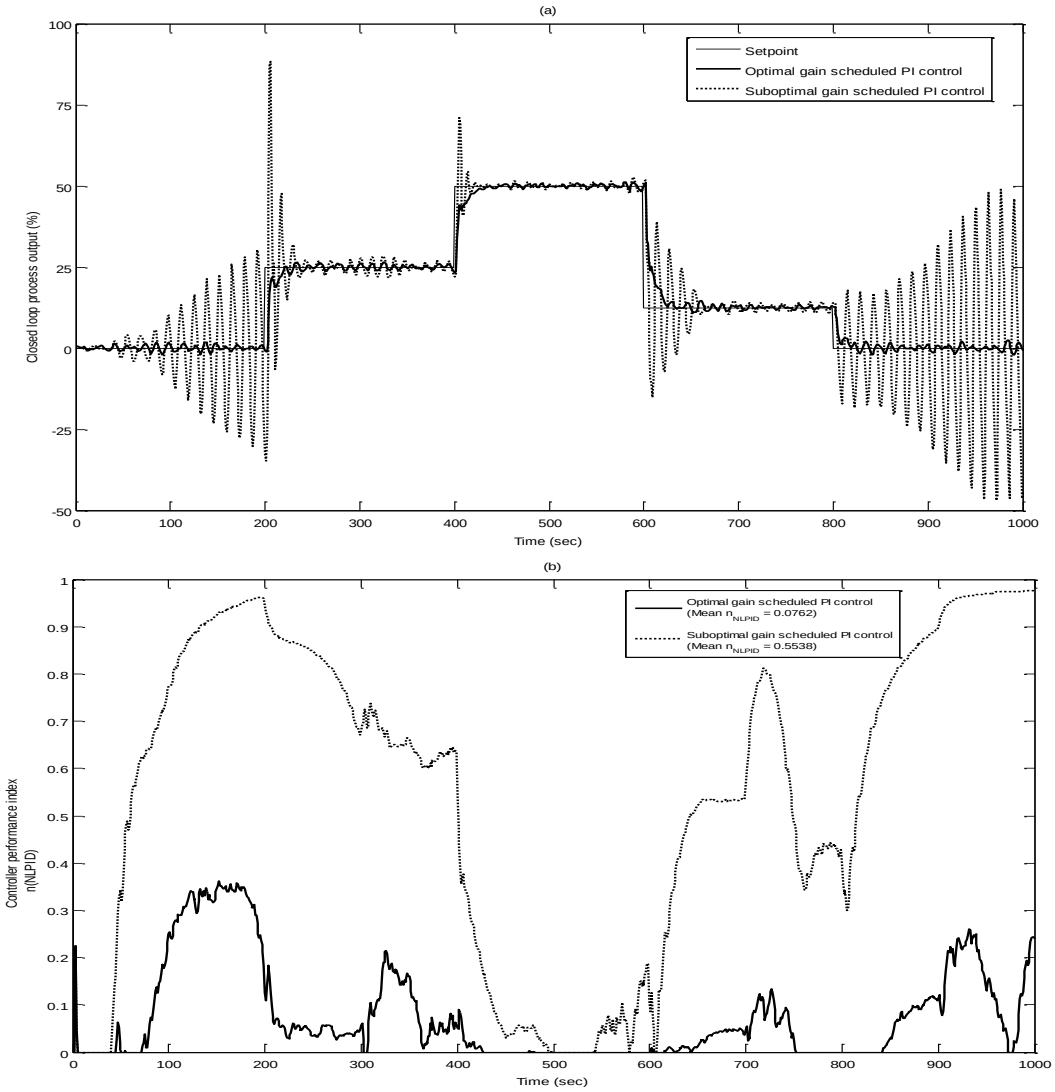

Figure 4.4: (a) Closed loop simulation following setpoints changes

(b) Dynamic NLCPA index for Example 1

4.5.3 Distribution analysis of the dynamic NLCPA index

To study the effects of different controller parameters on the distribution of $\eta_{NL_{PID}}$, the controller integral time constant (τ_i) for each operating region was increased progressively for the simulation case study presented in Section 4.5.2. In this instance, τ_i is chosen because of its substantial impact on the closed loop stability of the selected process. The controller integral time constant was increased to 1.5, 2, 2.5 and 3 times the optimal values of the integral time constants ($\tau_{i_{optimal}}$) at their respective operating points. Fig. 4.5 shows the kernel density estimate of the distribution of $\eta_{NL_{PID}}$ for variations in τ_i.

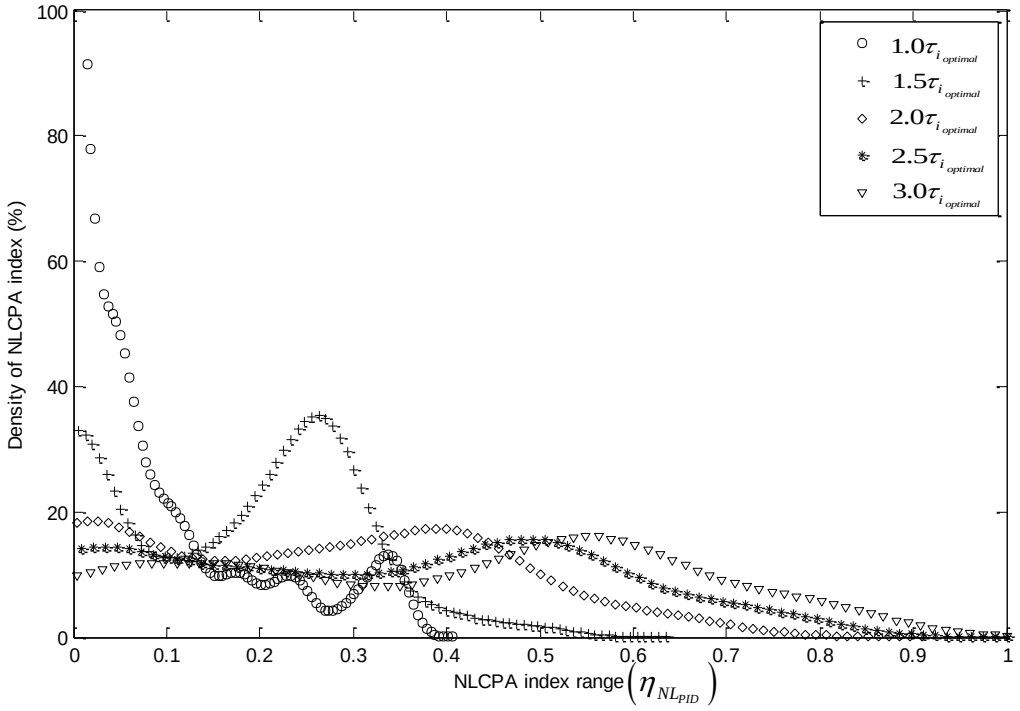

Figure 4.5: Kernel density estimates of $\eta_{NL_{PID}}$ for Example 1 with varying τ_i values.

With regards to Fig. 4.5, the optimal controller values for the NLCPA shows a narrow distribution falling between 0 and 0.4 since $\eta_{NL_{PID}} \to 0$. The main reason for this is attributed to the good performance of the closed loop when using optimal controller tuning parameters. Increasing the integral time (τ_i) parameter away from its optimal values, yields a broader distribution across the NLCPA range as $\eta_{NL_{PID}} \to 1$. This is due to the destabilizing effect of increasing τ_i on the control loop. Three times $\tau_{i_{optimal}}$ yields the worst control performance and has the lowest probability density estimate as $\eta_{NL_{PID}} \to 0$. Table 4.3 shows the variance from the mean of the closed loop error and the corresponding IAE. It is observed that the optimal controller results in the lowest error variance and mean $\eta_{NL_{PID}}$, with a strong correlation as the controller integral time constant is increased. This indicates that the proposed nonlinear index is capable of detecting increasingly poor closed performance when the controller parameters deviate from optimal settings.

Deviation from optimal τ_i	IAE	Error Variance	Mean $\eta_{NL_{PID}}$
$\tau_{i_{optimal}}$	26.24	5.522 x 10^{-3}	0.0763
$1.5\tau_{i_{optimal}}$	32.09	6.823 x 10^{-3}	0.1642
$2\tau_{i_{optimal}}$	38.5	8.233 x 10^{-3}	0.2427
$2.5\tau_{i_{optimal}}$	45.28	9.681 x 10^{-3}	0.3141
$3\tau_{i_{optimal}}$	52.31	11.14 x 10^{-3}	0.3846

Table 4.3: Error indices and the mean controller performance index for increasing integral time constants from Example 1.

4.6 SUMMARY AND CONCLUSIONS

This work has contributed a novel methodology for real time controller performance estimation of SISO nonlinear control loops. NNARMAX based identification procedures and advantages of the methodology have been discussed in this chapter and provide the theoretical foundation necessary for the development of the model based NLCPA.

It has been demonstrated through the use of a nonlinear simulation example that the methodology is effective in determining acceptable and poor closed loop performance when there are setpoint changes. An optimally tuned gain scheduled PID controller was chosen as a realistic benchmark for a broad class of nonlinear dynamic systems represented by the NNARMAX model. The next chapter provides details on real world application of the proposed methodology to a nonlinear pH reactor pilot plant.

Chapter 5

Implementation of the Model Based Nonlinear Controller Performance Assessment Index on pH Neutralization Pilot Plant

5.1 INTRODUCTION

The emphasis of this chapter is to present the results of the model based NLCPA framework developed in the previous chapter on real world process control loops. For the purpose of testing and analysing the proposed methodology, a pH neutralization pilot plant was designed and constructed in the Instrumentation Laboratory at the Department of Electronic Engineering, Durban University of Technology. A discussion of pH acid/base neutralization reaction is provided to demonstrate the intricacies involved in this highly nonlinear process.

In addition, a brief section of this chapter is devoted to the engineering design aspects of the pilot study plant with regards to the ABB™ FREELANCE™ DCS software and communication interface to MATLAB™ SIMULINK™. Important aspects of the practical challenges surrounding process control monitoring software tools are discussed. Finally, we implement the novel performance benchmarking tool developed in the previous chapter on real process control loops of the pilot study plant. Results of these experiments are presented and analysed for further discussion.

5.2 PILOT pH NEUTRALIZATION REACTOR

The control of pH is important in many chemical, wastewater and biological processes. It has been recognised in literature as being a non-trivial control problem (Shinskey, 1973; Gustafsson and Waller, 1983; McMillan, 1994; Narayanan *et al.*, 1997). Difficulties in acceptable pH control arise from strong process nonlinearity in which the process gain changes exponentially in a short range of the pH scale (McMillan, 1994; Lipták, 1995).

Given this fundamental nonlinear characteristic, the automatic controller also has to contend with process load disturbances, unsuitable valve sizing and in some cases, poorly designed processes. These characteristics can be so severe that classical linear feedback controller does not always achieve satisfactory performance (McMillan, 1994; Aström and Hägglund, 1995). Therefore it may be beneficial to provide some nonlinear compensation on these systems.

One such scheme is controller gain scheduling which is commonly employed on many nonlinear process control loops (Rugh and Shamma, 2000). As discussed in Chapter 4, this nonlinear approach is incorporated into the novel model based NLCPA benchmarking tool. The proposed model based NLCPA scheme is applied to the pH neutralization system that is characterised by severe nonlinearity around the pH neutralization point. Chemical process pH reaction nonlinearity is discussed in the next section through physico-chemical models of the designed CSTR pilot plant. A pH titration curve extracted from pilot plant data during initial field experiments shows the strong acid/strong base behaviour.

5.2.1 Description of nonlinear pH neutralization process

An illustration of the pH pilot plant that was constructed for the purpose of this study is shown in Fig. 5.1. For the sake of clarity, it is reduced to a simple process diagram as depicted by Fig. 5.2. In its simplest form, the plant consists of a CSTR in which an alkaline solution (Sodium Hydroxide - NaOH) from a tank is neutralised using a reagent (Sulphuric Acid - H_2SO_4). The control objective is to maintain the pH at a desired setpoint. This is not a trivial task due to the complex nature of the chemical process.

Figure 5.1: pH neutralization pilot plant used in real time experimentation.

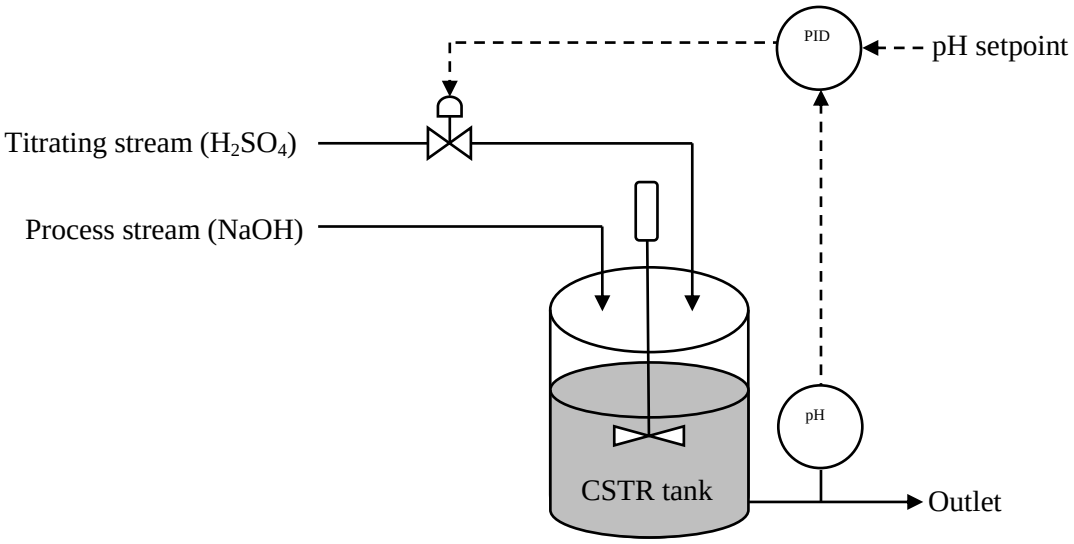

Figure 5.2: Simplified process diagram of the pH control plant.

The primary advantage of using the experimental setup is its availability to obtain process models, albeit on a relatively smaller scale in comparison to an industrial plant. Furthermore, there is an added flexibility in changing the control loop setpoint, the configuration strategy of the automatic controller, flow rates and pneumatic control valve hardware. These changes would not be possible to achieve in a full scale production facility that is normally running.

A detailed Process and Instrument Diagram (P&ID) of the plant is shown in Fig.5.3. Two holding tanks are used to store the process and titrating liquids. The liquids are pumped on demand via centrifugal pumps to the CSTR. Conductivity transmitters mounted inline are used to indicate the concentration levels of the acid and alkaline solutions respectively. Flow control valves regulate required volume of liquid into the CSTR for efficient neutralization. The outlet flow of the CSTR is controlled by a pneumatic valve that maintains a steady level in the tank at desired setpoint. Effluent from the CSTR tank is reserved in final product storage with some liquid returned to the CSTR to aid neutralization mixing during the control experiments. Nominal operating conditions for the plant are listed in Table 5.1.

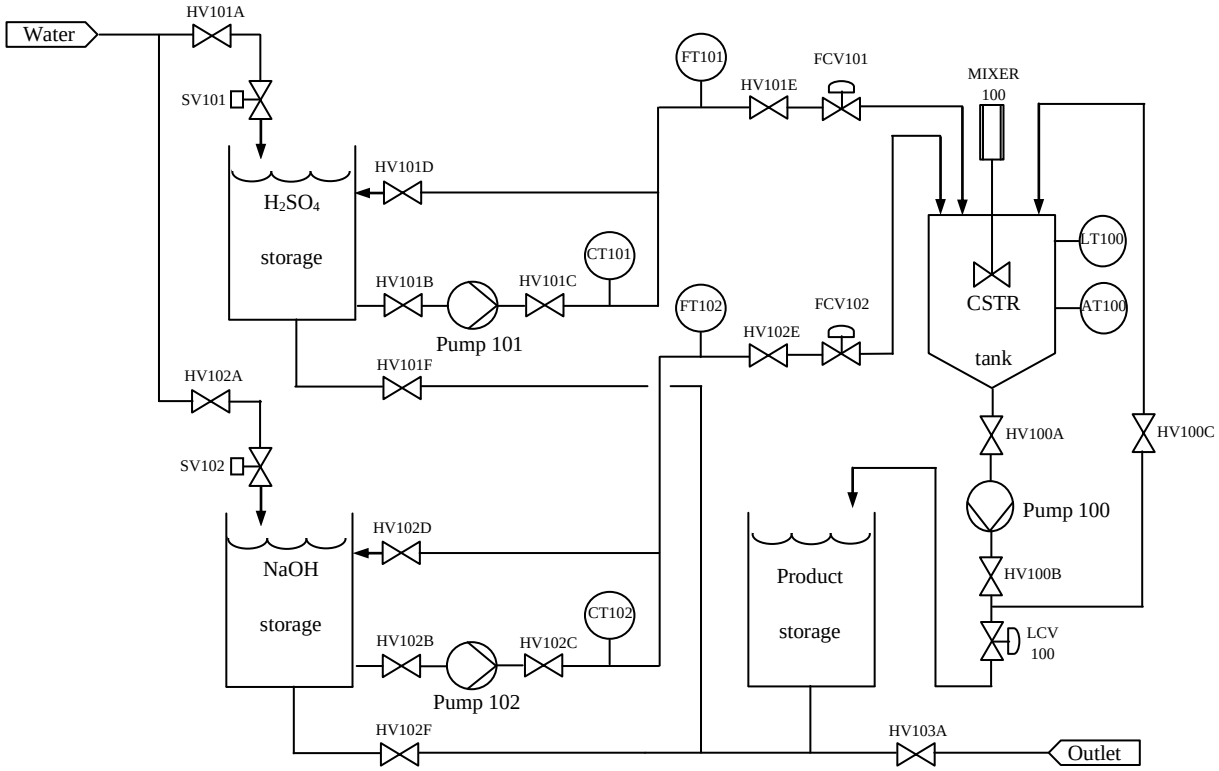

Figure 5.3: P&ID of the pilot study plant

Parameters of the CSTR plant	Value
Temperature	25 °C
Volume of the tank	125 liters
Steady state level of the tank	40 %
Steady state flow rate of NaOH	2.5 liters/min
Range of pH setpoint change	8.5 – 10.5
Concentration of influent process stream, NaOH	32.1×10^{-3} mol./liter
Concentration of titrating stream, H_2SO_4	6.53×10^{-3} mol./liter

Table 5.1: Typical operating conditions for the pH neutralization process

With the assumption that the CSTR tank's volume is constant and perfect mixing is achieved using an agitator blade, the following mixing pH theoretical dynamics can be deduced (McAvoy *et al.*, 1972; Gustafsson and Waller, 1983; Wright and Kravaris, 1991):

$$V_{CSTR}\frac{dx_a}{dt} = F_a C_a - (F_a + F_b)x_a \tag{5.1a}$$

$$V_{CSTR}\frac{dx_b}{dt} = F_b C_b - (F_a + F_b)x_b \tag{5.1b}$$

where:

V_{CSTR} - volume of the CTSR tank,

x_a - concentration of the acid solution in the CSTR,

x_b - concentration of the base solution in the CSTR,

F_a - acid flow rate (titrating stream),

F_b - base flow rate (process stream),

C_a – concentration of the acid entering the tank,

C_b – concentration of the base entering the tank.

As observed from Eq.(5.1a) and Eq.(5.1b), the concentration of the strong acid-strong base mixture in the CTSR tank dynamically changes with respect to time subject to the input flow streams. Therefore the *reaction invariants* in the tank for the acid (x_a) and base (x_b) species may be defined as:

$$x_a = [H_2SO_4] + [HSO_4^-] + [SO_4^{-2}] \tag{5.2}$$

$$x_b = [Na^+] \tag{5.3}$$

Neutralization chemical reactions for the experimental setup are given as:

$$2NaOH + H_2SO_4 = NaSO_4 + 2H_2O \tag{5.4}$$

Therefore the charge balance equation is represented by:

$$[Na^+]+[H^+]=[OH^-]+[HSO_4^-]+2[SO_4^{-2}] \tag{5.5}$$

Corresponding equilibrium constants that relate to the strong acid-strong base system given in Eq. (5.5) are:

$$[OH^-]=\frac{K_w}{[H^+]} \tag{5.6}$$

$$[HSO_4^-]=\frac{K_1[H_2SO_4]}{[H^+]} \tag{5.7}$$

$$[SO_4^{-2}]=\frac{K_2[HSO_4^-]}{[H^+]} \tag{5.8}$$

where, the ionic product of water is $K_w=1\times10^{-14}$. The two dissociation constants for the diprotic classified sulphuric acid is given by; $K_1=1\times10^{3}$ and $K_2=1.2\times10^{-2}$. Finally solving for the hydrogen ion $[H^+]$, the pH value can be calculated as:

$$pH=-\log_{10}[H^+] \tag{5.9}$$

The strong acid-strong base reaction results in a highly nonlinear characteristic around the equivalence point (McMillan, 1994) with the implication of severely affecting control loop performance. The titration curve for the experimental pilot plant is shown in Fig. 5.4, where it is observed that the pH process gain slope is steepest in the region between pH=6 and pH=8.7. This will have a negatively destabilizing effect on a conventional linear PID controller since the loop gain increases significantly in this region.

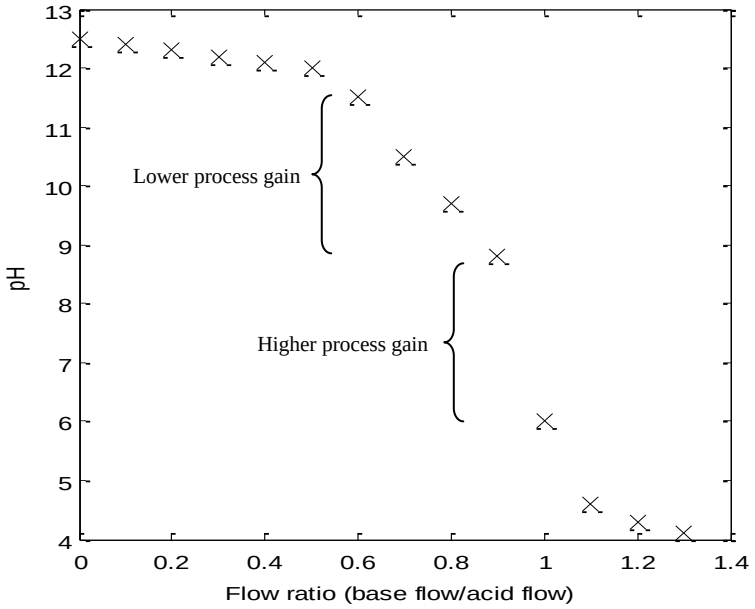

Figure 5.4: Titration curve for the pH neutralization reaction in the pilot plant

5.3 PROCESS CONTROL HARDWARE AND SOFTWARE USED IN THE EXPERIMENTS

An Open Process Control (OPC) server was established to transfer data bi-directionally from the DCS to MATLAB™ SIMULINK™ environment. ABB™ AC700 control hardware was used in the real time control of the process plant and connected to an Intel i7 personnel computer with 4 megabytes of random access memory running MATLAB™ OPC TOOLBOX™ and ABB™ FREELANCE™ programming software.

Experimental interface used in real time controller performance evaluation is shown in Fig.5.5. The advantage of this scheme will allow for implementation of the NLCPA on an external platform while computational power of the DCS is reserved for primary process control computations such as PID control and basic data manipulation.

Furthermore, the DCS platform is rather restricted to primitive function blocks (Hägglund, 2005) and higher level programming tools (for example; system identification and optimization computation) are more suited to a separate computer system that is connected to the DCS through the OPC server. The proposed performance index is computed in MATLAB™ and transmitted to the DCS in real time for presentation on the developed Human Machine Interface (HMI) as illustrated in Fig.5.6.

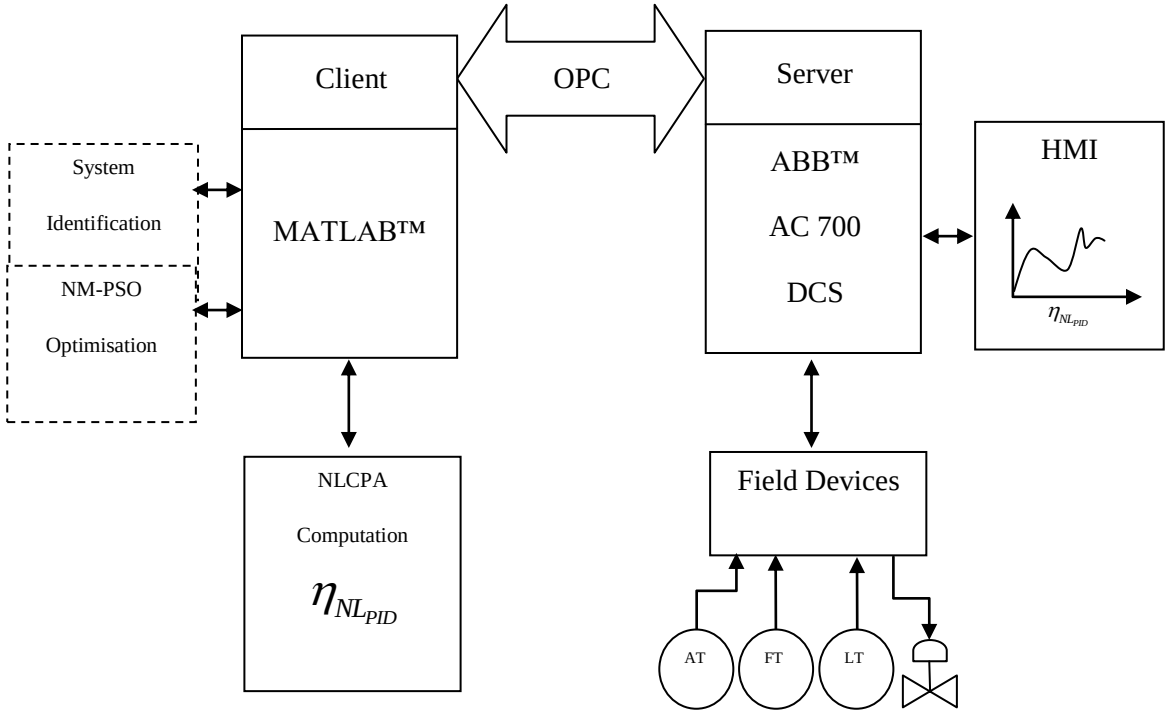

Figure 5.5: Connection between MATLAB™ and plant DCS using OPC TOOLBOX™

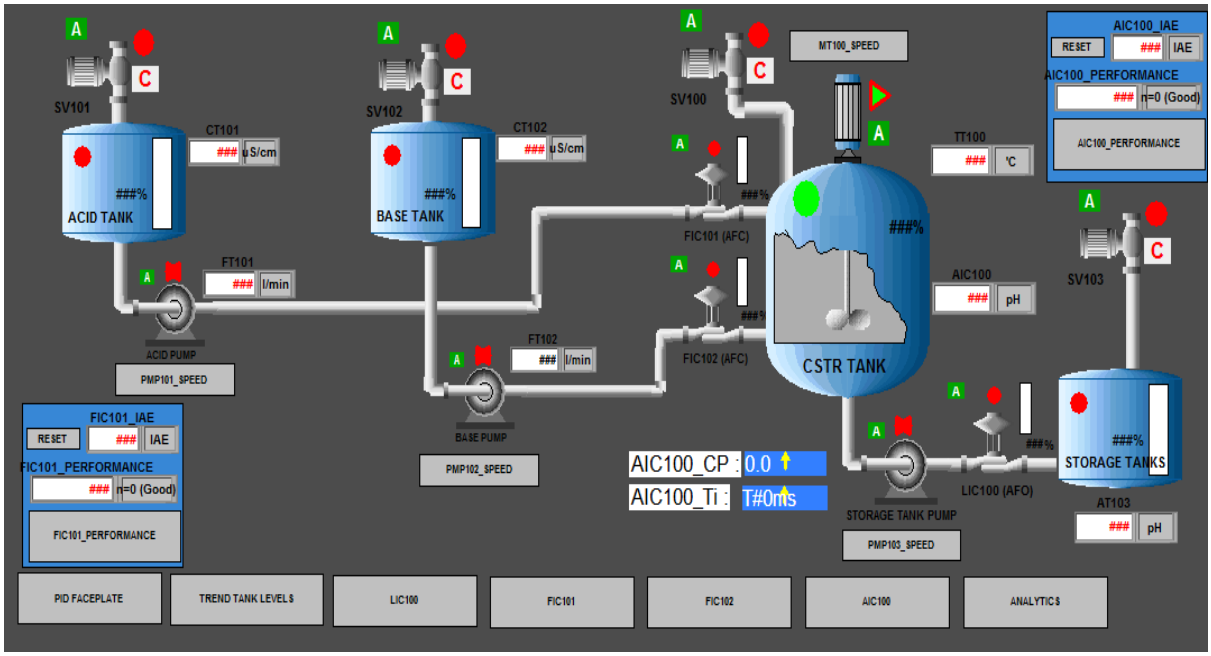

Figure 5.6: ABB™ AC700 DCS HMI indicating pH CSTR process information and real time dynamic NLCPA for pH (AIC100) and acid flow (FIC101) loops.

5.4 PRACTICAL IMPLEMENTATION OF THE PROPOSED MODEL BASED NLCPA BENCHMARK ON THE pH PLANT.

Given the full scale pH neutralization plant described in the previous sections, two nonlinear control loop case studies (pH control and acid flow control) are tested and analysed using the model based NLCPA methodology. Fixed constraints for each case study are given in Table 5.2. Sampling rate (T_s) for the flow control loop is 10 times faster than the pH control since it is very fast acting with small dead times. The number of regression variables (n_u, n_y, n_b) for the models were determined experimentally so as to minimize the modelling errors. Operating regions were chosen from the distinct process gain variations of the system. With regards to the pH control loop (AIC100), two operating regions were sufficient for the PID gain schedule design. This is shown by the two different process gains of the titration curve

in Fig.5.4. Similarly, the flow loop control loop (FIC101) was segmented into two regions for the PID gain scheduling design and is shown in Fig. 5.10. The NLCPA index was evaluated using the optimal and suboptimal PID gain scheduling. Details of the NLCPA application software written in MATLAB™ SIMULINK™ and ABB FREELANCE™ is shown in APPENDIX B.

Case study	Constraints													
	Sample time	Regression variables			Limits on PID settings						Limits on process output			
											Operating region 1		Operating region 2	
	T_s (sec)	n_y	n_u	n_k	$k_{c_{\min}}$	$k_{c_{\max}}$	$\tau_{i_{\min}}$ (sec)	$\tau_{i_{\max}}$ (sec)	$\tau_{d_{\min}}$ (sec)	$\tau_{d_{\max}}$ (sec)	$y^m{}_{\min}$ (%)	$y^m{}_{\max}$ (%)	$y^m{}_{\min}$ (%)	$y^m{}_{\max}$ (%)
pH control (AIC100)	1	2	2	1	0.1	10	100	1000	0	0	50	65	65	80
Flow control (FIC101)	0.1	1	2	1	0.1	20	0.1	10	0.01	1	0	25	25	50

Table 5.2: Constraints used in the determination of the optimal gain scheduled PID controller settings for respective operating regions.

5.4.1 Case study 1: Nonlinear pH neutralization control (AIC100)

Using step tests from the DCS controller output under open loop conditions (see Fig. 5.7), nonlinear CSTR pH dynamics were captured and analyzed for identification purposes. Fig. 5.8 reveals the results of the NNARMAX model output to the actual system behavior. A model fit of 88.44% was achieved.

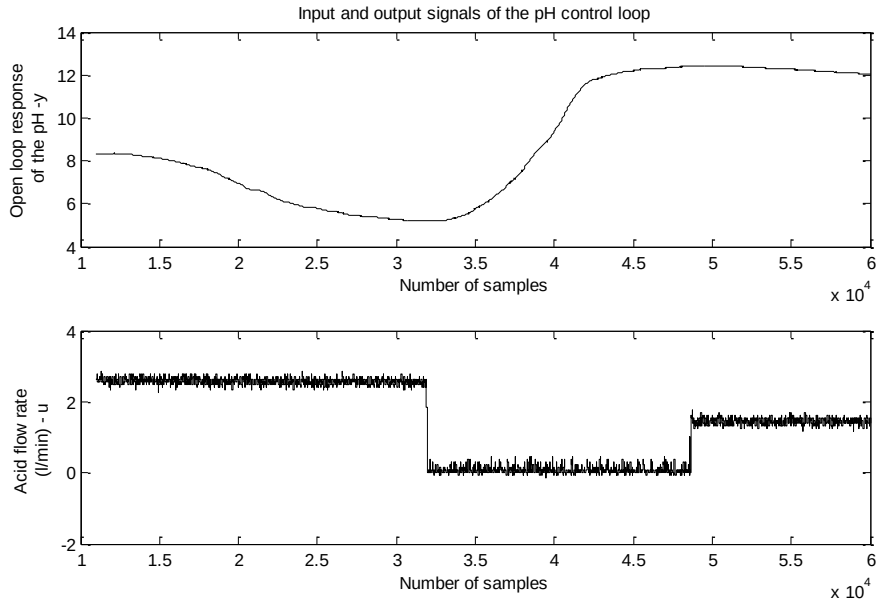

Figure 5.7: Open loop step test for pH (AIC100)

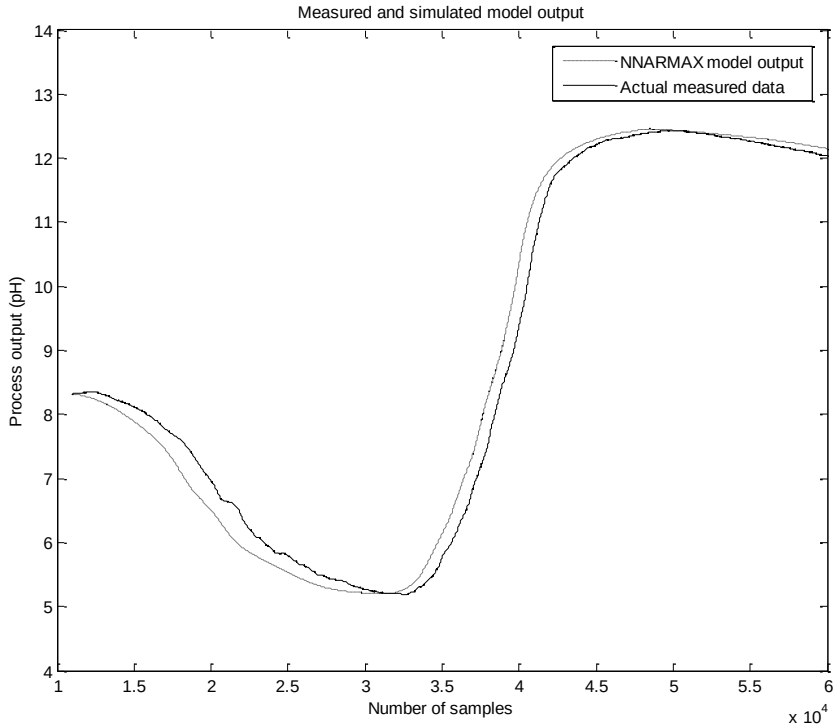

Figure 5.8: NNARMAX model output vs. actual system output for the pH loop (AIC100)

Results of the NM-PSO search algorithm for the optimal gain scheduled PID controller are shown in Table 5.3 at the respective operating segment. The suboptimal gain scheduled PID

controller settings was selected using the relay tuning method of Åström and Hägglund (1984) since the method can be applied in closed loop. Results of the real time plant experiments are shown in Figure 5.9.

CSTR pH control (AIC100)	PID gain scheduled settings					
	Operating region 1			Operating region 2		
	k_c	τ_i	τ_d	k_c	τ_i	τ_d
Suboptimal gain scheduled PID controller settings	5	687	0	5	687	0
Optimal gain scheduled PID controller settings	1.18	787	0	1.25	694	0

Table 5.3: The optimal controller parameters for pH control loop (AIC100) at the respective operating region

From Fig. 5.9(a) we observe that the optimal gain scheduled design resulted in an improved control performance when setpoint changes were made. Due to the large proportional gain of the suboptimal control design, it results in excessive oscillatory behavior particularly when the setpoint approaches the pH equivalence region where the pH process gain is very high. With regards to Fig. 5.9(b), the computed mean values of the NLCPA index for the suboptimal and optimal gain scheduled controllers are $\eta_{NL_{PID_{suboptimal}}} = 0.759$ and $\eta_{NL_{PID_{optimal}}} = 0.423$ respectively. The contrasting effects of different closed loop responses are clearly indicated by the proposed NLCPA index.

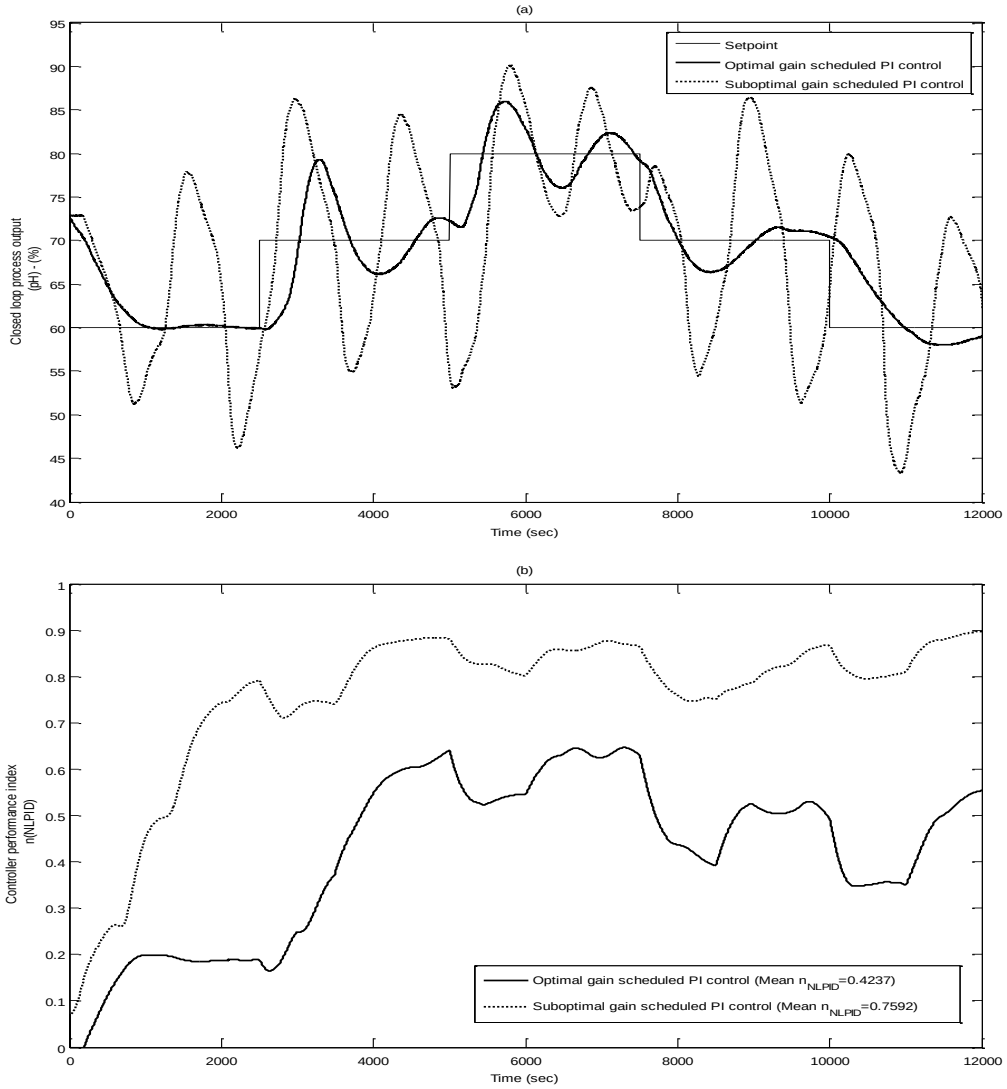

Figure 5.9: (a) Closed loop pH response following setpoint change for the fixed PID controller and optimal gain scheduled PID controller

(b) Dynamic NLCPA index

5.4.2 Case study 2: Acid flow rate control with valve nonlinearity (FIC101)

In this section, we apply the proposed methodology to a flow control loop in the pilot plant discussed in the previous example. Since nonlinearity may stem from the process itself or in the actuators of the control valves we focus attention to actuator nonlinearity in this case study. Actuator or valve nonlinearities are typically due to faults such as stiction, hysteresis, saturation, dead zone, and/or corroded valve seats (Choudhury *et al.*, 2004). The flow control valve (FCV101) which is responsible for controlling acid flow rate into the CSTR showed signs of hysteresis when stroked to full valve travel in manual mode (see Fig. 5.10). This has a nonlinear effect on the flow control loop, where at low flow rates (0 l/min to 3 l/min) the installed gain of the control valve is smaller when compared to higher flow rates (3 l/min to 7 l/min). Thus the flow control loop at low flow rates has marginally smaller overall loop gain dynamic when compared to higher flow rates.

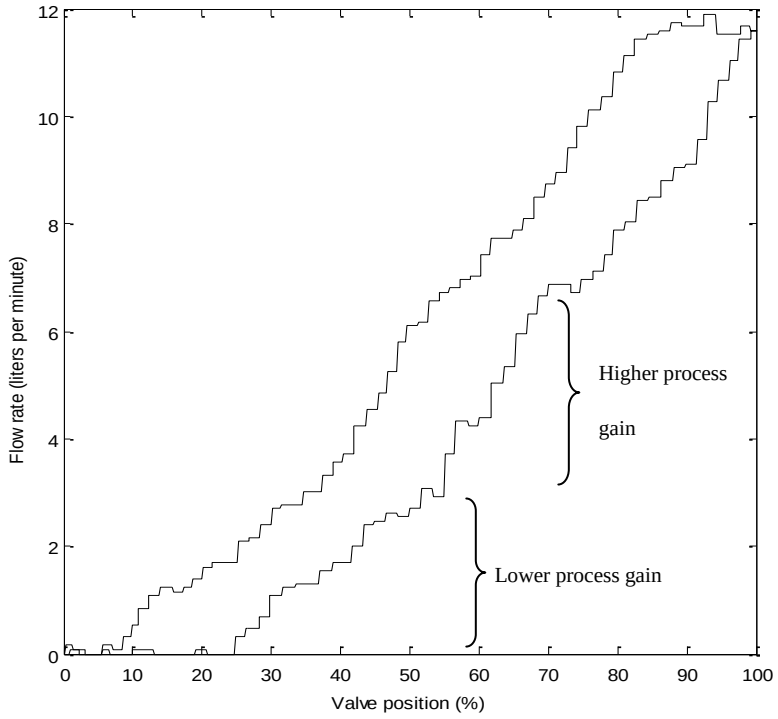

Fig.5.10: (a) Acid flow control valve (FCV101) with hysteresis nonlinearity

Open loop step test of the pneumatic control valve and flow dynamic characteristics are shown in Fig 5.11 and Fig 5.12 respectively. Nonlinear modeling of the dynamic flow rate behavior was captured with an 88.01% fit.

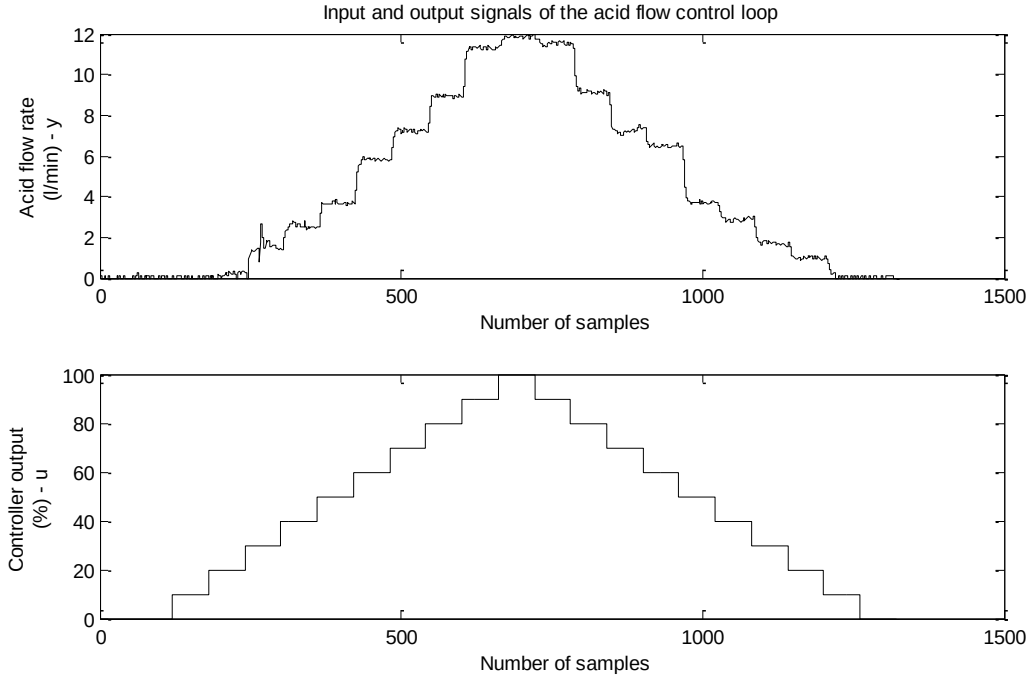

Fig. 5.11: Open loop step test for acid flow control valve with hysteresis (FIC101)

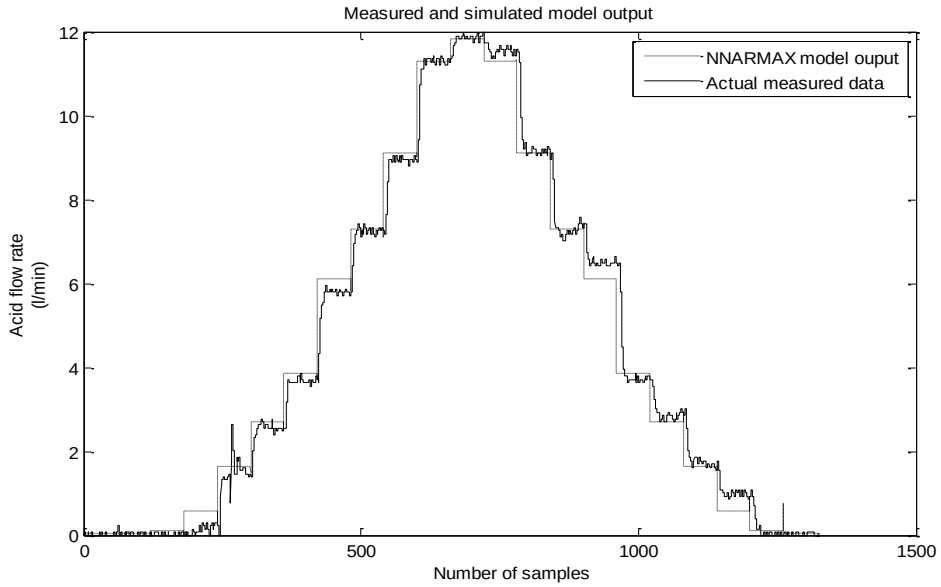

Fig. 5.12: NNARMAX model output vs. actual system output for the flow loop (FIC101)

Table 5.4 shows the PID parameters for the optimally tuned and suboptimal controller for each operating region. Suboptimal controller settings were derived using the relay tuning method (Åström and Hägglund, 1984) for the reasons provided in the previous section. With regards to the observations made from Fig 5.13(a), the suboptimal system shows constant oscillatory behavior at a higher setpoint flow rate of 42% and the optimal gain scheduled PID control yields improved setpoint tracking. Fig 5.13(b) shows the corresponding NLCPA index for closed loop control systems. The suboptimal PID gain schedule gives a the mean value of $\eta_{NL_{PID}} = 0.3023$. A peak value of $\eta_{NL_{PID}} = 0.795$ is observed at 241 seconds. In contrast, the optimal gain schedule PID controller gives a mean value of $\eta_{NL_{PID}} = 0.1542$. The presented case study demonstrates the efficacy of the proposed NLCPA methodology in detecting varying closed loop performance.

Acid flow control (FIC101)	PID gain scheduled settings					
	Operating region 1			Operating region 2		
	k_c	τ_i	τ_d	k_c	τ_i	τ_d
Suboptimal gain scheduled PID controller settings	4.1	1.37	0.38	4.1	1.37	0.38
Optimal gain scheduled PID controller settings	5.48	1.54	0.14	4.54	1.09	0.44

Table 5.4: PID gain scheduled parameters for acid flow control loop (FIC101) at the respective operating points

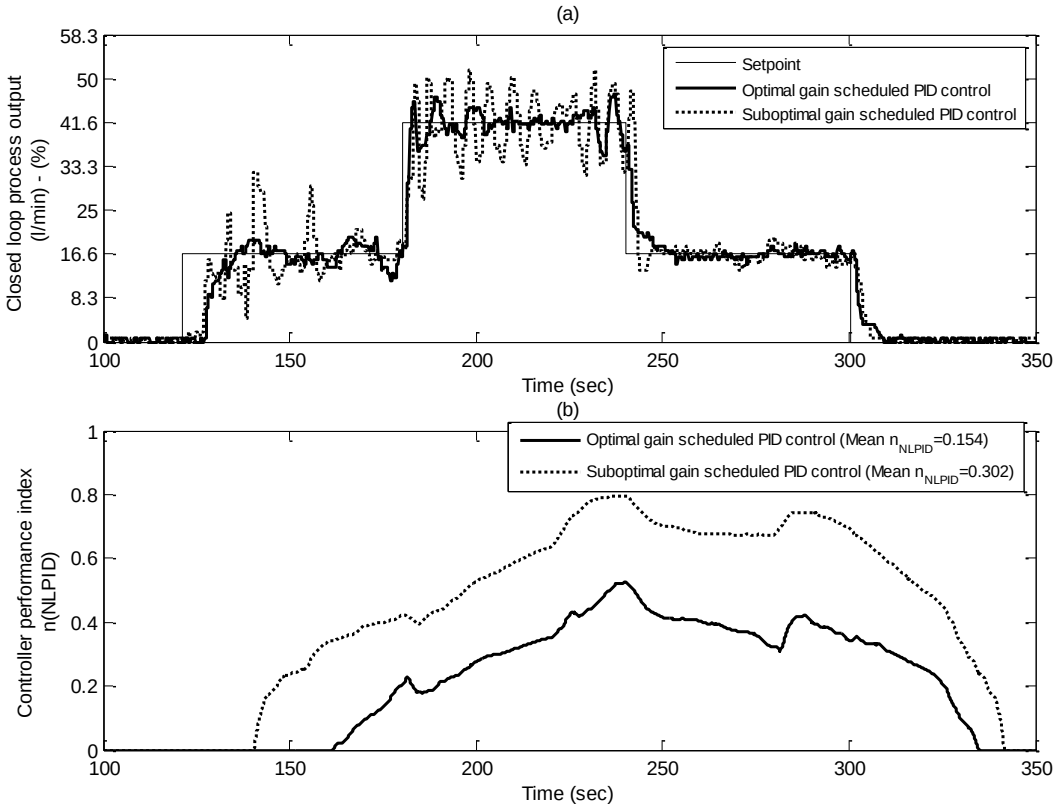

Fig 5.13: (a) Closed loop flow output following setpoint for optimal gain scheduled PID controller and fixed PID control.

(b) Dynamic NLCPA index.

5.5 SUMMARY AND CONCLUSIONS

This chapter presents the real world experiments conducted on a pH pilot study plant to test the efficacy of the proposed model based NLCPA framework for real time controller performance estimation of SISO nonlinear control loops. It has been demonstrated through the use of pH control that the methodology is effective in determining acceptable and poor closed loop performance when there are setpoint changes made.

The technique has been successfully implemented online using an OPC server interface that establishes access of the process control loop variables from the DCS in real time. This approach allows for convenient transfer of raw process data to the monitoring PC running the

NLCPA tool. Using the proposed NLCPA index, simple high alarms can be setup for each process control loop to alert the operator in the event of poor control loop behavior.

As a requirement, the proposed NLCPA method uses an open loop nonlinear model of the system. A noticeable drawback of the method is its dependence on the trained ANN model. If an inaccurate model is used then it may cause failure of the NLCPA methodology. In addition, adequate process excitation must be achieved for systematic nonlinear system identification. This may not be achievable during normal plant operation, hence an alternative data driven CPA methodology is described in the following chapter.

Chapter 6

Performance Diagnosis of Nonlinear Control Loops based on Multi-Class Support Vector Machines

6.1 INTRODUCTION

The aim of this chapter is to present a novel framework using Multi-Class Support Vector Machines (MC-SVMs) to classify the performance of closed loop SISO feedback controllers[1]. A SVM is trained to recognise descriptive statistical patterns originating from the autocorrelation function (ACF) of process data vectors from a linear time variant (LTV) FOPDT model with valve nonlinearity. ACF patterns emanating from different closed loop behaviours are used in the feature extraction procedure. Simulation studies and application to real world industrial data sets show that the MC-SVM classification tool is capable of detecting and diagnosing problematic control loops with very good accuracy and efficiency.

Unlike the use of model based CPA methods, the proposed framework relies only on the salient statistical features of the input data emanating from the ACF signal. Since MC-SVMs have not been used for CPA, their performance is still an open issue.

[1]A version of this chapter is accepted for publication by the Journal of Control Engineering and Applied Informatics.

6.2 EXPLOITING THE ACF FOR CPA

ACF is essentially cross correlation of a signal with itself at different lags(l). It gives a measure of how close the values of the variables are when measured at different time intervals. With a set of n data samples, the ACF is defined as (Karra and Karim, 2009; Howard and Cooper, 2010):

$$\rho(l) = \frac{\sum_{t=1}^{n-l}(y(t)-\bar{y})(y(t+l)-\bar{y})}{\sum_{t=1}^{n}(y(t)-\bar{y})^2} \tag{6.1}$$

where, y is the measured value of the signal at time t and $\bar{y}$ represents its mean. For control systems designed for setpoint tracking, $y(t)$ is replaced with the error signal $e(t) = r(t) - y(t)$ in Eq. (6.1).

It is well known in literature that the ACF of the process variable (PV) time series reveals important characteristics of closed loop behavior and is often used as a preliminary check (Karra and Karim, 2009; Howard and Cooper, 2010; Jelali, 2013). For instance, oscillatory signals possess certain unique mathematical properties that can be characterised by its sample ACF (Howard and Cooper, 2010). Further, Box *et al.* (1970) showed that the disturbance rejection characteristic of a control system output is related to the ACF coefficients. In the methodology presented by Howard and Cooper (2010), a second order continuous time model was fitted to the ACF curve. The damping coefficient was then used to define a relative damping index (RDI) which provides a measure of loop performance.

Performance measure falls into the categories of *sluggish* or *aggressive* closed loop behavior. Although the method is simple to understand and easy to implement it does depend heavily on the accuracy of the ACF curve fit. In order to present the novel NLCPA

methodology in a cohesive framework, a review of MC-SVMs is described in the subsequent sections. Several important terms and characteristic of the algorithm are discussed.

6.3 AN OVERVIEW OF MC-SVMs

Support vector machines (SVMs) are a powerful statistical learning theory approach to classification problems. This has been demonstrated in successful application of the algorithm in areas of image recognition, text detection and speech verification (Chapelle *et al.*, 1999; Yang *et al.*, 2005; Widodo and Yang, 2007; Kampouraki *et al.*, 2009). Motivation for it use in this work are its superior accuracy and generalization capabilities in comparison to ANNs, especially when a smaller number of samples are available in practice (Cortes and Vapnik, 1995). A review of SVMs in the research field of machine condition monitoring and fault diagnosis is given by Widodo and Yang (2007).

Typically SVMs are used to recognise special patterns from an acquired signal which are classified according to specific fault occurrence in the machine. Following signal acquisition, certain statistical features are extracted from the data for the purpose of determining the defining features of the specific fault. Such features are then considered suitable training patterns for recognition.

SVMs were originally developed for binary classification problems but can easily be effectively extended to multi-class problems (Yang *et al.*, 2005). The basic approach is to construct and combine several binary classifiers. One-against-one (OAO) applies pair-wise classification between the different classes while one-against-all (OAA) compares a given class with all the other classes grouped together (Widodo and Yang, 2007). OAO method constructs $k(k-1)/2$ classifiers where each one is trained on data from two classes. For

instance, if $k=5$ then 10 binary SVM classifiers need to be constructed rather than 5 as in the case of OAA approach. Although this requires a larger training time, the individual problems that need to be trained are significantly smaller and therefore we utilize OAO in this work.

Consider a set of N training samples $\{(\mathbf{x}_i, y_i)\}_{i=1,2,\ldots,N}$, with $\mathbf{x}_i \in \Re$ representing the input vectors and $y_i \in \{-1, +1\}$ denoting the class labels. With regards to Fig. 6.1, the black triangles correspond to the "Negative Class" and white circles represent the "Positive Class". The primary objective of the SVM algorithm is to orientate a separating hyperplane (H_0) between the two distinct classes such that the "Margin" (m) between the dotted lines is maximised. The optimal separating hyperplane is positioned at the centre of the margin. Bordering sample points close to the separating hyperplane which define the margin are called support vectors as shown by the grey triangles and circles. Once the support vectors have been selected, the remaining data points in the feature space become redundant since the classification decision process is solely based on the information provided by the particular support vectors.

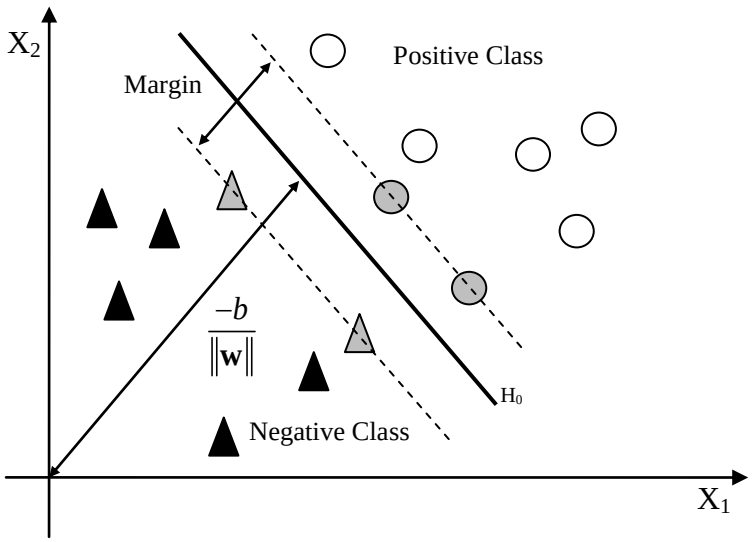

Figure 6.1: SVM classification of two classes

The points **x** which lie on the separating hyperplane satisfy the following condition:

$$f(\mathbf{x}) = \mathbf{w} \cdot \mathbf{x} + b = 0 \tag{6.2}$$

where, **w** is a normal vector to the separating hyperplane and *b* denotes the bias term used to define the position of the separating hyperplane. $|b| / \|\mathbf{w}\|$ is the perpendicular distance from the origin to the separating hyperplane and $\|\mathbf{w}\|$ is the Euclidean norm of $\mathbf{w}$. For linearly separable data, the margin is defined by the following constraints:

$$\mathbf{w} \cdot \mathbf{x}_i + b \geq +1 \text{ for } y_i = +1 \tag{6.3}$$

$$\mathbf{w} \cdot \mathbf{x}_i + b \leq -1 \text{ for } y_i = -1 \tag{6.4}$$

equivalent to:

$$y_i(\mathbf{w} \cdot \mathbf{x}_i + b) - 1 \geq 0, \quad i = 1, \ldots, N \tag{6.5}$$

The binary SVM classifier is written as:

$$f(\mathbf{x}) = sign(\mathbf{w} \cdot \mathbf{x}_i + b) \tag{6.6}$$

The decision function is based on the sign of $f(\mathbf{x})$ to classify input data either as +1 or -1. Given that there are many possibilities of separating hyperplanes in the feature space, the SVM classifier locates the hyperplane that best maximizes the separating margins between the two classes. With regards to Fig. 6.1, $m = \frac{2}{\|\mathbf{w}\|}$ represents the maximum distance between the hyperplanes. We subject *m* to Eq. (6.3) and (6.4) and replace it with its equivalent minimisation of the cost function:

$$J(\mathbf{w}) = \frac{1}{2}\|\mathbf{w}\|^2 \tag{6.7}$$

The optimisation problem given in Eq. (6.7) can be solved using quadratic programming but instead reformulated into its primal Lagrange (L_P) multiplier equivalent. This allows for efficient handling of constraints imposed by Eq. (6.5) and the training data only appears in the form of dot products between vectors. Conversion of Eq. (6.7) into its equivalent Lagrangian primal form with Karush-Kuhn-Tucker (KKT) conditions imposed yields:

$$L_P(\mathbf{w},b,\alpha)=\frac{1}{2}\|\mathbf{w}\|^2-\sum_{i=1}^{N}\alpha_i\left[y_i(\mathbf{w}\cdot\mathbf{x}_i+b)-1\right] \tag{6.8}$$

where, $\alpha=(\alpha_1,...,\alpha_i)$ represents non-negative Lagrange multipliers associated with constraints of Eq. (6.5).

Given Eq. (6.8), we find the derivative of L_P with respect to $\mathbf{w}$ and b, and simultaneously require that the derivatives of L_P with respect to all α vanish. For

$$\frac{\partial L_p}{\partial \mathbf{w}}=0 \quad \Rightarrow \quad \mathbf{w}=\sum_{i=1}^{N}\alpha_i y_i \mathbf{x}_i \tag{6.9}$$

and

$$\frac{\partial L_p}{\partial b}=0 \quad \Rightarrow \quad \sum_{i=1}^{N}\alpha_i y_i=0 \tag{6.10}$$

We substitute Eq. (6.9) and (6.10) into Eq. (6.8) to get the dual Lagrangian (L_D) formulation:

$$L_D(\mathbf{w},b,\alpha)=\sum_{i=1}^{N}\alpha_i-\frac{1}{2}\sum_{i,j=1}^{N}y_i y_j\alpha_i\alpha_j(\mathbf{x}_i\cdot\mathbf{x}_j) \tag{6.11}$$

Given Eq. (6.11), the task is to solve for the Lagrangian multiplier (α) that maximizes the function:

$$W(\alpha) = \sum_{i=1}^{N} \alpha_i - \frac{1}{2} \sum_{i,j=1}^{N} y_i y_j \alpha_i \alpha_j (\mathbf{x}_i \cdot \mathbf{x}_j) \tag{6.12}$$

subject to, $\alpha_i \geq 0, \quad i = 1, \ldots, N, \quad \sum_{i=1}^{N} \alpha_i y_i = 0$

Solving the dual optimization problem yields the Lagrangian multipliers necessary to express **w** in Eq. (6.6). This leads to the decision function given by:

$$f(\mathbf{x}) = sign\left(\sum_{i,j=1}^{N} y_i \alpha_i (\mathbf{x}_i \cdot \mathbf{x}_j) + b \right) \tag{6.13}$$

However in most real world applications, the sampled data may contain overlapping points which makes linear separation unattainable. Therefore a restricted number of misclassifications should be allowed around the margin. In this case, a set of slack variables; $\beta_i \geq 0, i = 1, ..., N$ are introduced. This represents the distance by which the linearity constraint is violated and is given by:

$$y_i (\mathbf{w} \cdot \mathbf{x}_i + b) \geq 1 - \beta_i, \ \beta_i \geq 0, \quad i = 1, \ldots, N \tag{6.14}$$

Hence, the modified cost function of Eq. (6.7) which accounts for the extent of the constraint violations becomes:

$$J(\mathbf{w}, \beta) = \frac{1}{2} \|\mathbf{w}\|^2 + c \sum_{i=1}^{N} \beta_i \tag{6.15}$$

where ‘c’ represents a user defined positive regularization constant. In this instance $c=1$ yielded the best cross validation results during trials using new data. The constant controls the stringency of the constrained violations and therefore defines the trade-off between a large margin and misclassification error. As before, the dual Lagrangian multipliers need to be formulated and solved in order to articulate the decision function.

If a linear boundary is unable to separate the two classes effectively, then the input data is mapped into a high-dimensional feature space through nonlinear mapping. Within this high-dimensional feature space, a separating hyperplane is constructed that linearly separates the class groups. This is achieved using nonlinear kernel vector functions, $\mathbf{\Phi(x)} = (\phi_1(\mathbf{x}),\ldots,\phi_q(\mathbf{x}))$ to map the *m*-dimensional input vector $\mathbf{x}$ onto the *q*-dimension feature space. In this work, linear, polynomial (Poly) and radial basis function (RBF) kernel functions are tested in the proposed CPA methodology and represented as:

$$K(\mathbf{x}_i,\mathbf{x}_j) = \left[\mathbf{\Phi}(\mathbf{x}_i)\cdot\mathbf{\Phi}(\mathbf{x}_j)\right] \tag{6.16}$$

Substituting Eq. (6.16) into Eq. (6.13), the SVM decision function becomes:

$$f(\mathbf{x}) = sign\left(\sum_{i,j=1}^{N} y_i\alpha_i\left[\mathbf{\Phi}(\mathbf{x}_i)\cdot\mathbf{\Phi}(\mathbf{x}_j)\right]+b\right) \tag{6.17}$$

Formulation of the OAO SVM classifier requires training data from the *ith* and *jth* classes. $y_i \in \{1,...,k\}$, where *k* denotes the number of classes and is *5* for this study. The following modification results in minimization of the binary classification given by:

$$J\left(\mathbf{w},\beta\right) = \frac{1}{2}\left\|\mathbf{w}^{ij}\right\|^2 + c\sum_t \beta_t^{ij} \tag{6.18}$$

subject to the constraints

$$(\mathbf{w}^{ij})^T \phi(\mathbf{x}_t) + b^{ij} \geq 1 - \beta_t^{ij} \qquad \text{for} \quad y_t = i,$$

$$(\mathbf{w}^{ij})^T \phi(\mathbf{x}_t) + b^{ij} \leq -1 + \beta_t^{ij} \qquad \text{for} \quad y_t = j,$$

and

$$\beta_t^{ij} \geq 0, \qquad \text{for } j = 1, 2, \ldots, q.$$

Where, the training data $\mathbf{x}_t$ is mapped to a higher dimensional space by kernel function ϕ. The binary classification problem is therefore modified to include combinations of SVMs from different classes (OAO) as illustrated in Fig.6.2. If sign $((\mathbf{w}^{ij})^T \phi(\mathbf{x}) + b^{ij})$ decision gives **x** in the *i*th class, then the vote for the *i*th class is incremented by one, otherwise the *j*th class is increased by one. New input vectors are predicted to belong to a certain class using the largest vote as the selection criteria. We now advance to explain feature extraction for developing the MC-SVM for the CPA problem.

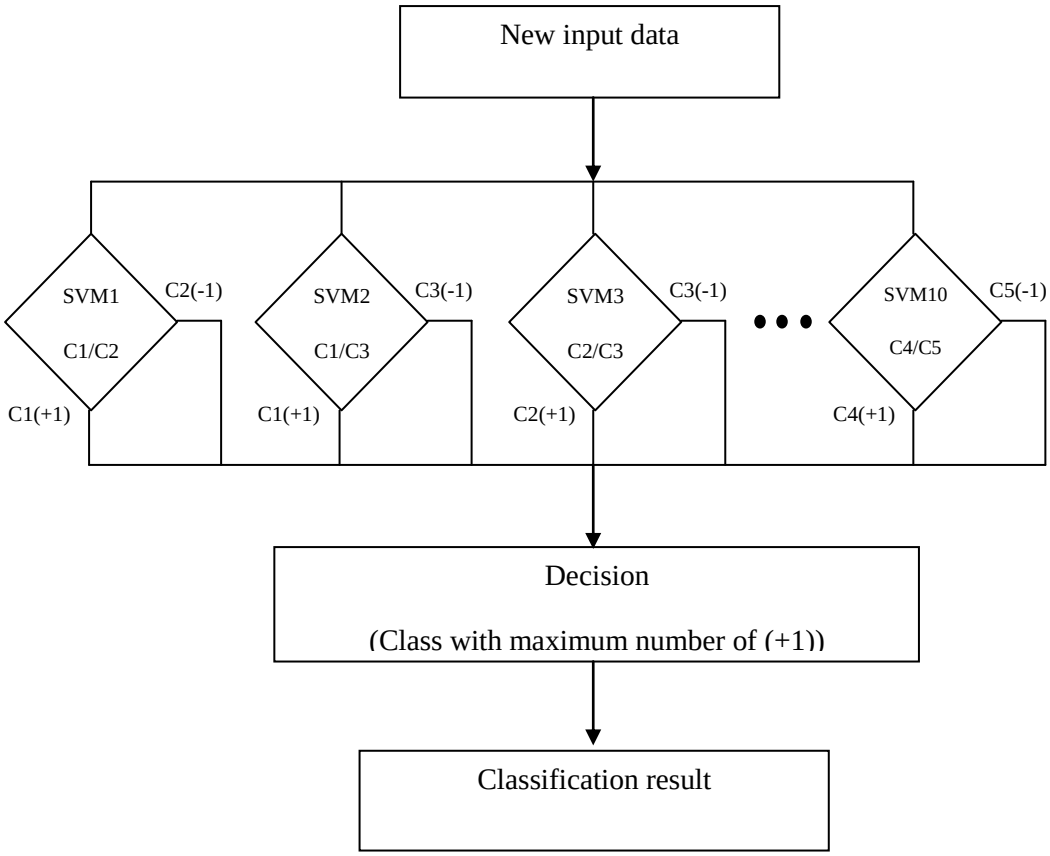

Figure 6.2: MC-SVM based “one-against-one” strategy used in the study

6.4 DEVELOPMENT OF THE DATA DRIVEN NLCPA TOOL

6.4.1 SISO nonlinear system description

Consider a negative closed loop feedback system shown in Fig. 6.3. The destabilizing effects of FCE nonlinearity, load and noise disturbances are taken into account. As mentioned previously the process is represented as a LTV FOPDT model given by:

$$G_p(s) = \frac{K_p \exp^{-\theta_p s}}{T_p s + 1} \tag{6.19}$$

where, Kp , Tp and θ_p represent the process gain, time constant and plant dead time respectively.

Using the process model in Eq. (6.19), simulations were conducted under different operating conditions with a conventional PI controller. Varying conditions such as valve static friction nonlinearity (Choudhury *et al.*, 2005), stochastic sensor noise and load disturbances behaviours were used to replicate real world conditions.

For each respective transfer function, the values of Kp ,Tp and θ_p were varied to simulate nonlinear time varying effects. Using simulated process data from these systems, the corresponding ACF patterns from the process output and control error was recorded. In the next section, statistical analysis is conducted on the ACF patterns for use on the novel MC-SVM CPA scheme.

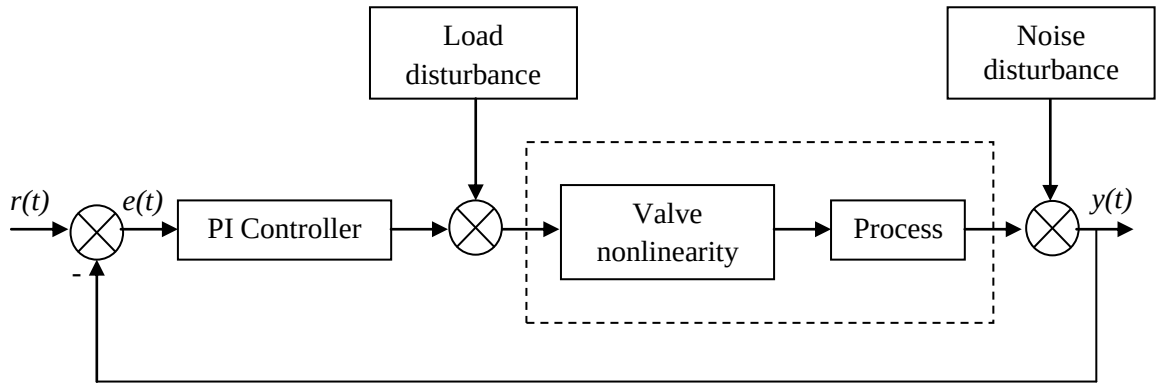

Figure 6.3: Closed loop feedback system under consideration with valve nonlinearity and external disturbances

6.4.2 Proposed ACF feature extraction and automated MC-SVM CPA

At first, we present ACF results for different closed loop performance conditions commonly encountered in most processes. Then, simple statistical features describing the different classes are used for feature extraction. Finally, these distinguishing features are used to train a MC-SVM classification utility for controller performance diagnosis. Fifteen key ACF patterns presented in Fig. 6.4 highlight the findings of the simulation study. The observed ACF features fall into five distinct classes with labels indicating the proposed controller performance classification criteria.

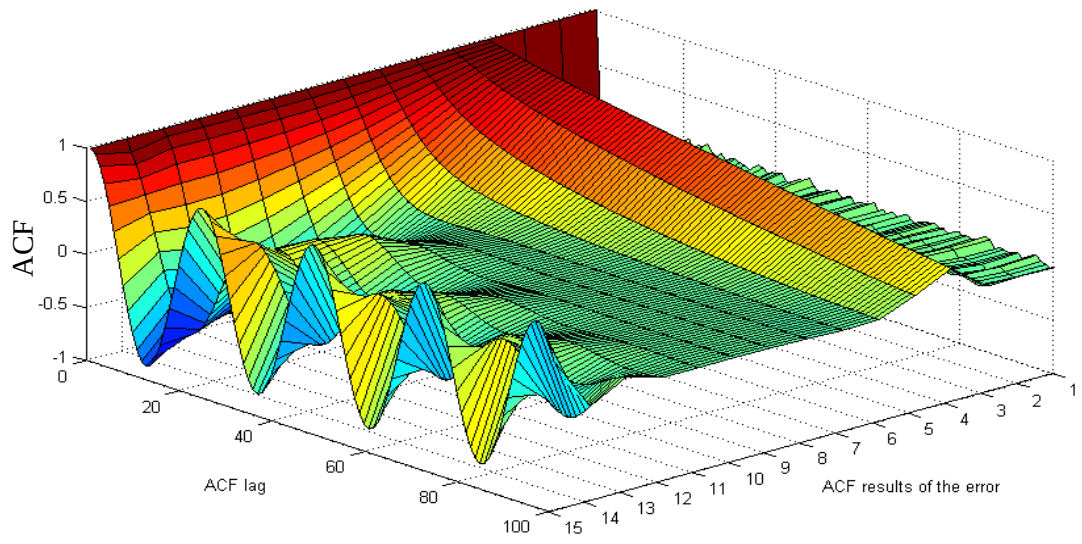

ACF number	Class	Label	Characteristic	SVM Label[2]
1-3	C1	Noise	High SNR	1
4-6	C2	Sluggish	Detuned system	2
7-9	C3	Acceptable	Optimal response	3
10-12	C4	Aggressive	Underdamped system	4
13-15	C5	Oscillatory	Limit cycling	5

Figure 6.4: Fifteen ACF signatures corresponding to different closed loop performance data

[2]The choice of SVM classification label number is inconsequential and may be replaced with other numerical indices relating to specific class description.

These classes were selected based on the following occurring system behaviour; high signal to noise ratio (C1), detuned systems which act slowly (C2), satisfactory performance with fast settling time and minimal overshoot (C3), high gain systems with large overshoots and longer settling time (C4), and systems which exhibit constant oscillatory behaviour (C5).

Simple box plots (see Fig. 6.5) of the ACF patterns (ACF1-ACF15) for each class (C1-C5) reveal several important characteristics. The distinguishing features of the ACF lag coefficients (ρ) are described below.

i) Mean:

$$\bar{\rho} = \frac{1}{l}\sum_{i=1}^{l}\rho(i) \tag{6.20}$$

where $\bar{\rho}$ is the mean value of the ACF coefficients for each subset class. In this work, the number of lags *(l)* is computed using the number of samples *(n)* by the relationship $l=n/5$. The data sampling rate is therefore an important consideration which provides a suitable length of data necessary to represent the whole picture of process activity. Howard and Cooper (2008) recommend sampling data at ten times the overall time constant of the process.

ii) Variance:

$$\text{var}(\rho) = \frac{1}{l}\sum_{i=1}^{l}(\rho(i) - \bar{\rho})^2 \tag{6.21}$$

provides a measure of dispersion of the set of ACF ρ-values for each class. Small variance indicates that the ACF lag coefficients are close to the mean, whereas a larger value will indicate data is spread out away from the mean.

iii) Interquartile range:

$$iqr(\rho) = Q_3 - Q_1 \tag{6.22}$$

is the relative statistical probability distribution of ACF ρ-values between the upper 75% (Q_3) and lower 25% (Q_1) quartiles.

iv) Skewness:

$$\gamma(\rho) = \frac{\frac{1}{l}\sum_{i=1}^{l}(\rho(i) - \bar{\rho})^3}{\left(\sqrt{\frac{1}{l}\sum_{i=1}^{l}(\rho(i) - \bar{\rho})^2}\right)^3} \tag{6.23}$$

describes the measure of symmetry of the probability distribution of ACF ρ-values. Normally distributed data that are symmetrical around its mean will have $\gamma(\rho) = 0$.

By considering the descriptive statistical analysis (Eq. 6.20-6.23) on the ACF coefficients (ρ), a summary of the feature extraction is presented in Fig.6.6 and Table 6.1.

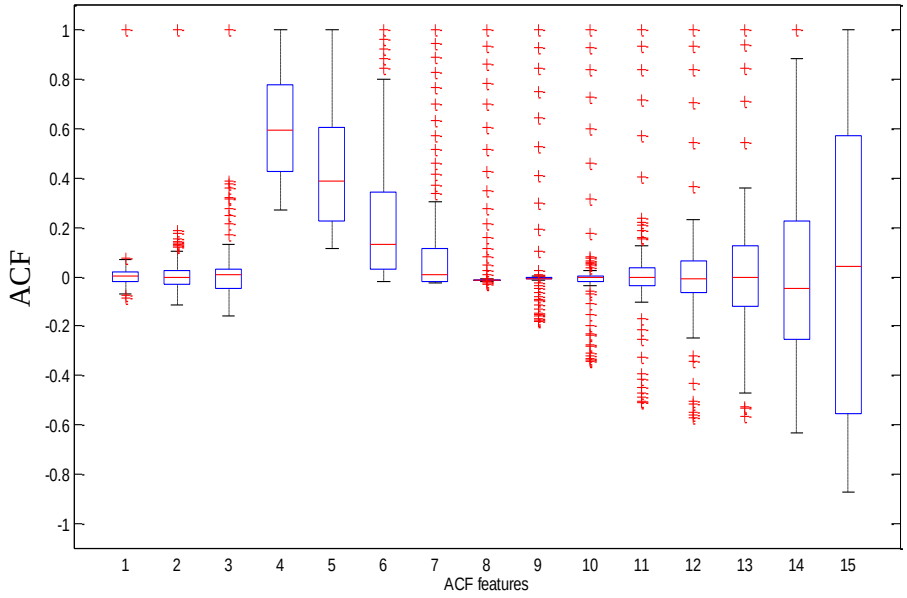

Figure 6.5: Box plot representation for each ACF signature

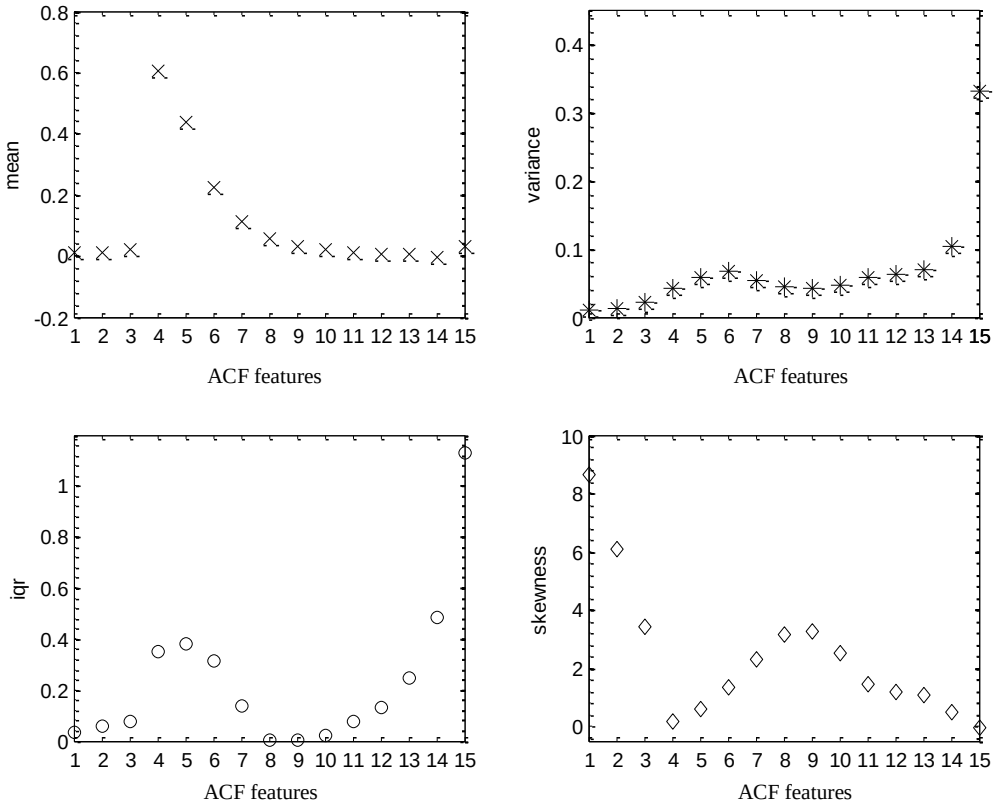

Figure 6.6: Features extracted from ρ-values of the data sets

Description of each class condition	MC-SVM label	ACF pattern	Feature sets			
			mean ($\bar{\rho}$)	variance ($\text{var}(\rho)$)	interquartile range ($iqr(\rho)$)	skewness ($\gamma(\rho)$)
Noise (C1)	1	1	0.0115	0.0108	0.0353	8.6175
	1	2	0.0114	0.0137	0.0575	6.1085
	1	3	0.0197	0.0219	0.0769	3.4351
Sluggish (C2)	2	4	0.6060	0.0433	0.3512	0.1610
	2	5	0.4346	0.0589	0.3799	0.5933
	2	6	0.2257	0.0665	0.3133	1.3235
Acceptable (C3)	3	7	0.1109	0.0545	0.1352	2.3157
	3	8	0.0580	0.0452	0.0034	3.1429
	3	9	0.0328	0.0432	0.0047	3.2357
Aggressive (C4)	4	10	0.0199	0.0473	0.0196	2.5271
	4	11	0.0129	0.0594	0.0743	1.4299
	4	12	0.0050	0.0638	0.1295	1.1718
Oscillatory (C5)	5	13	0.0034	0.0690	0.2464	1.0922
	5	14	-0.0046	0.1032	0.4816	0.4598
	5	15	0.0303	0.3323	1.1296	-0.0648

Table 6.1: Extracted ρ -values used in training the MC-SVM classifier tool.

6.4.3 Summary of automated MC-SVM CPA diagnostic procedure

Given the template results illustrated in Fig 6.6, a MC-SVM is trained to recognise the statistical patterns. Three sets of data were chosen for each class to improve the generalisation capabilities of the classification tool. New input data can be categorised into one of the classes belonging to C1 to C5. The MC-SVM CPA is summarised as follows:

Step 1: Collect plant data. $y(t)$ for disturbance rejection systems or $e(t)$ for setpoint tracking. Ensure adequate data sampling and sufficient process activity.

Step 2: Compute ACF coefficients (ρ) using Eq.6.1.

Step 3: Extract statistical features of ρ using Eqs. 6.20-6.23.

Step 4: Apply new input features to the trained MC-SVM classification algorithm, Eq.6.17.

Step 5: Report on classification result (C1 to C5).

Step 6: Go to step 1 when new data set available.

6.5 SIMULATION EXPERIMENTAL RESULTS AND ANALYSIS

The following experiments were conducted on simulated data sets to test the accuracy and efficiency of the proposed CPA tool. All simulation work was conducted in MATLAB™ SIMULINK™ using an Intel core i5 CPU running at 2.5 GHZ with 4 GB of RAM. A graphical user interface (GUI) was developed to interpret closed loop data sets and is shown in Fig. 6.7. Details of the GUI CPA diagnostic software tool are shown in APPENDIX C.

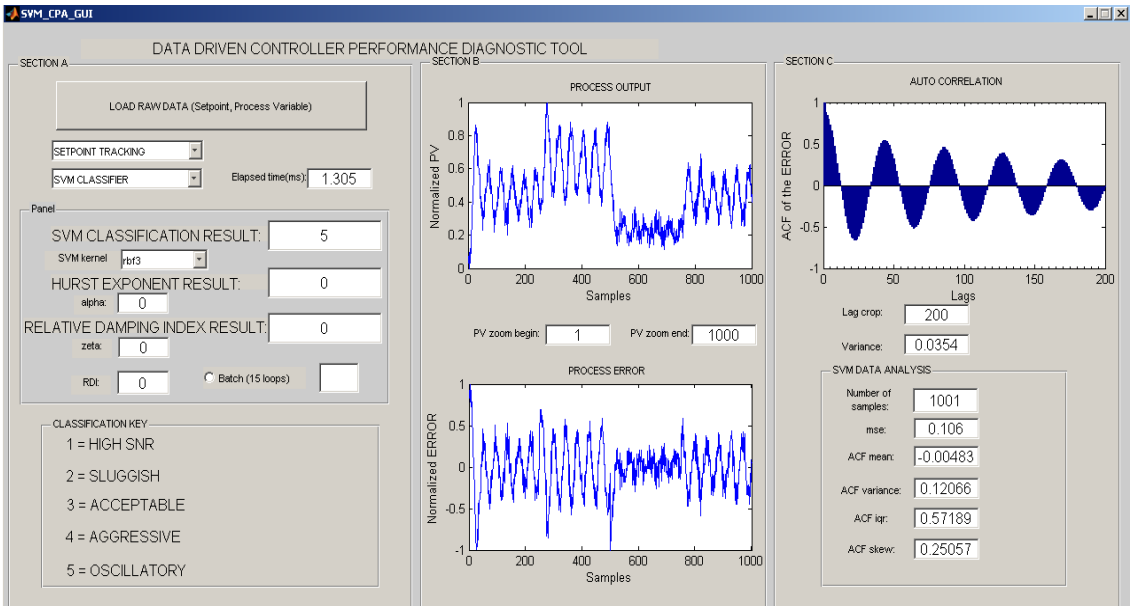

Figure 6.7: Data driven CPA diagnostic GUI used in the experiments

6.5.1 MC-SVM kernel selection

Performance of the MC-SVM is reliant on the choice of kernel function used to transfer input data to a higher dimensional space. The choice is data dependant and currently there are no well established guidelines to achieve a satisfactory performance (Yang *et al.*, 2005).

Table. 6.2 highlights the results of different kernels used in the simulation study using generated data from the FOPDT model given by Eq. 6.8. d_{poly} is the degree of the polynomial (Poly) and the width of the Radial Basis Function (RBF) kernel is given by g_{RBF} . Percentage misclassification is the main criteria for evaluating the performance of the SVM.

Preliminary test results showed this criteria ranged from 4.8% to 31.2% with RBF ($g = 3$) outperforming linear and polynomial kernel types.

Kernel function $K(x_i, x_j)$	Kernel type	No. of support vectors	Training time (ms)	% Misclassification
$x_i^T.y_i$	Linear	14	0.78	16.8 %
$\left(x_i^T.y_i\right)^{d_{poly}}$	Poly 1 $\left(d_{poly}=1\right)$	14	0.48	15.2 %
	Poly 2 $\left(d_{poly}=2\right)$	13	0.46	21.6 %
	Poly 3 $\left(d_{poly}=3\right)$	13	0.46	32.1 %
$\exp\left\{\left(-\frac{1}{g_{RBF}}\right)\left\|x_i-y_i\right\|^2\right\}$	RBF $\left(g_{RBF}=1\right)$	15	0.49	16.3 %
	RBF $\left(g_{RBF}=2\right)$	15	0.51	10.4 %
	RBF $\left(g_{RBF}=3\right)$	15	0.49	4.8 %

Table 6.2: Kernel selection test results from 875 simulated process data sets

6.5.2 Simulation case study

Given the satisfactory performance of the MC-SVM classifier with RBF$\left(g_{RBF}=3\right)$kernel mapping function, we now advance to show the results of the method applied to typical process models found in industry (Spinner *et al.*, 2014). Table 6.3 shows the plant and corresponding disturbance models used in the experiments with varying degrees of control difficulty as indicated by the controllability ratio $\left(0 \le \frac{\theta_p}{T_p} \le 10\right)$.

Effects of control valve static friction were also considered with a stick band of $S_v = 5$ and jump band in the range of $0 \le J_v \le 20$. Disturbance models were driven with a zero mean white noise sequence of variance; $\sigma_a^2 = 1\times10^{-3}$. The proposed method was compared to the Relative Damping Index (RDI) (Howard and Cooper, 2010) and the Hurst Exponent (HE) (Srinivasan *et al.*, 2012; Pillay and Govender, 2014) controller performance benchmarks and presented in Table 6.4.

Case study	Plant model	Disturbance model
1	$G_p(s) = \frac{1\exp^{-5s}}{(10s+1)}$	$D(s) = \frac{1}{(10s+1)}$
2	$G_p(s) = \frac{1}{(s+1)^4}$	$D(s) = \frac{1}{(s+1)^4}$
3	$G_p(s) = \frac{1\exp^{-3s}}{(15s+1)(5s+1)(2s+1)}$	$D(s) = \frac{1}{(17s+1)(4s+1)(s+1)}$
4	$G_p(s) = \frac{1\exp^{-5s}}{(s+1)^3}$	$D(s) = \frac{1}{(s+1)^3}$
5	$G_p(s) = \frac{1\exp^{-10s}}{(s+1)(s+2)(s+3)}$	$D(s) = \frac{1}{(s+1)(s+2)(s+3)}$

Table 6.3. Simulated process and disturbance models

	MC-SVM	HE	RDI
Average test time (ms)	1.3	823	609
% Misclassification	3.1 %	30.4 %	12.3 %

Table 6.4. Results of 65 simulated experiments

Results indicate an improved performance over the set of simulated data with the proposed classification scheme. The HE method failed to detect loop excessive oscillations which were caused by valve static fiction. Average computational time for the MC-SVM method is very fast in comparison to the other methods. This is due to the efficiency of the MC-SVM algorithm even with 15 support vectors defining the model. The other methods are hampered by computational burden in model fitting and data integration complexities over varying finite window lengths. The main drawback of the proposed method is that adequate process data is required in order to provide an appropriate ACF. This may take a long period of time if the process dynamics are characteristically slow.

6.6 SUMMARY AND CONCLUSIONS

In this chapter a novel control loop assessment diagnostic tool using the MC-SVM has been presented. A NLCPA framework using MC-SVMs were used in the development of the utility. The extracted features are easily obtained using simple statistical analysis of the ACF data. Simulation results demonstrate the methodology's effectiveness in classifying different closed loop behaviours. A level of 96.9 % classification accuracy was obtained using RBF $\left(g_{RBF} = 3\right)$ kernel type. In pursuit of further improving the accuracy of the method, the problem of feature selection is an open issue. In the following section, the proposed technique is applied to real world data.

Chapter 7

Implementation of the MC-SVM Diagnostic Tool on Real World Data

7.1 INTRODUCTION

The aim of this chapter is to apply the proposed MC-SVM CPA tool on real world data sets. Experimental data from the full scale pilot plant discussed in Chapter 5 and data from a pulp and paper mill are used to demonstrate the method. Live data was recorded at prescribed sampling rates on the pulp and paper plant DCS and analysed using the developed GUI CPA software. An overview of the hardware and software architecture used in the study is illustrated in Fig. 7.1.

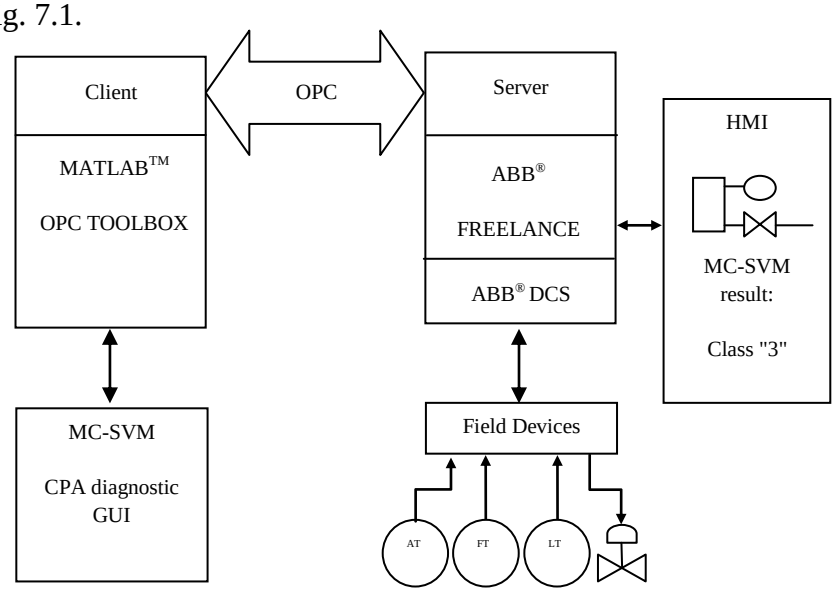

Figure 7.1: ABB™ DCS and MC-SVM CPA GUI architecture

7.2 EXPERIMENTAL EVALUATION OF PILOT SCALE PROCESS DATA

7.2.1 Assessing the performance of the MC-SVM CPA tool on the pH neutralization pilot plant

Data acquired from the pH control (AIC100) and acid control (FIC101) loops were assessed using the new classification methodology. The control objective for both loops were setpoint tracking using the same suboptimal and optimal gain scheduling controller parameters as given in Table 5.3 and Table 5.4 from Chapter 5.

7.2.1.1 Observations and analysis of the results

The experimental loop evaluation results for AIC100 and FIC101 is given in Fig. 7.2 and Fig. 7.3 respectively. In these figures, graphs (a)-(c) show the closed loop response data and the ACF of the error signal from the suboptimal gain scheduled PID controller. Similarly graphs (d)-(f) show controller responses and the ACF of the error using the optimal gain scheduled PID controller. Table 7.1 gives the final loop assessment results obtained for each respective control loop.

For both loops, the suboptimal controller settings resulted in severe closed loop oscillations which are correctly identified as belonging to class “C5” by the MC-SVM CPA tool. Optimal gain schedule controller settings resulted in improved closed loop responses for both case studies as indicated by class “C3”. Visual inspection of process output confirms the agreement between the automatic NLCPA utility and the actual closed loop responses.

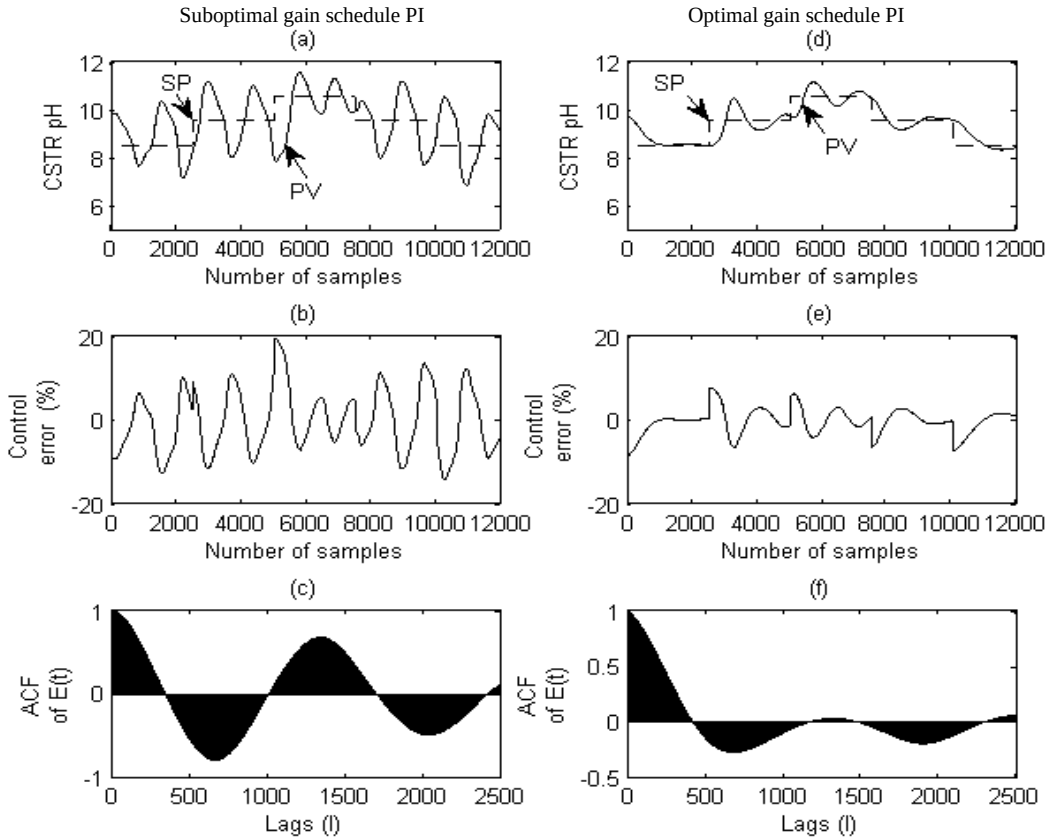

Figure 7.2: CSTR pH SP tracking control. (a) and (d) n=12000 samples of pH data, (b) and (e) control error, (c) and (f) ACF (l=2500) of the control error

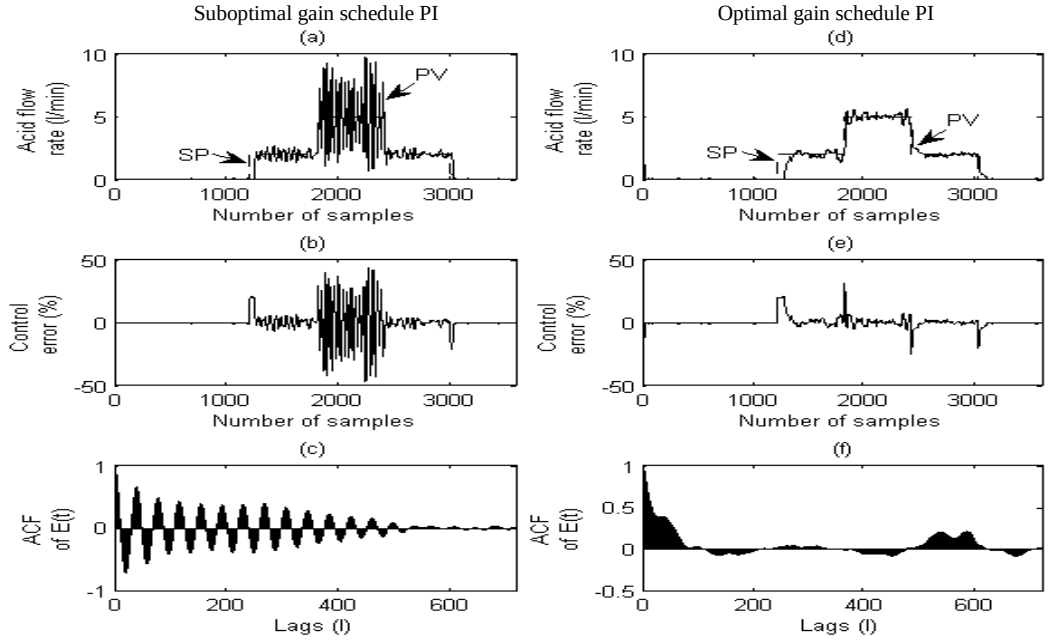

Figure 7.3: Acid flow rate SP tracking control. (a) and (d) n=3500 samples of flow rate data, (b) and (e) control error, (c) and (f) ACF (l=700) of the control error

MC-SVM CPA results for pH CSTR plant loops (AIC100-CSTR pH and FIC101-acid flow rate)						
Loop	PID gain schedule	Class	$\bar{\rho}$	var(ρ)	$iqr(\rho)$	$\gamma(\rho)$
AIC 100	Suboptimal	C5 (oscillatory)	-0.016	0.234	0.832	0.282
	Optimal	C3 (acceptable)	0.013	0.078	0.192	2.008
FIC 101	Suboptimal	C5 (oscillatory)	0.004	0.054	0.223	0.206
	Optimal	C3 (acceptable)	0.052	0.023	0.079	2.921

Table 7.1: pH neutralization pilot plant pH and acid flow control loop assessment results

7.2.2 Assessing the performance of the MC-SVM CPA tool on a flow loop experiencing control valve stiction

In this section, actual data from a flow control loop experiencing control valve stiction nonlinearity is assessed using the new NLCPA classifier tool. Control valve stiction, which is a common occurrence in many industrial control loops (Horch, 2000; Hägglund, 2002a; Choudhury *et al.*, 2004; He *et al.*, 2007) is one of the main problems affecting control loop performance and ultimately product quality (Scali and Ghelardoni, 2008).

Generally loop oscillations are caused by any one or the combinations of limit cycles caused by the valve stiction or process nonlinearities (He *et al.*, 2007). Although many well established methods exits for the detection and quantification of control valve stiction (Choudhury *et al.*, 2004; Singhal and Salsbury, 2005; Yamashita, 2006; He *et al.*, 2007; Scali

and Ghelardoni, 2008), here we present a simple but effective use of the MC-SVM CPA methodology for detection of loop oscillation caused by valve stiction.

The method will therefore complement well known stiction quantification methods and can be used to detect loop oscillations as a first step towards detecting unsatisfactory closed loop behaviour. Once oscillations have been confirmed by the NLCPA index, then further investigation into the source of the nonlinearity can be investigated using the established methodologies previously mentioned. A simple schematic of the flow loop under inspection is shown in Fig. 7.4. Control valve stiction was manually introduced into the pneumatic control valve by hardware manipulation of the positioner cam unit as described in Sewdass *et al.* (2014).

The control valve was setup accordingly to give three different closed loop responses as shown in Fig. 7.5. Response indicated by graph (a) clearly indicates the presence of control valve stiction nonlinearity and graphs (b) and (c) shows response data with no valve stiction present. The difference between graphs (b) and (c) is attributed to different PID controller settings. These cases where selected to show the performance of the proposed classification index to processes with poor and acceptable controller tuning. n=1000 data points was sampled at $T_s = 0.1$ seconds. Closed loop response data and its corresponding ACF graphs are shown in Fig. 7.6 – Fig. 7.8. Table 7.2 gives the final NLCPA evaluation results.

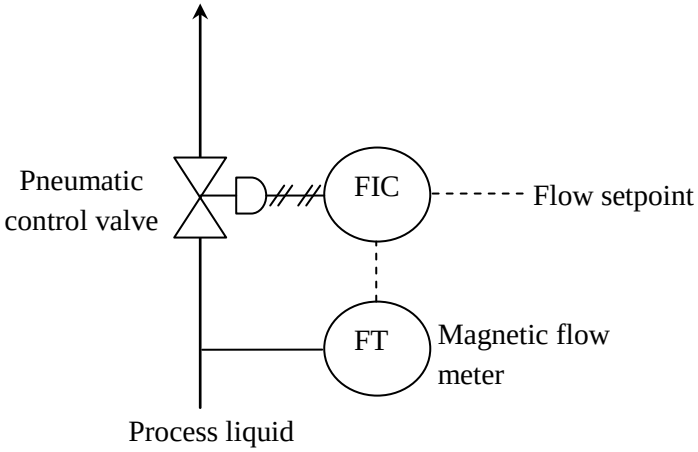

Figure 7.4: Flow control loop with control valve static friction

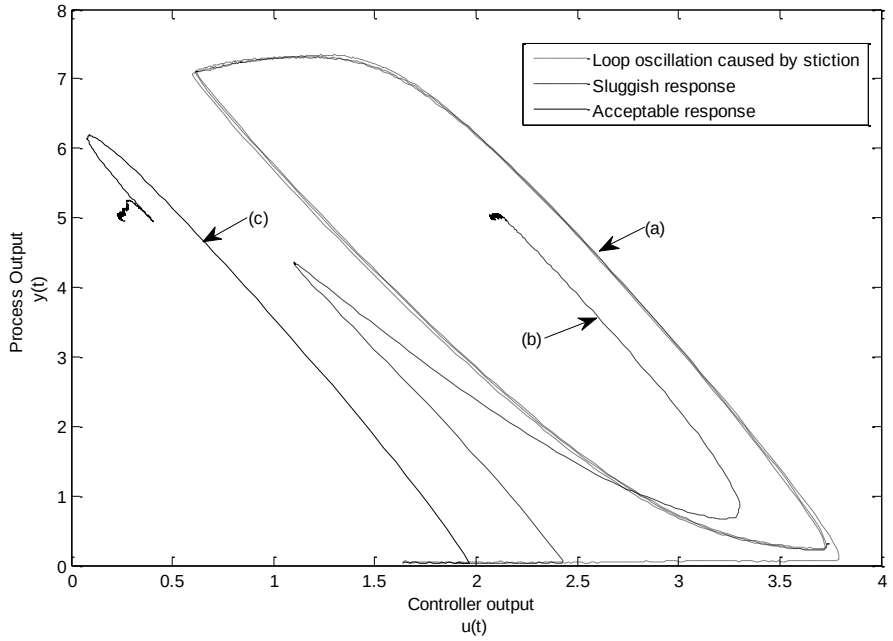

Figure 7.5: Controller output versus process output with: (a)-stiction response, (b)-overdamped response, (c) - acceptable response

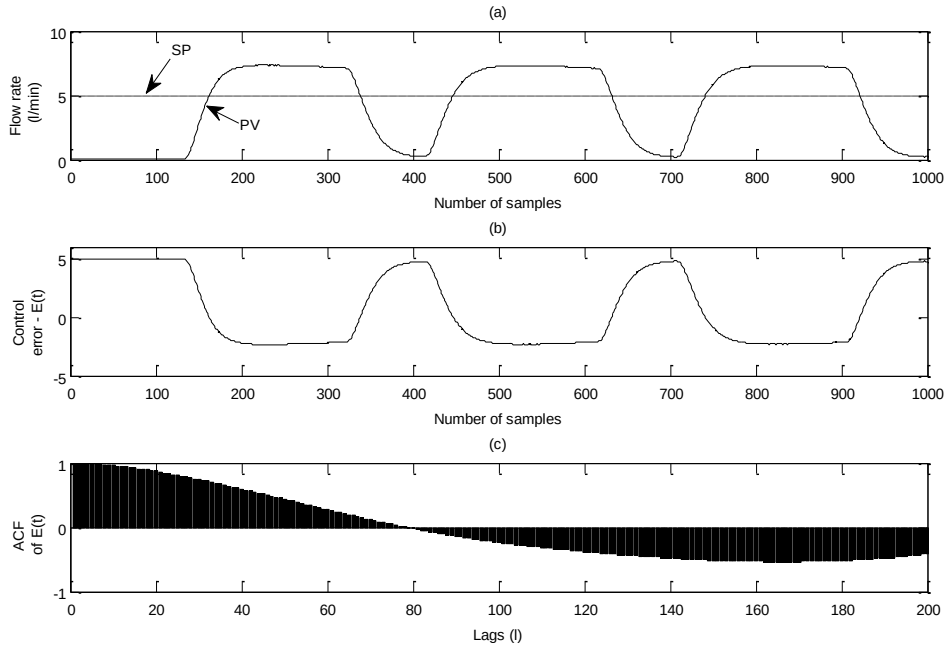

Figure 7.6: Flow rate SP tracking control with control valve stiction ($k_c = 0.38 \quad ; \tau_i = 8.63$). (a) flow rate response to setpoint change, (b) control error, (c) ACF (l=200) of the control error

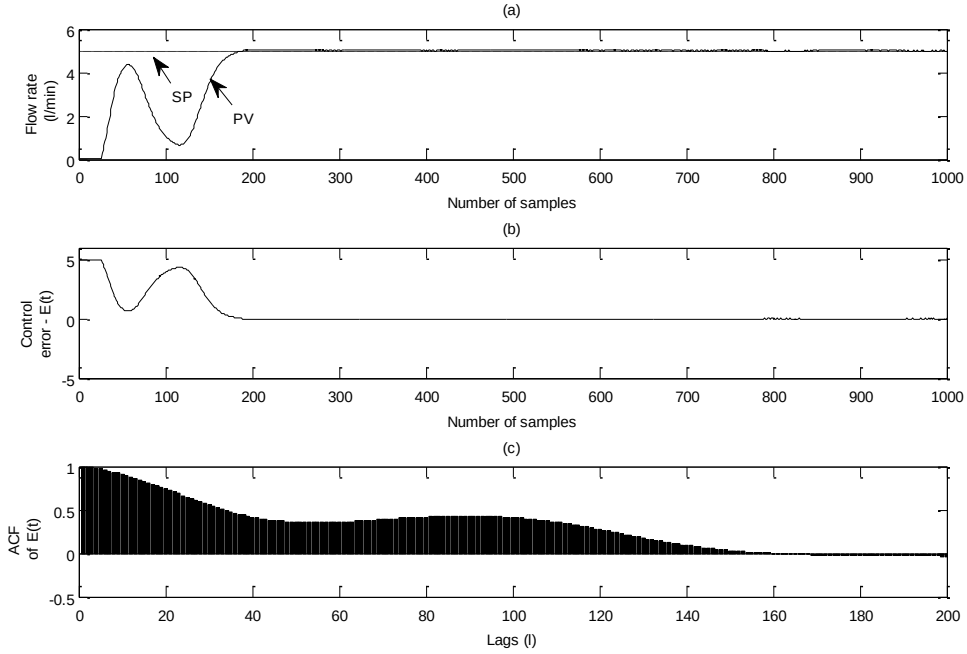

Figure 7.7: Flow rate SP tracking control with no control valve stiction and detuned PI controller. $\left(k_c = 0.38 \quad ; \tau_i = 8.63\right)$. (a) flow rate response to setpoint change, (b) control error, (c) ACF (l=200) of the control error

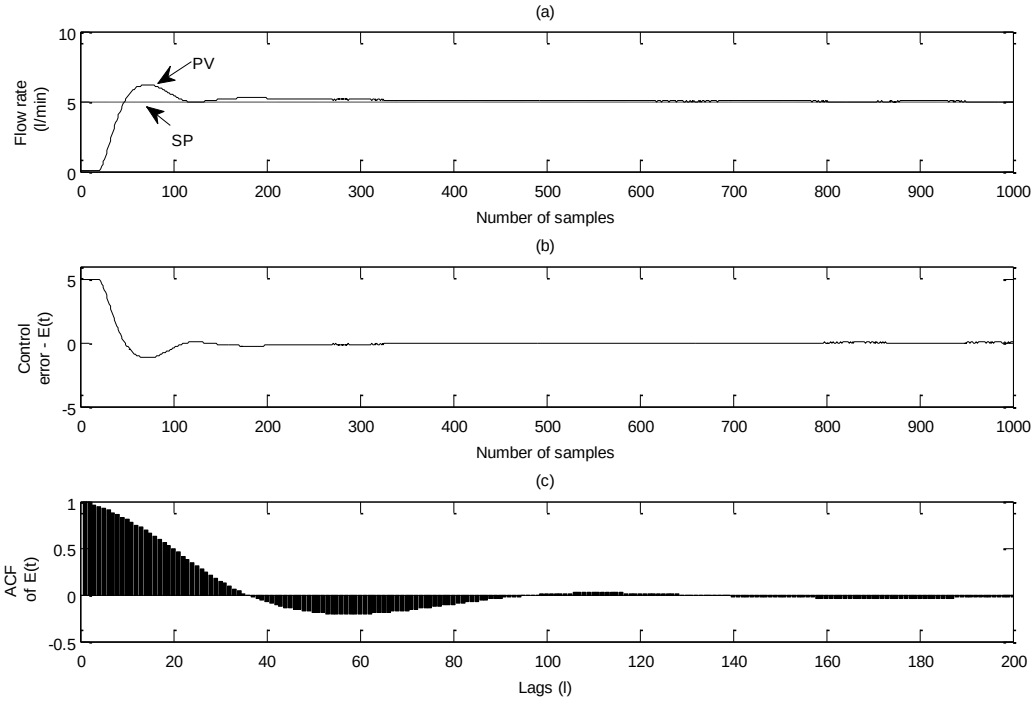

Figure 7.8: Flow rate SP tracking control with no control valve stiction and tuned PI controller. $\left(k_c = 0.33 \quad ; \tau_i = 10.0\right)$. (a) flow rate response to setpoint change, (b) control error, (c) ACF (l=200) of the control error

MC-SVM CPA results for flow loop							
Loop	Stiction present	MSE	Class	$\bar{\rho}$	var(ρ)	$iqr(\rho)$	$\gamma(\rho)$
Flow	Yes	9.880	C5	-0.019	0.273	0.903	0.699
	No	1.793	C2	0.312	0.076	0.393	0.589
	No	0.772	C3	0.047	0.072	0.061	2.210

Table 7.2: Flow control loop assessment results

7.2.2.1 Observations and analysis of the results

Observations of the experimental results show that when severe stiction is present it results in limit cycles around the setpoint. A relatively large mean square of the error (MSE) has resulted because of the control valve fault and is correctly defined as oscillatory (class C5) by the MC-SVM classifier. Removal of the valve stiction fault from the control valve positioner yields an improved closed loop response. Assessment results indicate a sluggish closed loop response (class "C2") as the PI controller parameters require fine tuning.

Application of the finely tuned PI settings on the flow control loop now results in faster setpoint tracking ability with minimal undershoot and a substantially smaller MSE value. A classification result of acceptable behaviour (class "C3") was recorded with the proposed methodology. In summary, there is agreement between the MSE of the closed loop response data and the resultant classifier results of the benchmarking index. Furthermore, the method performs satisfactorily in the presence of valve stiction nonlinearity. Although the NLCPA detects the presence of the nonlinearity it cannot identify the type of nonlinearity.

7.3 EXPERIMENTAL EVALUATION OF INDUSTRIAL DATA

7.3.1 Assessment of MC-SVM CPA on steam desuperheater control

The MC-SVM CPA method was also applied to real industrial data sets from a steam temperature desuperheater control obtained from the utility section of a local pulp and paper mill. Steam desuperheater control is often regarded as challenging due to its high order nonlinearity and load dependency (Lee *et al.*, 1997; Zhang *et al.*, 2012). Steam temperature is regulated at 200 °C using a desuperheater unit, cooling water valve and a PI temperature controller with a temperature sensor located downstream as illustrated by Fig. 7.9.

Fig. 7.10 (a-c) and Table 7.3 highlights the findings using initial data acquired from the plant DCS. 250 data points of the process outlet steam temperature *y(t)* and control error *e(t)* were obtained at a sample rate of 15 seconds. With a setpoint step increase to 210 °C, the steam temperature showed highly oscillatory behaviour.

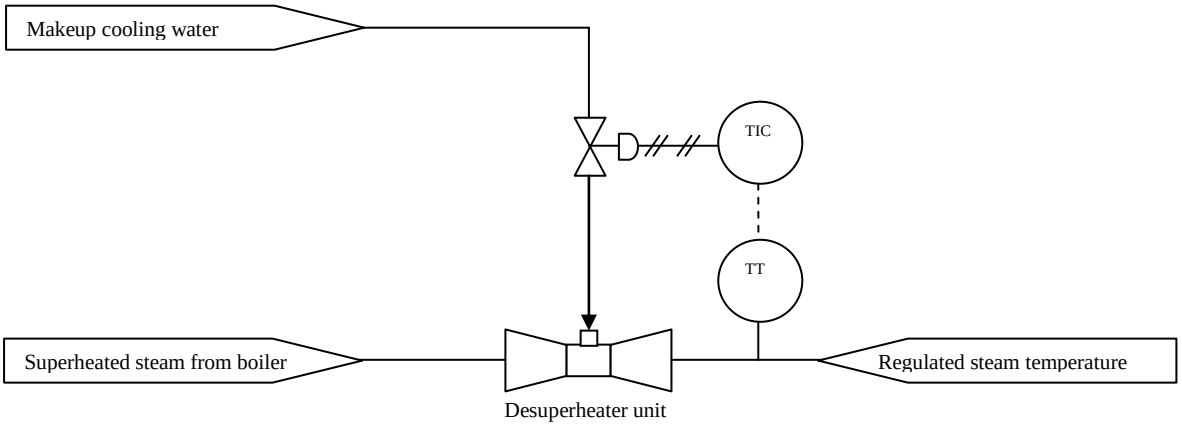

Figure 7.9: Simplified P&ID of desuperheater control from Pulp and Paper mill utility section

Applying the industrial data through the MC-SVM classifier correctly identified the closed loop as belonging to “Class 5” category. Visual inspections of the data trend show signs of oscillatory behaviour around the steam setpoint.

Upon further investigation, the automatic controller was discovered to have inappropriate parameter settings and was later fine-tuned, the results of which are shown in Fig.7.10 (d-f) and Table 7.3. Improved controller performance using the new PI parameters was verified by the MC-SVM classifier output indicating “Class 2” performance. Control loop shows substantial improvement as indicated by the lower MSE value.

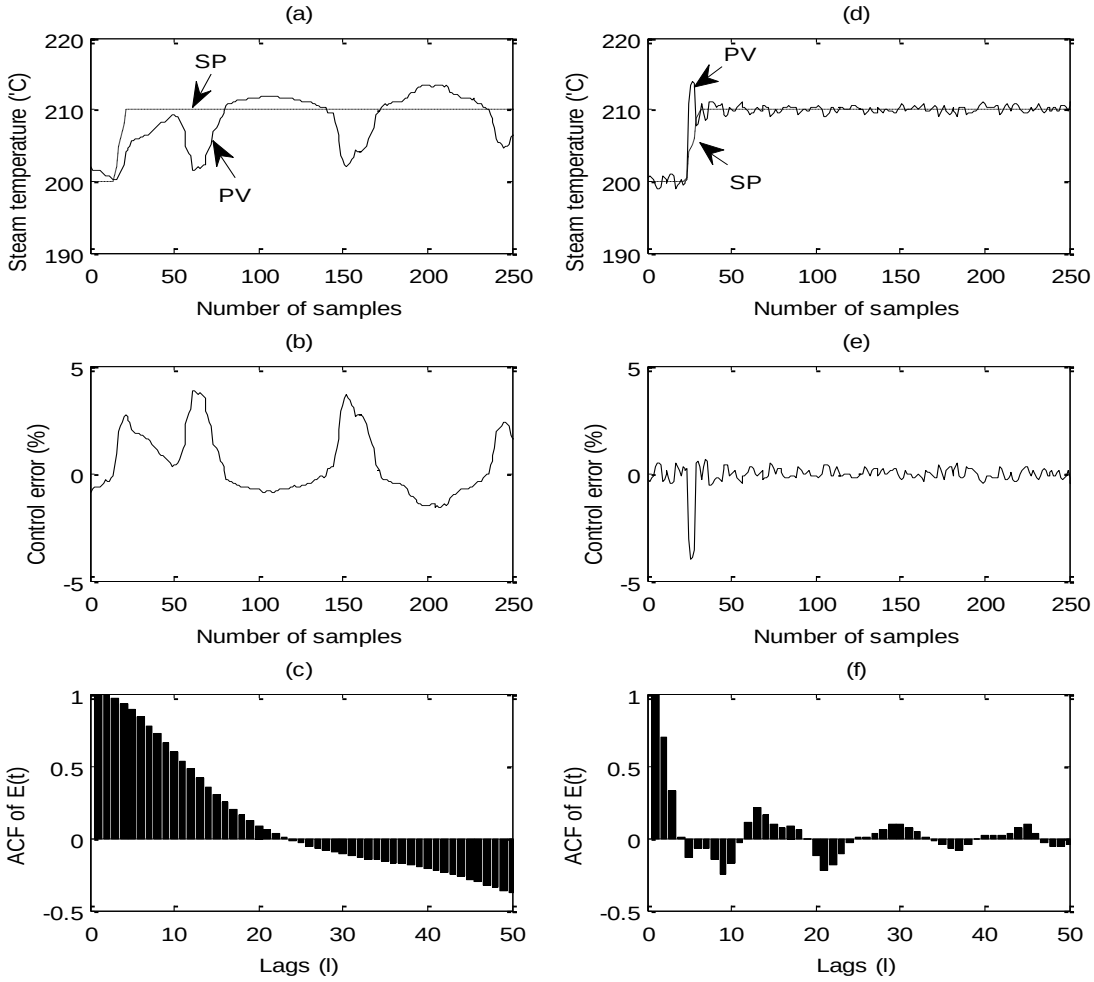

Figure 7.10: Data set of steam temperature desuperheater control and its corresponding MC-SVM result. (a-c) Initial response. (d-f) Fine-tuned response.

MC-SVM result for steam temperature desuperheater control						
	Class	MSE	$\bar{\rho}$	var(ρ)	$iqr(\rho)$	$\gamma(\rho)$
Initial	C5	0.368	0.115	0.178	0.597	0.849
Tuned	C3	0.171	0.029	0.039	0.130	3.004

Table 7.3: Assessment results of the steam temperature desuperheater control loop

7.4 SUMMARY AND CONCLUSIONS

The experimental study presented in this chapter has demonstrated the effectiveness of the proposed classification utility on real world data. Several loops were chosen based on their intrinsic nonlinear characteristics. The proposed methodology provides a means of assessing control loop performance operating under nonlinear constraints effectively and efficiently. With regards to its practical implementation, the GUI provides a simple and effectual means of classifying closed behaviour via computer interfaced system linked to a plant DCS.

Chapter 8

Summary of Study, Recommendations and Conclusions

8.1 SUMMARY OF THE RESEARCH STUDY

The main objectives of this research study have been to develop novel controller performance assessment methodologies for SISO feedback control systems, in which the closed loop experiences the destabilizing effects of nonlinear behaviour operating within the control channel.

Based on the fact that currently there are limited NLCPA schemes to effectively diagnose different closed loop behaviour operating under process and control valve nonlinearities, the main intent has been to develop new methodologies with process model knowledge and also with minimal process loop information requirements. Therefore two NLCPA schemes have been proposed and tested in detail using computer simulations and real data extracted from a full scale pilot pH neutralization reactor plant and pulp and paper mill. Algorithms were developed and implemented on well-known programming platforms and computer interfaced to the plant control hardware.

In the design of the model based NLCPA benchmark, NNARMAX models of simulated and real process systems were constructed using only I/O data. As with most designs that rely on a process model, insufficient and/or inapt data may lead to poor model estimation and will negatively impact on the NLCPA tool presented in this study. It is therefore important that a

sound and tractable nonlinear model be used for determining optimal PID controller settings since it is used directly in the real time benchmarking index.

The novel model based NLCPA index provides an alternative to the well-known MVC benchmark and considers process nonlinearities inherent in the control loop. The benchmark provides important insight by comparing an optimal gain scheduled nonlinear PID type controller to a suboptimal gain scheduled PID controller operating on the actual process. As evident from the case studies presented in this thesis, enhancement of suboptimal controller performance can be made as suggested by the nonlinear benchmarking index.

In many industrial situations, higher-level performance tests for the purpose of model extraction is usually not permitted, therefore a model free approach has pragmatic significance. By utilizing MC-SVMs a data driven approach is used to classify closed loop performance. This was achieved using only ACF signatures from routine data records and rudimentary statistical feature extraction. No other knowledge is required other than the fact that process dynamics following setpoint changes are fully captured by the ACF pattern.

For the data sets examined in the thesis, a high degree of accuracy from the proposed MC-SVM classification tool was achieved. Furthermore, classification results were obtained rapidly, which is an important consideration when dealing with a typical modern industrial facility which may have over a thousand control loops in operation.

8.2 RECOMMENDATIONS FOR EXTENDING THE WORK

The following recommendations are provided to extend the work presented in this thesis:

(i) For the model based NLCPA design, an assumption is made that the dynamic NNARMAX model captures essential nonlinear characteristic behaviour of the process. However, alternative nonlinear techniques may be applied to capture the systems transient behavior, such as fuzzy logic schemes.

(ii) Design of the optimal PID controller settings was based on minimization of the IAE; however it is possible to use other traditional time domain transient specifications such as minimal overshoot or rapid settling time. Such specifications would have significant industrial appeal since the NLCPA can be tailored to meet desired control objectives for individual control loops.

(iii) A variance trade-off between the process output and controller output can be used in the PID optimization routine by incorporating variance of the controller output with the process output variance in the controller design.

(iv) By complementing the proposed MC-SVM CPA tool with other existing data driven CPA indices, a simple voting system can be developed that may lead to loop assessment results with higher degree of accuracy and robustness to process uncertainties.

8.3 CONCLUDING REMARKS

This research has proposed two new CPA methodologies that can be applied to systems operating under nonlinear constraints. From the results and analysis presented in this thesis, these methodologies can effectively diagnosis closed loop performance of nonlinear processes. The performance assessment utility has practical significance to industry since it is capable of detecting unsatisfactory process behaviour, thereby aiding in reduction of production variances and wastage. The developed benchmarks should be of interest to control practitioners in the field of process control and industrial automation systems. Simple human machine interfaces have been developed to aid in the presentation of the new benchmarking indices in real time.

References

1. Agrawal, P. and Lakshminarayanan, S. (2003). Tuning proportional-integral-derivative controllers using achievable performance indices. *Industrial & engineering chemistry research*, 42 (22): 5576-5582.

2. Anbumani, K., Patnaik, L. and Sarma, I. (1981). Self-tuning minimum-variance control of nonlinear systems of the Hammerstein model. *IEEE Transactions on Automatic Control*, 26 (4): 959-961.

3. Antsaklis, P. J. (1990). Neural networks for control systems. *Neural Networks, IEEE Transactions on*, 1 (2): 242-244.

4. Astrom, K. J. 1970. *Introduction to stochastic control theory*. Courier Dover Publications.

5. Aström, K. J. and Hägglund, T. (1995). PID controllers: theory, design and tuning.

6. Åström, K. J. and Hägglund, T. (1984). Automatic tuning of simple regulators with specifications on phase and amplitude margins. *Automatica*, 20 (5): 645-651.

7. Åström, K. J. and Hägglund, T. 2006. *Advanced PID control*. ISA-The Instrumentation, Systems, and Automation Society; Research Triangle Park, NC 27709.

8. Bezergianni, S. and Georgakis, C. (2000). Controller performance assessment based on minimum and open-loop output variance. *Control Engineering Practice*, 8 (7): 791-797.

9. Bhat, N. V., Minderman Jr, P. A., McAvoy, T. and Wang, N. S. (1990). Modeling chemical process systems via neural computation. *Control Systems Magazine, IEEE*, 10 (3): 24-30.

10. Billings, S., Jamaluddin, H. and Chen, S. (1992). Properties of neural networks with applications to modelling non-linear dynamical systems. *International journal of control*, 55 (1): 193-224.

11. Bittanti, S. and Piroddi, L. (1997). Nonlinear identification and control of a heat exchanger: a neural network approach. *Journal of the Franklin Institute*, 334 (1): 135-153.

12. Box, G. E., Jenkins, G. M. and Reinsel, G. C. 1970. *Time series analysis: forecasting and control*. Wiley. com.

13. Bozdogan, H. (1987). Model selection and Akaike's information criterion (AIC): The general theory and its analytical extensions. *Psychometrika*, 52 (3): 345-370.

14. Chapelle, O., Haffner, P. and Vapnik, V. N. (1999). Support vector machines for histogram-based image classification. *Neural Networks, IEEE Transactions on*, 10 (5): 1055-1064.

15. Chen, S. and Billings, S. (1989). Representations of non-linear systems: the NARMAX model. *International journal of control*, 49 (3): 1013-1032.

16. Chen, S., Billings, S. and Grant, P. (1990). Non-linear system identification using neural networks. *International journal of control*, 51 (6): 1191-1214.

17. Chen, J. and Huang, TC. (2004). Applying neural networks to on-line updated PID controller for nonlinear process control. *Journal of Process Control*, 14 (1): 211-230.

18. Choudhury, M., Shah, L. and Thornhill, N. (2004). Diagnosis of poor control-loop performance using higher-order statistics. *Automatica*, 40 (10): 1719-1728.

19. Choudhury, M. S., Thornhill, N. F. and Shah, S. L. (2005). Modelling valve stiction. *Control Engineering Practice*, 13 (5): 641-658.

20. Cortes, C. and Vapnik, V. (1995). Support-vector networks. *Machine learning*, 20 (3): 273-297.

21. Cybenko, G. (1989). Approximation by superpositions of a sigmoidal function. *Mathematics of control, signals and systems*, 2 (4): 303-314.

22. Desborough, L. and Harris, T. (1992). Performance assessment measures for univariate feedback control. *The Canadian Journal of Chemical Engineering*, 70 (6): 1186-1197.

23. Desborough, L. and Miller, R. 2002. Increasing customer value of industrial control performance monitoring-Honeywell's experience. In: Proceedings of *AIChE symposium series*. New York; American Institute of Chemical Engineers; 1998, 169-189.

24. Eberhart, R. C. and Kennedy, J. 1995. A new optimizer using particle swarm theory. In: Proceedings of *Proceedings of the sixth international symposium on micro machine and human science*. New York, NY, 39-43.

25. Ender, D. B. (1993). Process control performance: Not as good as you think. *Control Engineering*, 40 (10): 180-190.

26. Eriksson, P.-G. and Isaksson, A. J. 1994. Some aspects of control loop performance monitoring. In: Proceedings of *Control Applications, 1994., Proceedings of the Third IEEE Conference on*. IEEE, 1029-1034.

27. Ettaleb, L. 1999. Control loop performance assessment and oscillation detection. PhD thesis, University of British Columbia.

28. Funahashi, K.-I. (1989). On the approximate realization of continuous mappings by neural networks. *Neural Networks*, 2 (3): 183-192.

29. Grimble, M. (1988). Generalized minimum variance control law revisited. *Optimal Control Applications and Methods*, 9 (1): 63-77.

30. Grimble, M. J. (2005). Non-linear generalized minimum variance feedback, feedforward and tracking control. *Automatica*, 41 (6): 957-969.

31. Gustafsson, T. K. and Waller, K. V. (1983). Dynamic modeling and reaction invariant control of pH. *Chemical Engineering Science*, 38 (3): 389-398.

32. Hägglund, T. (1995). A control-loop performance monitor. *Control Engineering Practice*, 3 (11): 1543-1551.

33. Hägglund, T. (2002a). A friction compensator for pneumatic control valves. *Journal of Process Control*, 12 (8): 897-904.

34. Hägglund, T. 2002b. Industrial applications of automatic performance monitoring tools. In: Proceedings of *IFAC World Congress, Barcelona Spain*.

35. Hägglund, T. (2005). Industrial implementation of on-line performance monitoring tools. *Control Engineering Practice*, 13 (11): 1383-1390.

36. Hanna, J., Upreti, S., Lohi, A. and Ein-Mozaffari, F. (2008). Constrained minimum variance control using hybrid genetic algorithm–An industrial experience. *Journal of Process Control*, 18 (1): 36-44.

37. Harris, T., Seppala, C. and Desborough, L. (1999). A review of performance monitoring and assessment techniques for univariate and multivariate control systems. *Journal of Process Control*, 9 (1): 1-17.

38. Harris, T. and Yu, W. (2007). Controller assessment for a class of non-linear systems. *Journal of Process Control*, 17 (7): 607-619.

39. Harris, T. J. (1989). Assessment of control loop performance. *The Canadian Journal of Chemical Engineering*, 67 (5): 856-861.

40. Harris, T. J. and Seppala, C. T. 2002. Recent developments in controller performance monitoring and assessment techniques. In: Proceedings of *AICHE Symposium Series*. New York; American Institute of Chemical Engineers; 1998, 208-222.

41. Haykin, S. (2004). A comprehensive foundation. *Neural Networks*, 2 (2004)

42. He, Q. P., Wang, J., Pottmann, M. and Qin, S. J. (2007). A curve fitting method for detecting valve stiction in oscillating control loops. *Industrial & engineering chemistry research*, 46 (13): 4549-4560.

43. Henson, M. A. and Seborg, D. E. (1994). Adaptive nonlinear control of a pH neutralization process. *Control Systems Technology, IEEE Transactions on*, 2 (3): 169-182.

44. Hinich, M. J. (1982). Testing for Gaussianity and linearity of a stationary time series. *Journal of time series analysis*, 3 (3): 169-176.

45. Horch, A. 2000. Condition monitoring of control loops. PhD thesis, Royal Institute of Technology.

46. Horch, A. and Isaksson, A. J. (1999). A modified index for control performance assessment. *Journal of Process Control*, 9 (6): 475-483.

47. Howard, R. and Cooper, D. (2010). A novel pattern-based approach for diagnostic controller performance monitoring. *Control Engineering Practice*, 18 (3): 279-288.

48. Huang, B. 1998. Multivariate statistical methods for control loop performance assessment. PhD thesis, University of Alberta.

49. Huang, H.-P. and Jeng, J.-C. (2002). Monitoring and assessment of control performance for single loop systems. *Industrial & engineering chemistry research*, 41 (5): 1297-1309.

50. Hugo, A. J. (2006). Performance assessment of single-loop industrial controllers. *Journal of Process Control*, 16 (8): 785-794.

51. Hunt, K. J., Sbarbaro, D., Żbikowski, R. and Gawthrop, P. J. (1992). Neural networks for control systems—a survey. *Automatica*, 28 (6): 1083-1112.

52. Hussain, M. A., Kittisupakorn, P. and Daosu, W. (2001). Implementation of neural-network-based inverse-model control strategies on an exothermic reactor. *Science Asia*, 27: 41-50.

53. Ingimundarson, A. and Hägglund, T. (2005). Closed-loop performance monitoring using loop tuning. *Journal of Process Control*, 15 (2): 127-133.

54. Jain, M. and Lakshminarayanan, S. (2004). A Filter Based Approach for Estimation of PI Achievable Performance. *DYCOPS-6, Boston, MA*,

55. Jelali, M. (2006). An overview of control performance assessment technology and industrial applications. *Control Engineering Practice*, 14 (5): 441-466.

56. Jelali, M. 2013. *Control Performance Management in Industrial Automation: Assessment, Diagnosis and Improvement of Control Loop Performance*. Springer.

57. Joe Qin, S. (1998). Control performance monitoring—a review and assessment. *Computers and Chemical Engineering*, 23 (2): 173-186.

58. Julien, R. H., Foley, M. W. and Cluett, W. R. (2004). Performance assessment using a model predictive control benchmark. *Journal of Process Control*, 14 (4): 441-456.

59. Kadali, R. and Huang, B. (2002). Controller performance analysis with LQG benchmark obtained under closed loop conditions. *ISA transactions*, 41 (4): 521-537.

60. Kampouraki, A., Manis, G. and Nikou, C. (2009). Heartbeat time series classification with support vector machines. *Information Technology in Biomedicine, IEEE Transactions on*, 13 (4): 512-518.

61. Karra, S. and Karim, M. N. (2009). Comprehensive methodology for detection and diagnosis of oscillatory control loops. *Control Engineering Practice*, 17 (8): 939-956.

62. Kendra, S. J. and Çinar, A. (1997). Controller performance assessment by frequency domain techniques. *Journal of Process Control*, 7 (3): 181-194.

63. Ko, B. S. and Edgar, T. F. (2001). Performance assessment of constrained model predictive control systems. *AIChE Journal*, 47 (6): 1363-1371.

64. Ko, B. S. and Edgar, T. F. (2004). PID control performance assessment: The single-loop case. *AIChE Journal*, 50 (6): 1211-1218.

65. Kozub, D. J. 2002. Controller performance monitoring and diagnosis. Industrial perspective. In: Proceedings of *Proc. 15th IFAC Triennial World Congress*, Barcelona, Spain,:xxx-xxx

66. Lee, S.H., Kong, J. and Seo, J.H. (1997). Observers for bilinear systems with unknown inputs and application to superheater temperature control. *Control Engineering Practice*, 5 (4): 493-506.

67. Leith, D. J. and Leithead, W. E. (2000). Survey of gain-scheduling analysis and design. *International journal of control*, 73 (11): 1001-1025.

68. Leontaritis, I. and Billings, S. A. (1985). Input-output parametric models for non-linear systems part I: deterministic non-linear systems. *International journal of control*, 41 (2): 303-328.

69. Lightbody, G. and Irwin, G. W. (1997). Nonlinear control structures based on embedded neural system models. *IEEE Transactions on Neural Networks*, 8 (3): 553-567.

70. Lipták, B. G. 1995. *Process measurement and analysis*. Butterworth Heinemann.

71. Liu, S., Liu, J., Feng, Y. and Rong, G. (2014). Performance assessment of decentralized control systems: An iterative approach. *Control Engineering Practice*, 22 (2014) :252-263.

72. Lynch, C. and Dumont, G. (1996). Control loop performance monitoring. *IEEE Transactions on Control Systems Technology*, 4 (2): 185-192.

73. Maboodi, M., Khaki-Sedigh, A. and Camacho, E. F. (2015). Control Performance Assessment for a Class of Nonlinear Systems Using Second Order Volterra Series

Models based on Nonlinear Generalized Minimum Variance Control. *International journal of control*: 1-20.

74. Majecki, P. and Grimble, M. (2004a). Controller performance design and assessment using nonlinear generalized minimum variance benchmark: scalar case. Control 2004, xxx-xxx.

75. Majecki, P. and Grimble, M. J. 2004b. GMV and restricted-structure GMV controller performance assessment multivariable case. In: Proceedings of *American Control Conference, 2004. Proceedings of the 2004*. IEEE, 697-702.

76. McAvoy, T. J., Hsu, E. and Lowenthal, S. (1972). Dynamics of pH in controlled stirred tank reactor. *Industrial & Engineering Chemistry Process Design and Development*, 11 (1): 68-70.

77. McMillan, G. K. 1994. *pH measurement and control*. Instrument Society of America.

78. Miao, T. and Seborg, D. E. 1999. Automatic detection of excessively oscillatory feedback control loops. In: Proceedings of *International Conference on Control Applications, Hawaii, USA*. 38.

79. Narayanan, N. L., Krishnaswamy, P. and Rangaiah, G. (1997). An adaptive internal model control strategy for pH neutralization. *Chemical Engineering Science*, 52 (18): 3067-3074.

80. Narendra, K. S. and Parthasarathy, K. (1990). Identification and control of dynamical systems using neural networks. *Neural Networks, IEEE Transactions on*, 1 (1): 4-27.

81. Nelder, J. A. and Mead, R. (1965). A simplex method for function minimization. *The computer journal*, 7 (4): 308-313.

82.Nikias, C. L. and Mendel, J. M. (1993). Signal processing with higher-order spectra. *IEEE signal processing magazine*, 10 (3): 10-37.

83. O'Dwyer, A. 2009. *Handbook of PI and PID controller tuning rules*. World Scientific.

84. Ordys, A. W., Uduehi, D., Johnson, M. A. and Thornhill, N. 2007. *Process control performance assessment: from theory to implementation*. Springer.

85. Pillay, N. and Govender, P. 2013. Constrained Minimum-Variance PID Control using Hybrid Nelder-Mead Simplex and Swarm Intelligence. In: Proceedings of *ICAART (2)*. 330-337.

86. Pillay, N. and Govender, P. (2014). A Data Driven Approach to Performance Assessment of PID Controllers for Setpoint Tracking. *Procedia Engineering*, 69: 1130-1137.

87. Pillay, N., Govender, P. and Maharaj, O. (2014). Controller performance assessment of servomechanisms for nonlinear process control systems. *Proceedings of the World Congress on Engineering and Computer Science 2014*, 2: 918-923.

88. Poulin, E. and Pomerleau, A. 1996. PID tuning for integrating and unstable processes. In: Proceedings of *Control Theory and Applications, IEE Proceedings-*. IET, 429-435.

89. Rao, T. S. and Gabr, M. (1980). A test for linearity of stationary time series. *Journal of time series analysis*, 1 (2): 145-158.

90. Rengaswamy, R., Hägglund, T. and Venkatasubramanian, V. (2001). A qualitative shape analysis formalism for monitoring control loop performance. *Engineering Applications of Artificial Intelligence*, 14 (1): 23-33.

91. Rugh, W. J. and Shamma, J. S. (2000). Research on gain scheduling. *Automatica*, 36 (10): 1401-1425.

92. Sales, K. and Billings, S. (1990). Self-tuning control of non-linear ARMAX models. *International journal of control*, 51 (4): 753-769.

93. Scali, C. and Ghelardoni, C. (2008). An improved qualitative shape analysis technique for automatic detection of valve stiction in flow control loops. *Control Engineering Practice*, 16 (12): 1501-1508.

94. Sendjaja, A. Y. and Kariwala, V. (2009). Achievable PID performance using sums of squares programming. *Journal of Process Control*, 19 (6): 1061-1065.

95. Sewdass, S., Pillay, N., Moorgas, K. and Govender, P. 2014. Control Valve Stickband Compensator. In: Proceedings of *World Congress*. 1260-1265.

96. Shahni, F. and Malwatkar, G. (2011). Assessment minimum output variance with PID controllers. *Journal of Process Control*, 21 (4): 678-681.

97. Shinskey, F. G. 1973. *pH and pION control in process and waste streams*. John Wiley & Sons, Inc.

98. Shoukat Choudhury, M., Shah, S. L. and Thornhill, N. F. (2004). Diagnosis of poor control-loop performance using higher-order statistics. *Automatica*, 40 (10): 1719-1728.

99. Singhal, A. and Salsbury, T. I. (2005). A simple method for detecting valve stiction in oscillating control loops. *Journal of Process Control*, 15 (4): 371-382.

100. Sivalingam, S. and Hovd, M. (2011). Controller performance monitoring and assessment. *Selected Topics on Constrained and Nonlinear Control*: 27.

101. Spinner, T., Srinivasan, B. and Rengaswamy, R. (2014). Data-based automated diagnosis and iterative retuning of proportional-integral (PI) controllers. *Control Engineering Practice*, 29: 23-41.

102. Srinivasan, B., Spinner, T. and Rengaswamy, R. (2012). Control loop performance assessment using detrended fluctuation analysis (DFA). *Automatica*, 48 (7): 1359-1363.

103. Sun, Z., Qin, S. J., Singhal, A. and Megan, L. (2013). Performance monitoring of model-predictive controllers via model residual assessment. *Journal of Process Control*, 23 (4): 473-482.

104. Swanda, A. P. and Seborg, D. E. 1999. Controller performance assessment based on setpoint response data. In: Proceedings of *American Control Conference, 1999. Proceedings of the 1999*. IEEE, 3863-3867.

105. Tan, K., Huang, S. and Ferdous, R. (2002). Robust self-tuning PID controller for nonlinear systems. *Journal of Process Control*, 12 (7): 753-761.

106. Thornhill, N., Huang, B. and Shah, S. (2003). Controller performance assessment in set point tracking and regulatory control. *International Journal of Adaptive Control and Signal Processing*, 17 (7-9): 709-727.

107. Thornhill, N. F. and Horch, A. 2006. Advances and new directions in plant-wide controller performance assessment. *IFAC Proceedings Volumes*, 39 (2): 29-36.

108. Tyler, M. L. and Morari, M. (1996). Performance monitoring of control systems using likelihood methods. *Automatica*, 32 (8): 1145-1162.

109. Vander Wiel, S. A., Tucker, W. T., Faltin, F. W. and Doganaksoy, N. (1992). Algorithmic statistical process control: concepts and an application. *Technometrics*, 34 (3): 286-297.

110. Veronesi, M. and Visioli, A. (2010a). An industrial application of a performance assessment and retuning technique for PI controllers. *ISA transactions*, 49 (2): 244-248.

111. Veronesi, M. and Visioli, A. (2010b). Performance assessment and retuning of PID controllers for integral processes. *Journal of Process Control*, 20 (3): 261-269.

112. Wang, W., Zhang, J. and Chai, T. (2000). A survey of advanced PID parameter tuning methods. *Acta Automatica Sinica*, 26 (3): 347-355.

113. Widodo, A. and Yang, B.-S. (2007). Support vector machine in machine condition monitoring and fault diagnosis. *Mechanical Systems and Signal Processing*, 21 (6): 2560-2574.

114. Wright, R. A. and Kravaris, C. (1991). Nonlinear control of pH processes using the strong acid equivalent. *Industrial & engineering chemistry research*, 30 (7): 1561-1572.

115. Yamashita, Y. (2006). An automatic method for detection of valve stiction in process control loops. *Control Engineering Practice*, 14 (5): 503-510.

116. Yang, B.-S., Han, T. and Hwang, W.-W. (2005). Fault diagnosis of rotating machinery based on multi-class support vector machines. *Journal of Mechanical Science and Technology*, 19 (3): 846-859.

117. Yu, W. 2007. Variance analysis for nonlinear systems. PhD thesis, Queens University.

118. Yu, W., Wilson, D. and Young, B. 2011a. A comparison of nonlinear control performance assessment techniques for hammerstein-wiener processes. In: Proceedings of *Advanced Control of Industrial Processes (ADCONIP), 2011 International Symposium on*. IEEE, 246-251.

119. Yu, W., Wilson, D., Young, B. and Harris, T. 2009. Variance decomposition of nonlinear systems. In: Proceedings of *Control and Automation, 2009. ICCA 2009. IEEE International Conference on*. IEEE, 738-744.

120. Yu, W., Wilson, D. I. and Young, B. R. (2010a). Control performance assessment for nonlinear systems. *Journal of Process Control*, 20 (10): 1235-1242.

121. Yu, W., Wilson, D. I. and Young, B. R. (2010b). Nonlinear control performance assessment in the presence of valve stiction. *Journal of Process Control*, 20 (6): 754-761.

122. Yu, W., Wilson, D. I. and Young, B. R. (2012). A comparison of nonlinear control performance assessment techniques for nonlinear processes. *The Canadian Journal of Chemical Engineering*, 90 (6): 1442-1449.

123. Yu, Z., Wang, J., Huang, B. and Bi, Z. (2011b). Performance assessment of PID control loops subject to setpoint changes. *Journal of Process Control*, 21 (8): 1164-1171.

124. Zhang, Z., Hu, L.-S. and Shi, W.-J. 2011. Estimation of benchmark performance for nonlinear control systems. In: Proceedings of *American Control Conference (ACC), 2011*. IEEE, 5079-5084.

125. Zhang, J., Zhang, F., Ren, M., Hou, G. and Fang, F. 2012. Cascade control of superheated steam temperature with neuro-PID controller. *ISA Transactions*, 51: 778-785.

126. Zhou, Y. and Wan, F. (2008). A neural network approach to control performance assessment. *International Journal of Intelligent Computing and Cybernetics*, 1 (4): 617-633.

127. Zhu, Q., Ma, Z. and Warwick, K. (1999). Neural network enhanced generalised minimum variance self-tuning controller for nonlinear discrete-time systems. *IEE Proceedings-Control Theory and Applications*, 146 (4): 319-326.

128. Ziegler, J. and Nichols, N. (1942). Optimum settings for automatic controllers. *trans. ASME*, 64 (11).

APPENDIX A

APPENDIX B

APPENDIX C